Ministero dell'Istruzione, dell'Università e della Ricerca

Università degli Studi di Palermo

Dottorato di Ricerca in
Scienze e Biotecnologie Mediche Sperimentali e Applicate:
***indirizzo* Genomica e Proteomica nella ricerca Oncologica ed Endocrino-Metabolica**

Ciclo XXV: 2012-2014

Settore Scientifico Disciplinare: BIO/06

PROTEOMIC IDENTIFICATION OF NOVEL MARKERS IN BREAST AND COLON CANCER

Tesi di Dottorato di:

Miriam Buttacavoli

Coordinatore:

Prof.ssa Carla Giordano

Tutor:

Dott.ssa Patrizia Cancemi

Ministero dell'Istruzione, dell'Università e della Ricerca

Università degli Studi di Palermo

PhD Programme in Experimental and Applied Medical Sciences and Biotechnology:

Genomics and Proteomics applied to Oncological and Endocrine – Metabolic research

Graduation year 2016

PROTEOMIC IDENTIFICATION OF NOVEL MARKERS IN BREAST AND COLON CANCER

PhD Thesis by:

Miriam Buttacavoli

Director of PhD Programme:

Prof.ssa Carla Giordano

Supervisor:

Dott.ssa Patrizia Cancemi

INDEX OF CONTENTS

BACKGROUND

Tumors are complex and variable diseases both in its presentation, development and clinical outcome. The same heterogeneity and variability exist at cellular and molecular level. Cancer is a multi-step process during which cells undergo profound metabolic and behavioral changes, leading them to proliferate in an excessive way, to escape surveillance by the immune system, and ultimately to invade distant tissues to form metastases. Currently, more than 1% of all human genes are implicated via mutation in cancer. It is now accepted that mutations in cancers can be divided into drivers and passengers (Haber DA and Settleman J, 2007). Driver mutations directly or indirectly confers a selective growth advantage to the cell in which it occurs, whereas passengers are co-travellers that do not contribute to cancer development. The functional alterations of these recurrently mutated genes, however, involve a small number of molecular, biochemical and cellular traits, referred as **hallmarks of cancer.**

These acquired capabilities include sustaining proliferative signaling, evading growth suppressors, resisting cell death, enabling replicative immortality, inducing angiogenesis, and activating invasion and metastasis, and represent an essential tool for understanding the heterogeneity of neoplastic diseases (*Fig. 1*) (Hanahan D and Weinberg RA, 2000).

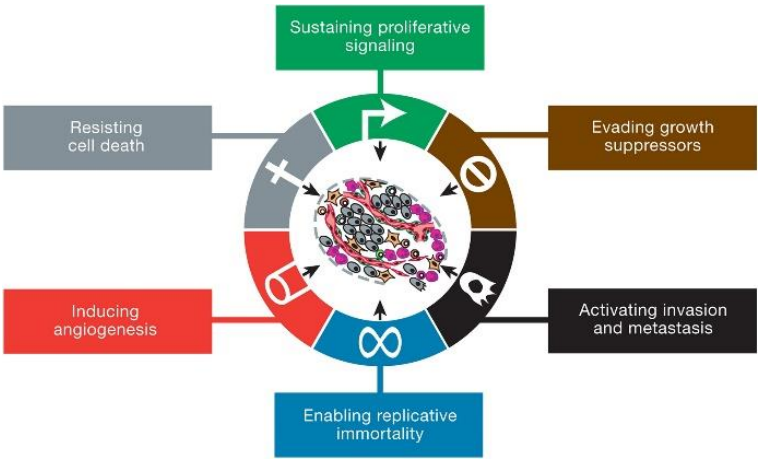

Figure 1. The Hallmarks of Cancer, proposed by Douglas Hanahan and Robert A. Weinberg.

Certainly, normal cells evolve progressively to a neoplastic state and they acquire a succession of these hallmark capabilities; the multistep process of carcinogenesis could be rationalized by the need of incipient cancer cells to acquire the traits that enable them to become tumorigenic and ultimately malignant. Normal tissues control the production and release of growth-promoting signals that ensure cell homeostasis and maintain the normal tissue architecture and function.

Cancer cells are able to **sustain proliferative signaling** in different ways: a) they may produce growth factor ligands themselves, resulting in autocrine proliferative stimulation; b) cancer cells may send signals to stimulate normal cells within the supporting tumor-associated stroma, which respond by supplying the cancer cells with various growth factors (paracrine proliferative stimulation). Cancer cells may display high levels of membrane receptors or mutated receptors resulting in constitutive activation of downstream signaling circuits involved in cell growth and cell cycle progression that in turn influence other cell-biological properties, such as cell survival and energy metabolism. For example, the epidermal GF receptor (EGF-R/erbB) is upregulated in stomach, brain, and breast tumors, while the HER-2/neu receptor is overexpressed in stomach and mammary carcinomas (Slamon DJ et al., 1989; Yarden Y and Ullrich A , 1988). Moreover, mutations in the catalytic subunit of phosphoinositide 3-kinase (PI3-K) isoforms were detected in an array of tumor types, which serve to hyperactivate the PI3-K signaling circuitry, including its key Akt/PKB signal transducer (*Fig. 2*).

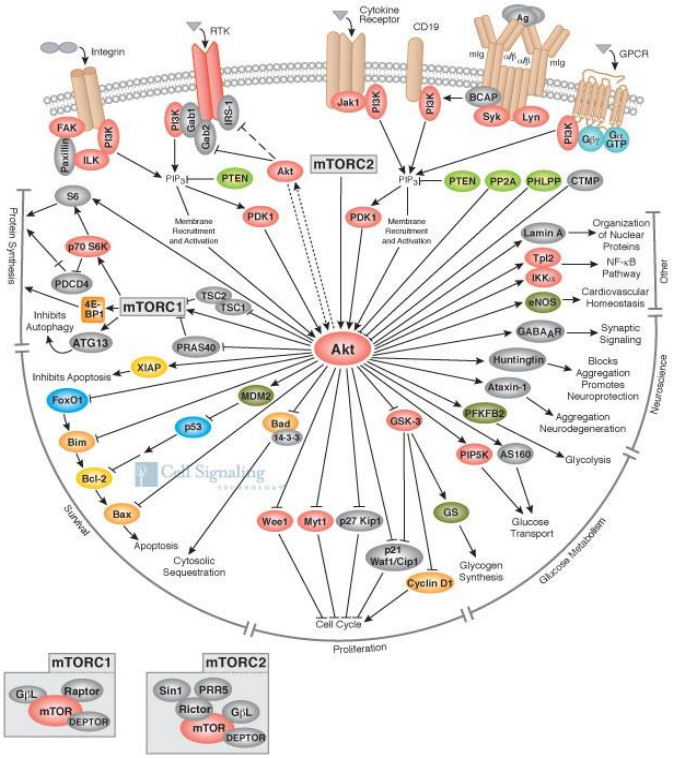

Figure 2. Picture illustrating the central role of Akt/PKB pathway in the cell.

Then, it is very important the negative feedback, because defects in these mechanisms are capable of enhancing proliferative signaling. A prototype of this type of regulation involves also the mTOR kinase, a coordinator of cell growth and metabolism that lies both upstream and downstream of the PI3-K pathway. In the circuitry of some cancer cells, mTOR activation results, via negative feedback, in the inhibition of PI3-K signaling. Thus, when mTOR is

pharmacologically inhibited in such cancer cells (such as by the drug rapamycin). The associated loss of negative feedback results in increased activity of PI3-K and its effector Akt/PKB, thereby reducing the antiproliferative effects of mTOR inhibition (Sudarsanam S and Johnson DE, 2010; O'Reilly KE et al., 2006).

In addition to the hallmark capability of inducing and sustaining positively growth-stimulatory signals, cancer cells must also **evade powerful programs** that negatively regulate cell proliferation. Many of these programs depend on the actions of tumor suppressor genes, in particular two prototypical tumor suppressors encode for the RB (retinoblastoma-associated) and TP53 proteins involved in cell growth and/or in senescence. Recent results have highlighted the complexity and the interconnections between the prototypical growth signaling circuity, centered around tyrosine kinase receptors and transduced by MAP kinase cascades and other important effector pathways such as extracellular matrix receptors (i.e integrines), cell-cell receptors (i.e cadherins), cytokines or antigrowth factors. These cascades are linked to each other via a variety of cross talking connections and can be linked with other pathways (*Fig. 3*).

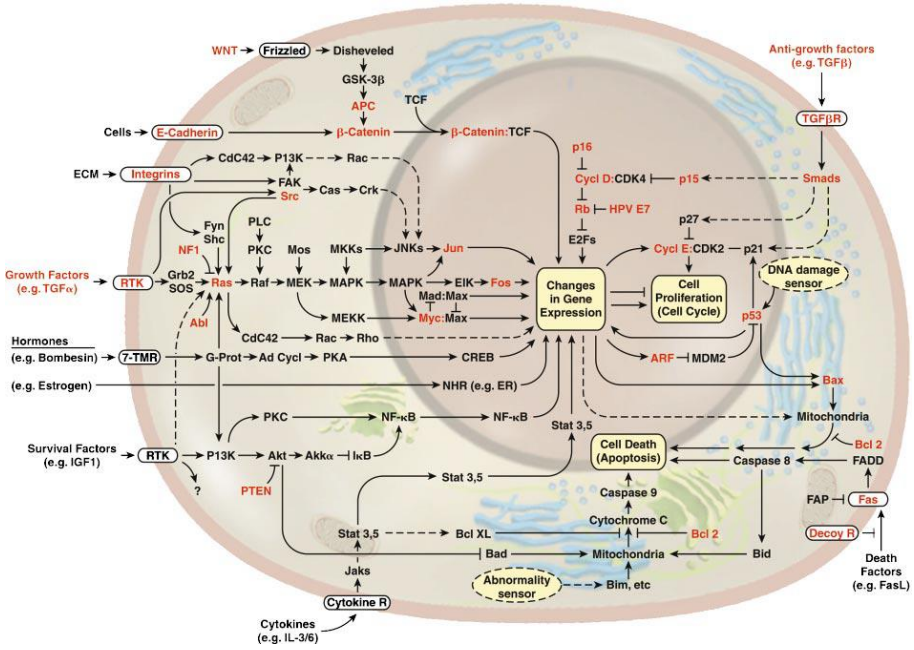

Figure 3. Cross-talking connections between signaling pathways involved in cancer.

Cancer cells during tumor progression are able to **resist to cell death**. Apoptosis is triggered in response to various physiologic stresses that culminates in disruption of cellular membranes, fragmentation of chromatin and apoptosis bodies' formation. Nevertheless, the apoptotic machinery is composed of both upstream sensors and downstream effector components. The sensors are able to monitor the extracellular death-inducing signals (the extrinsic apoptotic program), or signals of intracellular origin (the intrinsic program) and activate latent protease

(caspases 8 and 9), which initiate a cascade of proteolysis involving effector caspases responsible for the execution phase of apoptosis (*Fig. 4*). Many of the signals that elicit apoptosis converge on mitochondria, through the release of cytochrome C. The activation of apoptotic regulators and effectors is controlled by pro- and anti-apoptotic factors of the Bcl-2 family (Adams JM and Cory S, 2007). Bcl-2, Bcl-xL, Bcl-w, Mcl-1, A1 are inhibitors of apoptosis, acting in large part by binding to and by suppressing Bax and Bak, pro-apoptotic triggering proteins. Cancer cells have many strategies to evade apoptosis. Most common is the loss of TP53 tumor suppressor function, eliminating the critical damage sensor from the apoptosis-inducing circuitry. Alternatively, tumors may increase the expression of anti-apoptotic regulators (Bcl-2, Bcl-xL) or of survival signals (Igf1/2) and downregulate pro-apoptotic factors (Bax, Bim, Puma).

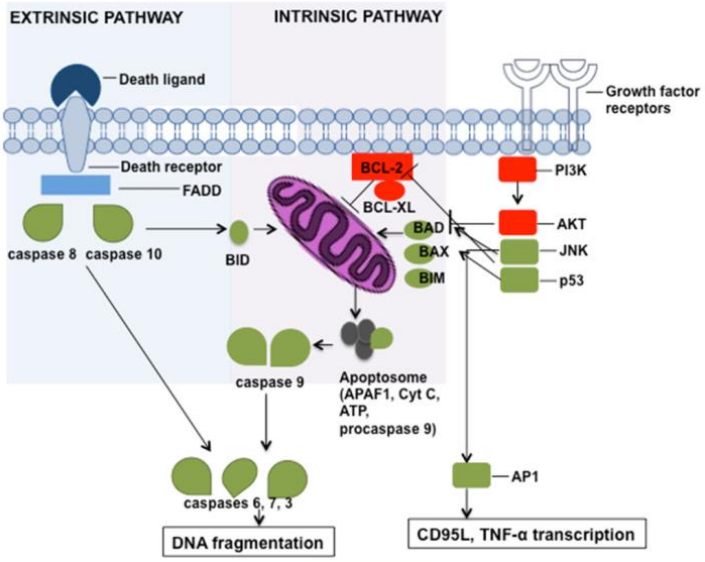

Figure 4. Extrinsic and intrinsic apoptotic signaling pathways.

An another important cell-physiologic response that can be strongly induced in certain states of cellular stress is the **autophagy**, enabling cells to break down cellular organelles (such as ribosomes and mitochondria) and allowing the resulting catabolizes to be recycled, used for biosynthesis and energy metabolism. Like apoptosis, the autophagy machinery has both regulatory and effector components (Mizushima N, 2007). Recently, it was revealed an interesting connection between the regulatory circuits governing autophagy, apoptosis, and cellular homeostasis, through the signaling pathway involving the PI3-K, AKT, and mTOR kinases, which is stimulated by survival signals to block apoptosis, similarly inhibits autophagy. When survival signals are insufficient, the PI3-K signaling pathway is downregulated, with the result that autophagy and/or apoptosis may be induced (Levine B and Kroemer G, 2008; Sinha S and Levine B, 2008). In the context of neoplasia, another important aspect related to cell death

is the **necrosis**. Necrotic cells, in fact, release proinflammatory signals into the surrounding tissue microenvironment. The immune inflammatory cells actively recruit are able to promote tumor progression fostering angiogenesis, cell proliferation and invasiveness. Other acquired capability of tumor cells is the **limitless replicative potential** in order to generate macroscopic tumors, in contrast with normal cells, which are able to progress through a limited number of successive cell growth and division cycles. In normal cells, repeated cycles of cell division induce senescence, a typically irreversible entrance into a not proliferative state, followed by cell death. The length of telomeric DNA regulates the senescence process (*Fig. 5*). The progressive shortening of telomeres, through successive cycles of replication, reduces their ability to protect the end of chromosomal DNA. In cancer cells, telomeres length is successfully maintained by the up-regulation of telomerase enzyme activity.

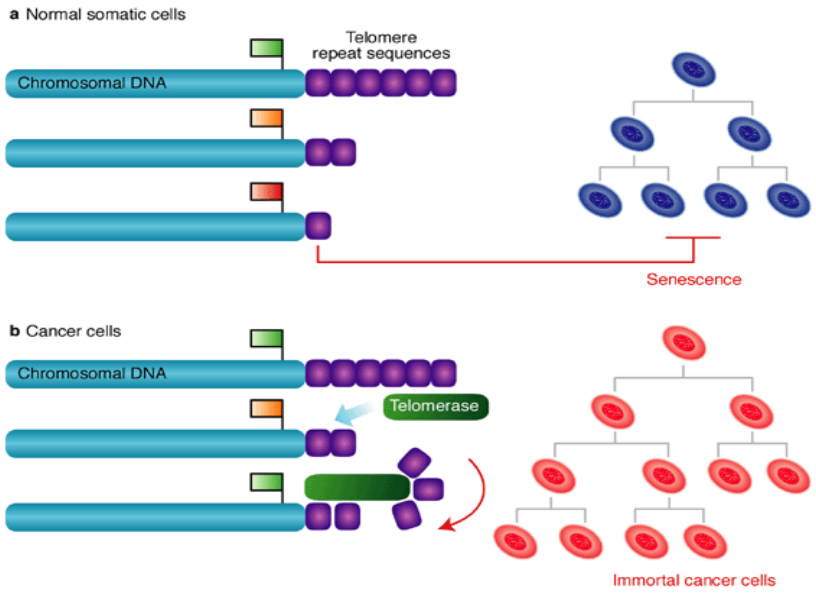

Figure 5. Regulation of telomere length in normal and cancer cells by telomerase (Molecular medicine, 2002).

For growth, emerging neoplasias must develop **angiogenic ability** (Bouck N et al., 1996; Hanahan D and Folkman J, 1996; Folkman J, 2006). This capability to induce and sustain angiogenesis seems to be acquired in a step (or steps) during tumor development, through an "angiogenic switch" from vascular quiescence (*Fig. 6*), by chancing the balance of angiogenesis inducers and countervailing inhibitors, for example involving altered gene transcription (increased expression of VEGF and/or FGFs or downregulated expression of inhibitors such as thrombospondin-1 or β-interferon). However, the tumor neovasculature is typically aberrant, with excessive vessel branching, distorted and enlarged vessels and microhemorrhaging. Moreover, the peri-tumoral inflammatory sustain the angiogenic switch. Additionally, VEGF

ligands can be sequestered in the extracellular matrix in latent forms that are subject to release and activation by extracellular matrix-degrading proteases (e.g., MMP-9).

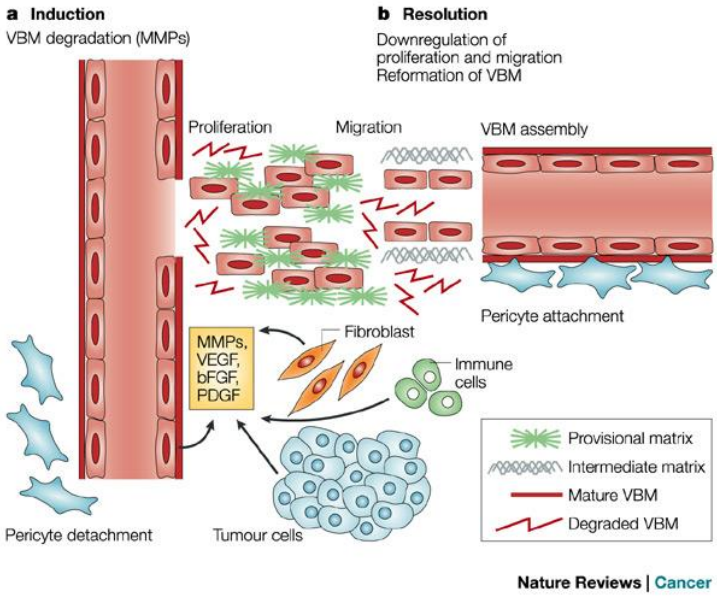

Figure 6. Picture representing the formation of new blood vessels from pre-existing vasculature (Folkman J, 2007).

The ability of tumor cells to spread from their original location to invade and colonize distant organ sites is the main feature that distinguishes benign from malignant cancers. The **metastatic process** consists of a series of genetic or epigenetic changes, during which cancer cells leave the original tumor site, enter lymph or blood circulation (a process called intravasasion), survive and migrate, and extravasate to colonize distant organs (Talmadge JE and Fidler IJ, 2010; Fidler IJ, 2003). The most common places of metastases are the liver, the brain, the bones, the lung and the adrenal glands. There is a propensity for certain tumors to seed in particular organs. This was first recognized by Stephen Paget in 1889. He formulated the "*seed and soil*" hypothesis, proposing that specific cancer cells (the seed) have an affinity for certain organs (the soil). For example, breast cancer cells that have a physiological need for calcium selectively metastasize to bone because they can use it as an abundant source of calcium. In general, cancer cells tend to metastasize in organs where blood and energy supplies are abundant (such as liver or lung) or that are separated from the immune system by a physical barrier (such as the brain). Initiation of metastasis requires releasing cells from cell-to-cell contacts and breaking of the basement membrane to penetrate into the underlying stroma and mesenchymal compartments. The epithelial-mesenchymal transition (EMT) is highly implicated by transformed epithelial cells, which can acquire the abilities to invade, to resist apoptosis and to disseminate (*Fig. 7*). Most solid tumors show an epithelial phenotype.

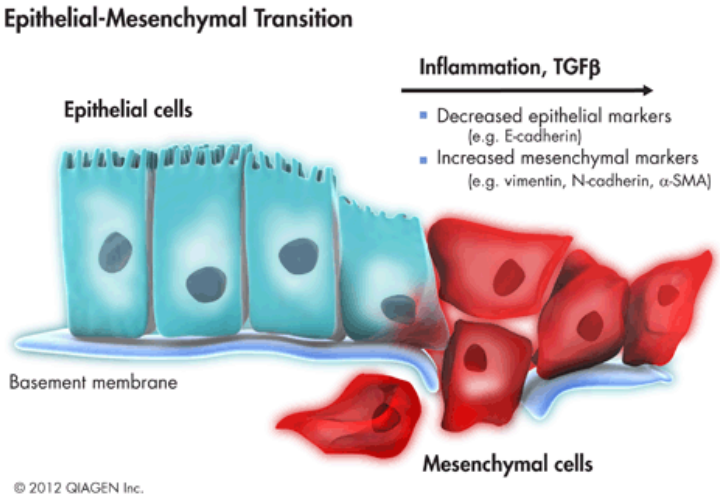

Figure 7. Picture representing the Epithelial-Mesenchymal Transition.

During tumor progression, this phenotype becomes altered and some cells undergo a transition to assume a more mesenchymal phenotype, characterized by a high migratory capacity. Conversely, during extravasation, the cells undergo a reverse mesenchymal-epithelial transition, which regenerates high proliferative status and allows formation of a metastasis with a morphology that resembles the primary tumor. A landmark of Epithelial-Mesenchyme Transition (EMT) is the loss of E-cadherin expression associated with the switch from cytokeratin to vimentin expression. Invasive cancer cells show increased expression of many enzymes, as well as decreased expression of their regulators, involved in the degradation of components of the ECM. One important group of such enzymes is the matrix metalloproteinases (MMP). The MMP family contains a diverse group of enzymes with different substrate preference (collagenase, gelatinase, stromelysin). All family members include a leader domain, a propeptide domain and a highly conserved catalytic domain containing a zinc atom involved in substrate binding. MMPs play important roles during normal development and morphogenesis, and their activities are tightly regulated. Activation depends upon cleavage of the leader domain and is regulated by endogenous MMP inhibitors, which include a-2 macroglobulin and tissue inhibitors of metalloproteinases (TIMPs). An imbalance between MMPs and naturally occurring MMP inhibitors may cause an excess of extracellular matrix destruction, allowing cancer cells to invade surrounding tissues and to metastasize. Two of the most studied MMPs are MMP-2 and -9 (gelatinase A and B, respectively).

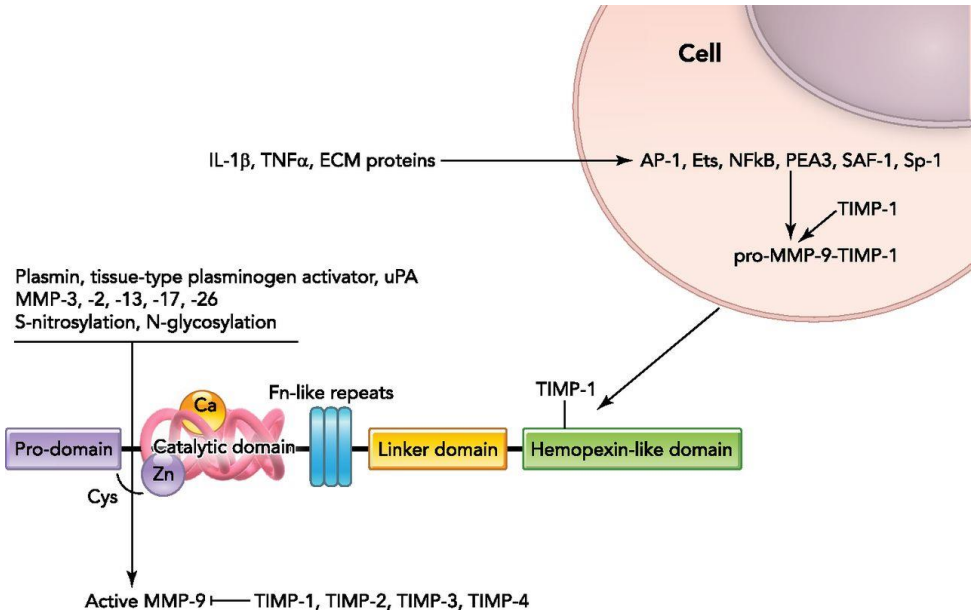

Figure 8. Structure, transcription and translation regulating factors of MMP-9.

There is clear evidence for increased levels of active forms of MMP-2 and/or MMP-9 in bladder, breast, colon, prostate, lung, esophageal and gastric cancer tissues (Kurizaki T et al., 1998). This increased expression can take place in cancer cells and/or in surrounding normal stromal cells, indicating that cancer cells can somehow induce stromal cells to secrete factors that facilitate migration, invasion and, ultimately, metastasis. Urokinase plasminogen activator (uPA) is also frequently upregulated in cancer. It controls the synthesis of plasmin, which degrades laminin and activates gelatinases (*Fig. 8*). Thus, upregulation of these enzymes in cancer can lead to proteolytic cascades that degrade the basement membranes and components of the stroma. Besides their direct role in degrading ECM components, MMPs are also indirectly involved in promoting metastasis through their roles in angiogenesis: MMP-9 induces the release and the activation of VEGF-ligands sequestrated in the ECM in latent forms. Furthermore, proteases also contribute to sustained tumor growth by the ectodomain cleavage of membrane-bound pro-forms of growth factors, and the release of peptides that are mitogenic and chemotactic for cancer cells. The overexpression of gelatinases in primary tumors has been shown to correlate with grade or stage in many solid cancer types. Moreover, they often predict disease-free survival after treatment, or correlate to overall cancer-specific survival. The expression of MMP-2 and MMP-9 is not necessarily coordinated in all tumors, and their value as potential prognostic indicators varies, e.g. in the case of breast carcinoma (Scorilas A et al., 2001; Talvensaari-Mattila A et al., 1998; Turpeenniemi-Hujanen T, 2005). As consequence of the invasion process, neoplastic cells penetrate the underlying interstitial stroma where they may interact actively with the host cells. Recent cancer studies have acknowledged the active

roles that tumor stroma can play in carcinogenesis, focusing on the abnormal communication between tumor cells and their microenvironment. The extracellular environment of primary tumors may be depicted as a complex microecosystem (*Fig. 9*), in which the neoplastic cells, the extracellular matrix, mesenchymal cells, blood and lymphatic vessel, and a variety of active factors play a dynamic role in cancer progression. There is no doubt that the system is extremely intricate since each component may send and receive signals from all the others, and once activated, each cell type may modulate the responses and modify the repertoire of signals. Ultimately the collective orchestration of these cross-talks between neoplastic cells and host cells may have permissive or restrictive effects on the angiogenic processes and on the propensity of neoplastic cells to form metastasis. Previous works by our group demonstrated the important role of some components of the tumor microenvironment (i.e fibroblasts, proteoglycans, collagens) on breast cancer proteomics (Cancemi P et al., 2010; Pucci-Minafra I et al., 2007; Pucci-Minafra I et al., 2008).

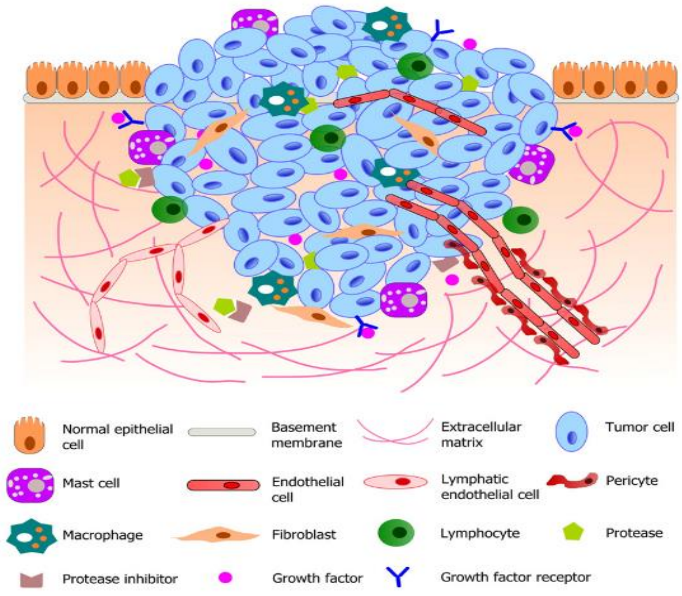

Figure 9. Schematic illustration of tumor microenvironment and its components which collectively contribute to the tumor-stromal interaction and tumor progression (Joyce JA, Pollard JW, 2009; Koontongkaew S, 2013).

As was already suggested in Hanahan D., 2000, the numerous signaling molecules affecting cancer cells operate as nodes and branches of reprogrammed circuits deriving by circuits operating in normal cells. Recently, the original interpretation of these circuits was solidified and the catalog of signals and the interconnections of their signaling pathways were expanded. Other two additional hallmarks of cancer cells have been proposed to be functionally important for cancer development and labeled as emerging hallmarks (*Fig. 10*): the first involves the capability to modify, or reprogram, cellular metabolism in order to most effectively support neoplastic proliferation. The second allows cancer cells to evade immunological destruction, in particular by T- and B-lymphocytes, macrophages, and natural killer cells. Additionally, two consequential characteristics of cancer cells facilitate acquisition of both core and emerging hallmarks: genomic instability in cancer cells, which generates random mutations including chromosomal rearrangements and inflammatory state of premalignant and malignant lesions driven by cells of the immune system (Hanahan D and Weinberg RA, 2011).

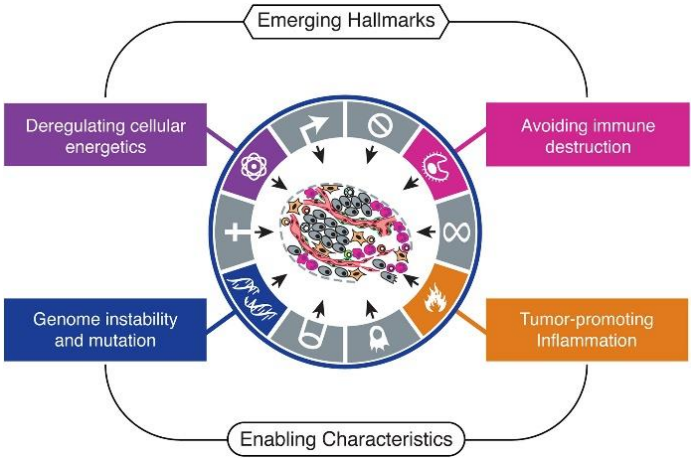

Figure 10. Emerging hallmarks and enabling characteristics by Douglas Hanahan and Robert A. Weinberg.

Cancer metabolism

Glucose is a primary source of energy. Under aerobic conditions, normal cells metabolize glucose to pyruvate via glycolysis in the cytosol, and subsequently convert pyruvate to carbon dioxide in the mitochondria for oxidative phosphorylation; under anaerobic conditions, conversion of pyruvate to lactic acid is favored with relatively low amounts of pyruvate being diverted to the mitochondria. In contrast, cancer cells primarily derive energy from glucose via glycolysis to lactic acid, even under highly aerobic conditions, a property first observed by Otto Warburg. The "*Warburg effect*" is much less energy-efficient than the oxidative phosphorylation pathway, but the production and secretion of lactic acid, markedly contributing

to metabolic acidosis commonly found in solid cancers (*Fig. 11*). An acidic pH can markedly impede the function of normal immune cells, promote the activation of proteolytic enzymes, and on the other hands, can contribute to activate apoptotic program in normal adjacent cells.

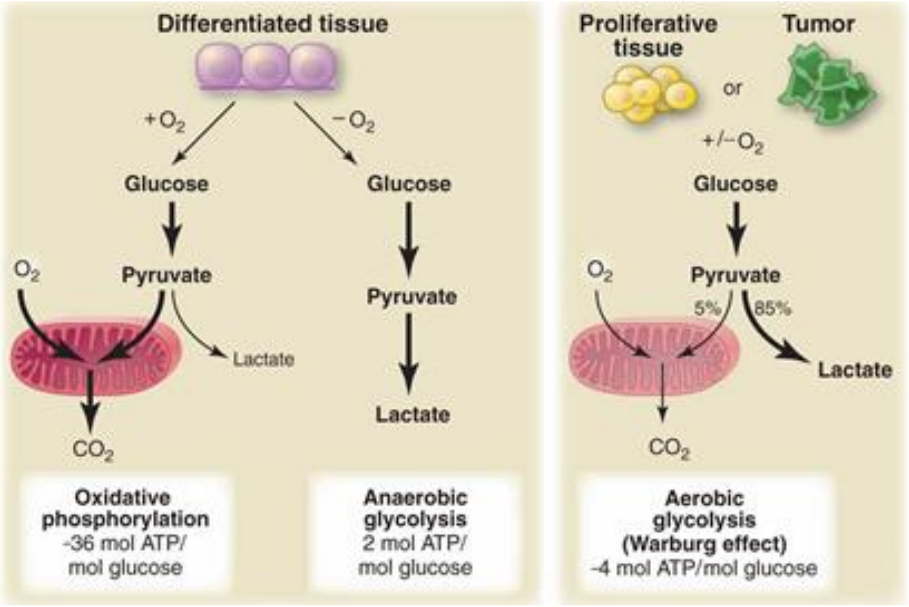

Figure 11. Schematic representation of the differences between oxidative phosphorylation, anaerobic glycolysis, and aerobic glycolysis (*Warburg effect*) (Vander Heiden MG et al. 2009).

Epigenetic control of tumor development

Historically, the term **epigenetics** was used to describe all biological phenomena that do not follow normal genetic principle. In a broader sense, epigenetics can be considered as an interface between genotype and phenotype. The importance of epigenetic principle is highlighted by the fact that all cells in any given organism share an identical genome with other cell types, yet they can exhibit strikingly different morphological and functional properties. Therefore, it is obvious that epigenetic events define the identity and proliferation potential of different cells in the body, features that are typically deregulated in cancer. Epigenetic inheritance includes DNA methylation, histone modifications and RNA-mediated silencing, all of which are essential mechanisms that allow the stable propagation of gene activity states from one generation of cells to the next.

DNA methylation

The best-studied epigenetic mechanism is DNA methylation. The methylation of DNA refers to the covalent addition of a methyl group to the 5-carbon (C5) position of cytosine bases that are located 5’ to a guanosine base. This is a very small chemical modification of the DNA

molecule that while it does not alter the DNA code, may have major regulatory consequences. Aberrant DNA methylation is tightly connected to a wide variety of human cancer. Two forms of aberrant DNA methylation are found in human cancer: the overall loss of 5-methyl-cytosine (global hypomethylation) and gene promoter-associated (CpG island specific) hypermethylation (*Fig. 12*).

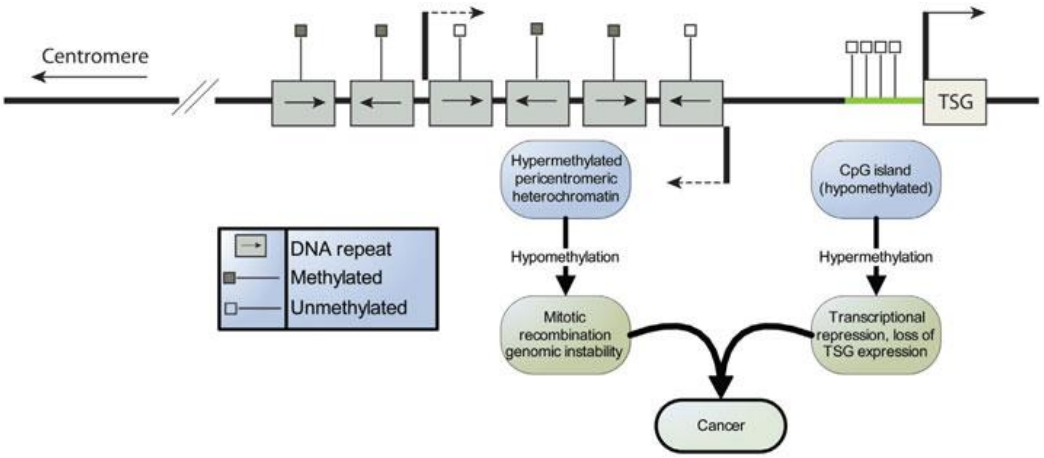

Figure 12. DNA methylation and cancer.

While the precise consequences of genome-wide hypomethylation are still debated (activation of cellular proto-oncogenes, induction of chromosome instability), hypermethylation of gene promoters is in turn associated with gene inactivation. When hypermethylated, gene promoters become unable to bind the factors that are responsible for gene expression. The gene thus becomes inactivated. A large number of studies indicated that the silencing of tumour suppressor genes and other cancer-related genes may occur through hypermethylation of their promoters.

miRNAs

Recently have been identified numerous microRNAs (miRNAs) that control EMT and govern microenvironmental remodeling and epithelial plasticity (Wright JA et al., 2010). miRNAs are small non-coding RNAs of 18–25 nucleotides in length that function as negative regulators. miRNAs post-transcriptionally regulate gene expression by either inhibiting mRNA translation or inducing mRNA degradation, and they participate in a wide variety of physiological and pathological cellular processes (e.g., proliferation, differentiation, apoptosis and development) by simultaneously controlling the expression levels of hundreds of genes.

Histone modifications

The post-translational acetylation and methylation of lysine residues in histone tails is another epigenetic process that can regulate gene expression. Histone acetylation typically results in an "open" chromatin configuration that facilitates the access of transcription factors to DNA and gene transcription, but the reverse scenario can silence tumor suppressor genes in cancer cells.

Breast and colon tissues

Breast and colon cancer represent two of the common cancers in human. In general, the development of cancers is influenced by a number of intrinsic (biological) and external factors. The intrinsic factors include the age (cancer generally is in fact considered to be an old age disease), hormonal status of the individual, family history (some cancers have a link with family occurrence) and genetic predisposition (expecially in the develpoment of genetic-specific cancer). The external factors include diet and life style. More than 50% of all cancers are related to the diet , for example high fat diet and obesity are associated with breast cancer. Moreover, the role of cigarette smoking is well estabilished in lung cancer. It is now emerging that the external factors can cause cancer because they add the free radical production in the body. Free radicals and reactive oxygen species (ROS) are produced during the normal metabolic process as well as by interaction with external agents. They include superoxide anions, hydroxyl radicals, peroxylradicals and hydroperoxylradicals, which interact with DNA, producing gene mutation and chromosomal instability.

Focusing the general features of the normal organization of the breast and intestinal ephitelium can help to understand the tissues changes during the respective tumorigenesis. The normal epithelial composition and organization of breast and colon reflect the specific functions of these tissues: mammmary gland is able to produce and secrete milk during lactation, while the intestine absorbs nutrients. Breast and colon ephitelia are composed of polarized cells, tightly connected to each other, caracherized by different specialized domains. Lateral domain contains specialized adherens junctions formed by cadherins. Tight junctions are located above adherens junctions towards the luminal surface and physically separate the apical membrane of cells. In the basolateral membrane are found integrins and other transmembrane proteins that anchor epithelial cells to the underlying basement membrane, an organizing scaffold comprised of specific extracellular matrix (ECM) molecules that are produced by the epithelium itself and surrounding fibroblasts (Nelson WJ et al., 2013).

Breast tissue overlies the ribs and chest muscles. The milk producing glandular epithelia of a woman's breast is contained within adipocyte tissue. A breast consists of 15–20 epithelial lobes, each develops numerous milk-producing lobules upon pregnancy (*Fig. 13*).

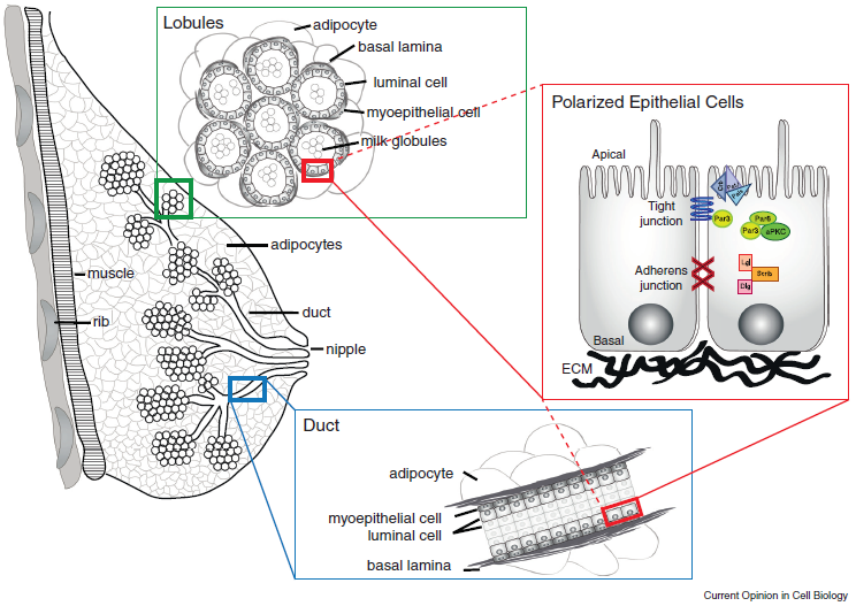

Figure 13. Schematized view of the normal tissue organization in breast.

Each lobule and lobe is connected to the nipple via ducts that transport milk. The lobules and ducts consist of a bilayered epithelium comprising an inner layer of milk-producing luminal epithelial cells and an outer layer of myoepithelium that contracts to generate milk flow. Luminal epithelial cells are polarized containing apical domains that face the lumen and basolateral domains that interface with the interior of the body. In breast tissue, cancer arise predominantly from the luminal epithelial cells of ducts or lobules (*Fig. 14*).

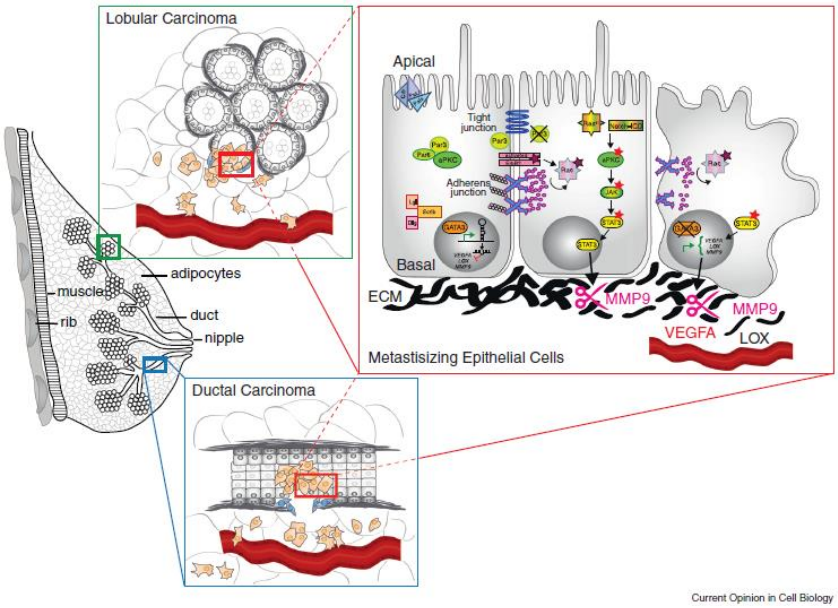

Figure 14. Relationship between cellular and tissue changes in breast cancer. Invasive lobular carcinoma (ILC) originates in the luminal cells of milk-producing lobules.

The **intestine** resides in the abdominal cavity and is essentially a long tube that connects the stomach to the rectum. It is divided into small and large intestine (colon). Both regions contain a number of different tissue layers (*Fig. 15*).

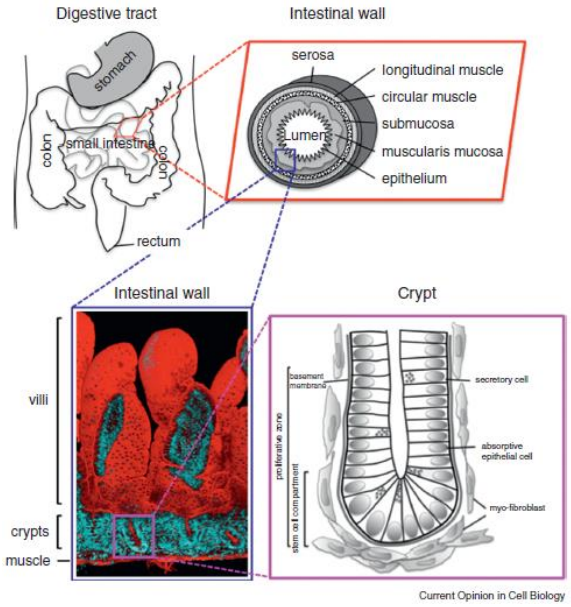

Figure 15. Schematized view of the normal tissue organization in intestine.

The outermost layer, the serosa, covers the intestine and is followed by two muscle layers that are perpendicular to each other. The outer longitudinal muscle layers run parallel to the intestinal axis and the inner, circumferential muscle layer circumnavigates the intestinal wall. The next layer is the sub-mucosa, which consists mostly ECM, contains blood and lymphatic vessels. The muscularis mucosa consists of myo-fibroblasts that reside directly underneath the basement membrane that underlies the epithelium lining the intestinal lumen. In colon only crypts are present. Crypts contain proliferative stem cells at their base that produce the different cell types normally present in the epithelium including secretory and absorptive epithelial cells. The epithelium in each crypt is surrounded by myo-fibroblasts. In the intestine and colon, cancer originates in the epithelium of the crypt and in the early tumor stages cells remain polarized, with an increased proliferation and decreased differentiation (*Fig. 16)*. Cellular polarity is lost at later stages and then cells invade the surrounding stroma.

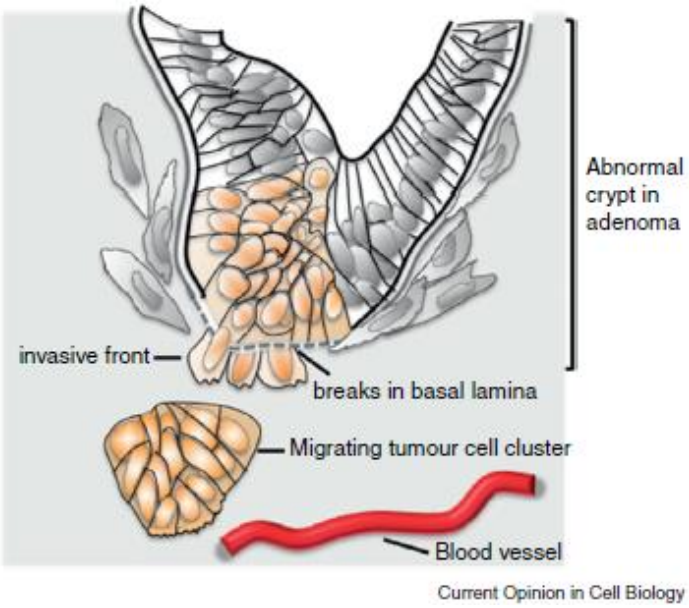

Figure 16. Relationship between cellular and tissue changes in colon cancer.

Breast cancer

Breast cancer is a highly heterogeneous disease under several distinct viewpoints. Indeed, different types of breast cancer exhibit variable histopathological and biological features, different clinical outcome and different response to systemic interventions. The histopathological classification of breast carcinoma is based on the diversity of the morphological features of the tumors. Breast cancer can be classified in carcinoma in situ (non-infiltrating) and infiltrating breast cancer. The first is characterized by uncontrollated proliferation of malignant epithelial cells, that do not exceed the basement membrane; in the infiltrating breast cancer, the epithelial cells break the basal lamina to invade and metastasise into different anatomical regions.

In breast cancer, the family history represents one of the strongest factor of risk. About 5-10% of all cases of breast cancer may have an hereditary basis. The two genes that confer susceptibility to the onset of breast cancer are BRCA-1 and BRCA-2, implicated in DNA repair mechanism, cell cycle checkpoint control, and maintenance of genomic stability. In the sporadic cases of breast cancer, alterations in proto-oncogenes are associated with the initiation, promotion and/or maintanance of tumors. Oncogenes often found to be overexpressed, include members of the myc and ras family (c-myc, H-ras1) and members of the EGF receptors (EGFR, erbB) family.

Clinical classification of breast cancer

Immunohistochemistry (IHC) represents a diagnostic tool to determine the stage and grade of a tumor and to identify the cell type and origin of a metastasis; moreover it allows to find the site of the primary tumor and provides the molecular classification of breast cancer into ER-positive and ER-negative categories.

Breast cancer is also routinely classified into HER-2 amplified or non-amplified categories by RNA and DNA in situ hybridization. In breast cancer, the status of hormone receptors (HRs) such as estrogen receptor (ER), progesterone receptor (PR), and HER-2, can act as prognostic or predictor of efficacy of the specific treatments. Patients with ER^+/PR^+ tumors will treated with antiestrogenes molecules. The human epidermal receptor protein-2 (HER-2) is an oncoprotein, which belongs to the epidermal growth factor receptor (EGFR) family and is expressed at low levels in breast duct epithelium. Approximately 10% to 30% of breast cancers demonstrate HER-2 gene amplification or protein overexpression and breast cancer patients are more likely to suffer from relapse and tend to have a shorter overall survival. Through the development of the monoclonal antibody trastuzumab, which targeted the HER-2 protein, the

amplification status of HER-2 becames also a highly predictive biomarker (Slamon DJ et al., 1987; Mass RD et al., 2005). Trastuzumab improves survival, response rates, and time to progression when used alone or in combination with chemotherapy. Overexpression and amplification of HER-2 can be detected in about 15% of all primary breast cancer, and this group of patients benefit significantly from anti-HER-2 therapies.

However, the current clinical parameters for breast cancer diagnosis, cure, and prognostic/predictive properties, appear inadequate to discriminate between cancer subtypes and to support proper therapeutic decisions. Indeed, patients with the same type and stage of disease often display significantly different clinical outcome and responses to therapy.

Molecular classification of breast cancer

In 2000, Perou and colleagues, using cDNA microarrays, proposed a strong correlation between phenotype and genotype. Based on the gene expression data, breast cancers were grouped into five major subsets with prognostic significance that might be related to different molecular features of mammary epithelial biology, such as the basal-like, normal breast-like, HER-2-positive, luminal A and luminal B subtypes. Tumors can further be separated into the ER^+ and ER^- branches. Several independent studied have reproduced those findings, observing that the various molecular subtypes have distinct clinical outcomes and responses to therapy. For instance, the luminal A subtype has the best prognosis, basal-like and HER-2 subtypes have the worst prognosis, and the luminal B subtype has an intermediate prognosis.

The above mentioned five molecular subtypes of breast cancer are conserved across ethnic groups and are already evident at the ductal carcinoma in situ (DCIS) stage (Yu K et al., 2004), suggesting distinct tumor progression pathways for each tumor type. It is proposed that each tumor subtype can be initiated by specific stem cell or progenitor cell (*Fig. 17b*), or determined by acquired genetic and epigenetic events (*Fig. 17a*).

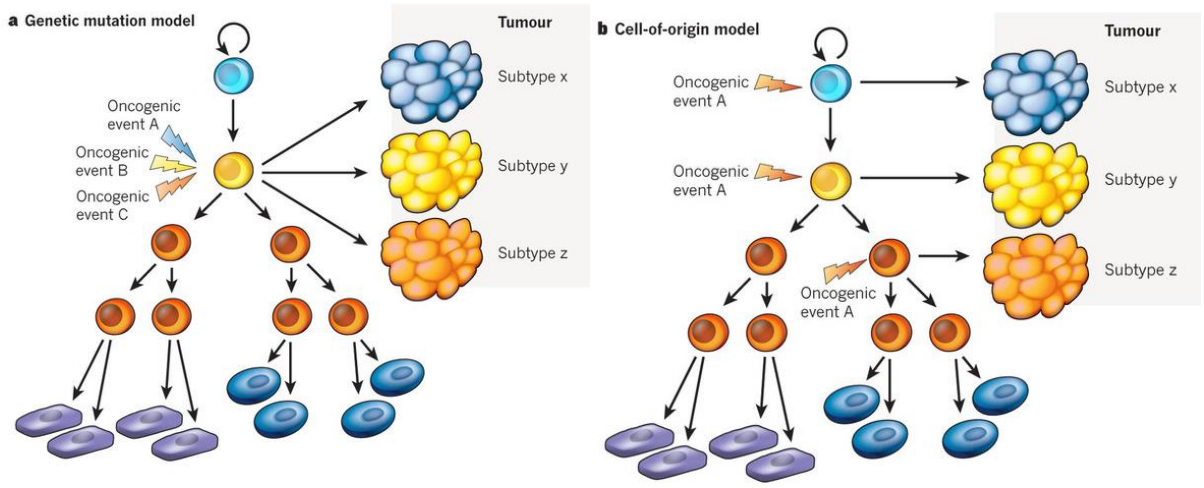

Figure 17. Two hypothetical models explaining the origin of breast tumor subtypes: a) the genetic (and epigenetic) mutation model; b) the cell-origin model (Visvader JE, 2011).

Gene signatures

Patients stratification according to their clinical prognosis is a desirable goal in cancer treatment. Reliable predictions on the basis of gene signatures could support appropriate therapeutic strategy.

Gene signatures can complement classic prognostic factors to obtain more accurate prognostic information. The main premise of these emerging tests is that they simultaneously quantify the expression of multiple genes and combine the gene expression measurements into prediction scores that may predict clinical outcome more accurately than any of the genes alone.

The 70-gene signature (MammaPrint; Agendia, Amsterdam, The Netherlands) and the 21-gene signature (OncoType; Genomic Health, Redwood City, CA) are being used in selected patients with early ER^+ disease to identify those women that will be cured even if they do not receive adjuvant chemotherapy (van de Vijver MJ et al., 2002; Paik S et al., 2004). These signatures have been extensively studied and are widely used in Europe and in USA. Both the 70-gene and the 21-gene signatures have predictive, in addition to prognostic, value. This means that, in women allocated to high-risk groups, adjuvant chemotherapy significantly improves disease-free survival (*Fig. 18*).

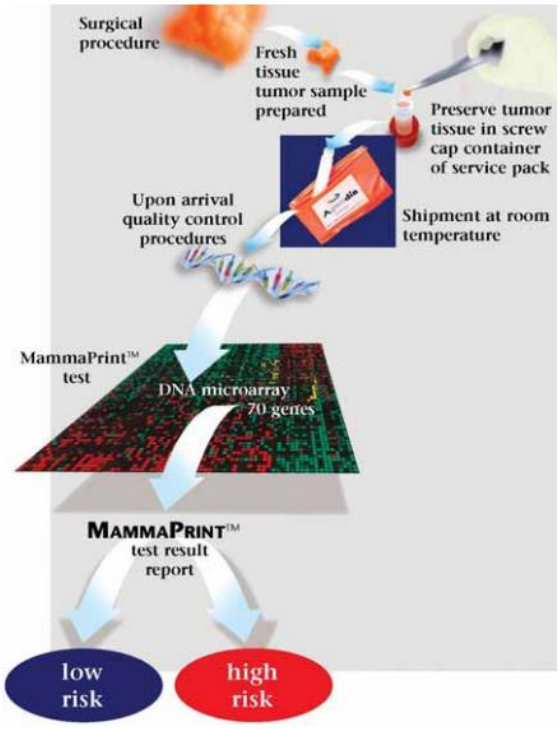

Figure 18. Commercial microarray products such as the Mammaprint and Oncotype DX (not shown) gene expression tests determine whether breast cancer is likely to recur and thus should be treated aggressively.

New emerging protein biomarkers in breast cancer

In the last years, the cancer research was aimed to improve the life quality of breast cancer patients. Unfortunatly, at the moment, there is no single treatment known for certain cure of breast cancer. A number of different types and forms of tumor markers exist, including: hormones, proteins, enzymes, glycoproteins, oncofetal antigens and receptors. Recently, other biomarkers are emerging to quantify the residual risk of patients and to indicate the potential value of additional treatment strategies.

✓ **Ki67**: Ki67, a proliferation marker, is a nuclear non histone protein associated with cellular proliferation, expressed in certain phases of the cell cycle namely S, G1, G2, and M phases, but is nonexisting in G0 (Gerdes J et al., 1984). The correlation of Ki67 and other biomarkers in invasive breast cancer has been studied intensively. In normal breast tissue, it was found that Ki-67 is also expressed at low levels (<3% of cells) in ER-negative cells, but not in ER-positive cells (Urruticoechea A et al., 2005). It was suggested also a correlation with HER-2, but this is not completely clear (Nicholson RI et al., 1993, Rudolph P et al., 1999).

The cell cycle represents the most important biological process controlling cell proliferation. Many oncogenes and suppressor genes encode proteins operating throughout the cell cycle, leading to eventually uncontrolled cell growth. Some cyclins for example behave like oncoproteins.

✓ **Cyclin D1** is a protooncogene that plays a critical role in G1 progression of the cell cycle. Its overexpression was found in many human cancers as a result of gene amplification or traslocations. High cyclin D1 expression statistically significantly correlate with lower tumor grade, estrogen and progesterone receptor positivity and lower proliferation activity in breast tumors and increased breast cancer specific survival and overall survival. Cyclin D1 expression has been shown in previous human breast cancer studies to correlate with positive ER status, the protein being predominantly expressed in the well-differentiated, lowgrade, slow-growing subtypes of breast cancer (Roy PG et al., 2006).

✓ **Cyclin E** is another G1 cyclin which can be expressed in many tumor cells and that acts as a positive regulator of cell cycle transition with peak levels of protein expression and enzymatic complex formation with cyclin-dependent kinase 2 in the G1 phase (Koff A et al., 1992). Altered expression of cyclin E protein as oncogene occurs in most of the breast tumor and increases with increase of grade and stage of the tumor, suggesting its potential as a new prognostic marker.

✓ Another group of proteins that is emerging as potentially important markers in multiple tumour types is the **S100** family. The S100 proteins are small acidic proteins (10–12 kDa) and

constitute the largest subfamily of the EF-hand calcium-binding proteins (25 members), involving in a large network of calcium-dependent, and independent protein–protein interactions. One reason of interest in this protein is because the majority of the S100 genes are clustered on a region of human chromosome 1q21 that is prone to genomic rearrangements. There is increasing evidence that altered expression of S100 family members is seen in many cancers including breast, lung, bladder, kidney, thyroid, gastric, prostate and oral cancers. S100 proteins are commonly up-regulated in tumours and this is often associated with tumour progression. S100 proteins are proposed to have intracellular and extracellular roles in the regulation of many diverse processes such as protein phosphorylation, cell growth and motility, cell-cycle regulation, transcription, differentiation and cell survival (*Fig. 19*).

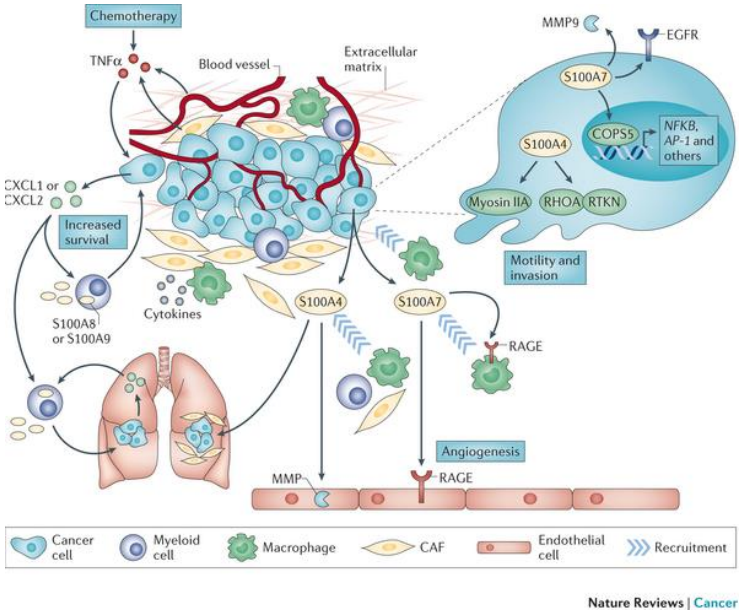

Figure 19. Intracellular and extracellular S100A4 and S100A7, and extracellular S100A8 and S100A9 mediate breast tumour progression and metastasis (Bresnick AR et al., 2015).

Several S100 members show altered expression levels in cancer cells compared to normal cells and are differentially expressed in various malignancies, according to types and stages of cancer (Zhang H et al., 2008; Wang G et al., 2008). Finally, a number of S100 proteins have been shown to interact with and to regulate various proteins involved in cancer and exert different effects on p53 activity (van Dieck J et al., 2009). Numerous members of the S100 protein family were screened contextually for through a large-scale proteomic approach, comparing proteomics among a large group of breast cancer patients, all diagnosed as ductal infiltrating carcinomas. Proteomics is presently the only system able to detect protein isoforms of potential

interest, which are not detectable by gene expression or immunohistochemical investigations. The results obtained strongly support the hypothesis that a significant deregulation of multiple S100 protein members is associated with breast cancer progression, and suggest that these proteins might act as potential prognostic factors for patient stratification. Qualitative analysis showed that some of the S100 protein members are ubiquitously expressed in all patients while others appeared more sporadic. Among the first, are: S100A2, S100A6, S100A11 and S100A13 (all isoforms, when present); the members with more or less sporadic appearance are: S100A8 (71%), S100A4 (57%) and S100A7 (51%, isoform a and 63%, isoform b). The quantitative evaluation showed that the expression levels of each S100 member was different among patients, but collectively, most of the S100 protein forms were statistically correlated. Moreover, it was investigated the prognostic potential of S100 proteins to predict distant metastatic relapse during a time lapse of three years from the surgical intervention. The most robust correlation with metastasis regarded primarily the protein S100A4, and secondly the protein S100A7 (Cancemi P et al., 2010).

Colorectal cancer

Colorectal cancer (CRC) is the third cause of cancer in men (10% of total) and the second cause of cancer in women after breast cancer (9.4% of total). Although the aetiology is not known, CRC is considered a multifactorial disease, an important role being attributed to the impact of environmental factors on a genetically prone land. Hereditary predisposition is considered an important factor in colorectal carcinogenesis, although 80% of colorectal neoplasms occur in the absence of a family history of CRC (Lynch HT et al., 2003).

A hypercaloric diet, high in fat and low in dietary fiber is positively correlated with the CRC occurrence. Obesity, western diet and lack of physical activity are common risk factors for both type 2 diabetes mellitus and for CRC (Dahm CC et al., 2010).

Likely breast cancer, colon cancer is a genetically heterogeneous disease, involving genetic and epigenetic alterations that transform normal colonic epithelium into cancer.

(*Tab. 1***)**.

Cancer hallmarks	Examples of involving factors in CRC
Growth signal autonomy	EGFR, KRAS, BRAF
Insensitivity to antiproliferative signals	P53, PTEN, APC
Unlimited replicative potential	TERT
Angiogenesis	VEGF
Escaping apoptosis	P53, MLH1
Invasion and metastasis	Cdc-42, RhoA GTPase
Reprogramming of cell metabolism	PI3K, AKT, c-MYC
Evading immune destruction	IL-8

PTEN = Phosphatase and tensin homolog; TERT = telomerase reverse transcriptase; VEGF = vascular endothelial growth factor; IL-8 = interleukin-8.

Table 1. Cancer hallmarks in relation to colorectal cancer.

Most cases of colorectal cancer (CRC) are sporadic and resulting from the accumulation of somatic genetic aberrations associated with a variety of environmental risk factors (Cunningham D et al., 2010; Søreide K et al., 2009). The remaining proportion of cases involve a familial genetic component. The genetic mutations responsible for sporadic colorectal cancer (not related to mutations genetically acquired) are the same that characterize the hereditary forms. The 1-5 % of inherited forms consists of polyposis forms (FAP, Familial Adenomatous Polyposis syndrome) and not polyposis forms (HNPCC, Hereditary Non Polyposis Colorectal Cancer or Lynch syndrome). Furthermore, 10% is characterized by other types of familial syndromes and 1% by the presence of chronic inflammation IBD (Inflammatory Bowel Disease), such as Ulcerative colitis and Crohn's disease. Numerous genetic aberrations accumulate including the inactivation of the adenomatous polyposis coli tumour suppressor

gene (APC) and activation of oncogenes such as K-*ras*, deletion of chromosome 18q and amplification of 20q (Pritchard CC et al. 2011). Cumulatively these genetic changes afford the tumour anti-apoptotic, pro-angiogenic and proliferative properties.

Molecular classification of colorectal cancer

Most adenomas in subjects with Lynch syndrome show loss of expression of a DNA mismatch repair protein (usually MLH1 or MSH2) and display a form of genetic instability characterized by the accumulation of numerous mutations, which specifically target repetitive sequences of DNA. These sequences occur most frequently in non-encoding microsatellite regions, hence the term *microsatellite instability* (MSI). After the inactivation of a DNA mismatch repair gene, it was possible detect mutations at a high frequency throughout the genome (*MSI-high*, MSI-H). CRCs with MSI have a diploid DNA content with few losses or gains of chromosomal regions. Genetic instability operate therefore on two levels, implicating two major pathways in colorectal carcinogenesis (*Fig. 20*).

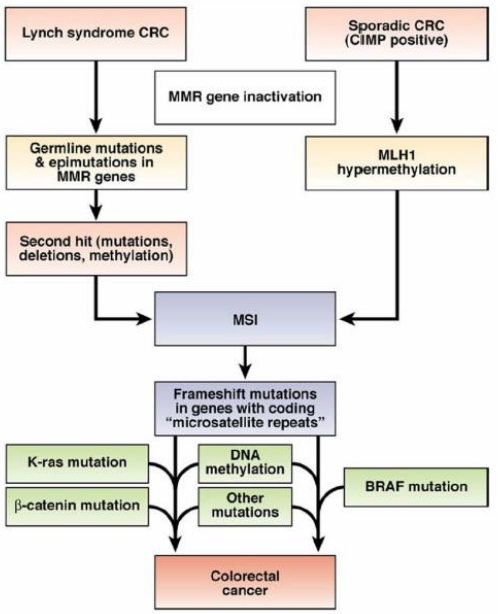

Figure 20. Two molecular pathways responsible for the development of CRC with MSI.

One is the *chromosomal instability* (CIN) pathway (adenoma–carcinoma sequence), affecting whole chromosomes or parts of chromosomes, in particular it is characterized by allelic losses on chromosome 5q (APC), 17p (p53), and 18q (DCC/ SMAD4), responsible for 85% of sporadic CRC; the other is a pathway that involves *microsatellite instability* (MSI), affecting DNA sequences, responsible for 15% of CRC. Recent studies have suggested that among these pathways there is some cross talk and these forms of instability are mutually exclusive, so that CRCs with CIN will be MS stable (MSS). A subset of non-MSI-H CRC shows MSI-L (*MSI-*

low). MSI-L CRCs were distinguished from both MSI-H and MSS CRCs on the basis of gene expression profiles and also differ from MSS CRCs in showing frequent instability in the trinucleotide repeat region of RAS-induced senescence 1 (RIS1).

Considering the underlying types of genetic instability and the presence of DNA methylation, physicians suggest five molecular subtypes of CRC (Jass JR, 2007):

1. CIMP-high, methylation of MLH1, BRAF mutation, chromosomally stable, MSI-H, origin in serrated polyps, known generally as sporadic MSI-H (12%).
2. CIMP-high, partial methylation of MLH1, BRAF mutation, chromosomally stable, MSS or MSI-L, origin in serrated polyps (8%).
3. CIMP-low, KRAS mutation, MGMT methylation, chromosomal instability, MSS or MSI-L, origin in adenomas or serrated polyps (20%).
4. CIMP-negative, chromosomal instability, mainly MSS, origin in adenomas (may be sporadic, FAP associated or MUTYH (formerly MYH) polyposis associated) (57%).
5. Lynch syndrome, CIMP-negative, BRAF mutation negative, chromosomally stable, MSI-H, origin in adenomas (3%) (described also as familial MSI-H CRC).

These groups may be conceived as completing a circle rather than representing the ends of a spectrum (*Fig. 21*). Overlaps between the groups are not excluded. For example, K-*ras* rather than BRAF mutation may occasionally occur in association with CIMP-high.

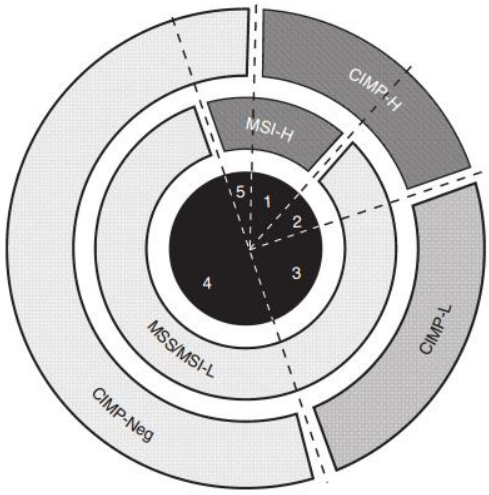

Figure 21. Derivation of molecular colorectal cancer groups 1–5 based on CpG island methylator phenotype (CIMP) status (H, high; L, low; Neg, negative) and DNA microsatellite instability (MSI) status (H, high; L, low; S, stable).

Clinical and morphological classification of colorectal cancer

It was demonstrated that each of the described subtypes correlates with particular morphologies, but it is not necessarily possible to recognize each group on the basis of morphological features alone. Certainly, primary basis for the classification of CRC is therefore molecular. Macroscopic appearance of CRC is influenced by evolutionary phase in the moment of discovery, several aspects being described: polypoid form, ulcero-vegetant, ulcerative and infiltrative form. The two major histological types of CRC tumors consist of epithelial and mesenchymal tumors (Fleming M et al., 2012). For uniformity and consistency in reporting, internationally accepted and used classification is that proposed by the WHO: adenocarcinoma, medullary carcinoma, colloid adenocarcinoma, "signet ring" squamous cell carcinoma, epidermoid carcinoma, adenosquamos, small cell carcinoma, undifferentiated carcinoma and other types (Puppa G et al. 2010).

Gene signatures

The CRC heterogeneity is considered to be one of the factors responsible for the considerable variability in treatment response among patients with the same stage of CRC. This emphasises the clear requirement to have defined methods to classify colorectal. As previously reported, a single gene mutation alone cannot explain the poor prognosis of colorectal cancer (CRC) that results from the progressive accumulation of genetic and epigenetic alterations that lead to cellular transformation and tumor progression. Currently, diagnosis, prognosis, and treatment decisions for CRC are based on the clinic pathologic analysis of the CRC tissue. The tumor stage, histological classification, presence or absence of lymph node and/or distant metastasis, and preoperative serum carcinoembryonic antigen levels have all been recognized as prognostic factors. The available diagnostic platforms include multigene-based assays and gene microarrays that may provide reliable information on the prognosis of a patient and/or their sensitivity to treatment. For these reasons, much work has been placed on the identification of novel molecular prognostic factors that alone or in combination with clinic pathologic factors may improve the prediction of clinical outcome and determine the appropriate therapeutic approach.

In a recent study (Shin IY et al., 2014), it was established a correlation between the expressions of six proteins, recently cited as prognostic factors in patients with CRC, and clinicopathologic factors. The examined proteins were Cathepsin D, TP53, COX-2, EGFR, c-erbB-2 and Ki-67. Wang and collaborators (2015) developed a 31-gene expression signature for the prediction of

relapse among patients with stage II/III CRC based on the combined use of gene expression profiling and TLDA (Taqman low-density array) analysis. The identification of 31 genes that are closely associated with outcomes in patients with CRC has clinical implications. Patients who have a higher risk of relapse could benefit from adjuvant therapy and those who have lower risk could be spared what may be unnecessary treatment.

There are two promising prognostic tests based on the expression levels of different gene panels: ColoPrint, a microarray-based expression profile that measures the expression levels of 18 genes, predicting accurately the risk of relapse in stage II colon cancer patients, and Oncotype DX, that includes 12 genes, consisting of 7 recurrence risk genes and 5 reference genes (Tan IB, Tan P, 2011). In an another previous study, an 18-gene signature (CD36, DHRS13, DUSP2, FAM198B, FKBP5, GLT25D2, GZMB, IL1B, ITGAM, ITPRIPL2, MYBL1, NEAT1, NUDT16, P2RY10, PDE4D, PDZK1IP1, SH2D2A, and VSIG10) was identified that could accurately differentiate between peripheral blood samples of CRC patients and controls. These results open an opportunity for the diagnosis and early detection of CRC (Xu Y et al., 2013).

Colorectal recurrence

Curative surgery is the best treatment option for patients with CRC, but tumor recurrence after resection, both local and distant, is associated with a high risk of cancer-related death. At the time of initial diagnosis, approximately two-thirds of patients with CRC undergo resection with curative intent, but 30%–50% of these patients relapse and die of their disease (Abulafi AM et al., 1994).

While some studies have defined early recurrence as being within the first 2 years after surgery, others have defined it as being within the first year or within the first 3 years after curative surgery (Cho YB et al., 2007). A number of these studies analyzed risk factors associated with recurrence or the survival period after recurrence. Approximately 60%–80% of recurrences develop within the first 2 years after surgery and cases of recurrence 5 years after surgery are rare.

Moreover, it was shown that the resection of hepatic colorectal metastases may produce long-term survival and cure (Fong Y et al., 1999). Seven factors were found to be significant and independent predictors of poor long-term outcome by multivariate analysis: positive margin, extrahepatic disease, node-positive primary, disease-free interval from primary to metastases <12 months, number of hepatic tumors >1, largest hepatic tumor >5 cm, and CEA level >200 ng/ml. Patients with up to two criteria can have a favourable outcome. Patients with three, four,

or five criteria should be considered for experimental adjuvant trials. Studies of preoperative staging techniques or of adjuvant therapies should consider using such a score for stratification of patients.

Identification of prognostic factors for recurrence might improve survival rates in patients with CRC after curative resection, as this would allow early detection and treatment. Previous studies have identified a number of factors including tumor stage, depth of invasion, the degree of vascular or perineural invasion, and serum levels of CEA and CA 19-9 as having statistically significant association with CRC recurrence. Using these factors as predictors of the recurrence interval, could further help in identifying high-risk patients and in making decisions regarding postoperative therapy. An elevated postoperative CA 19-9 level, venous invasion, and advanced N stage were found to be significant risk factors for early recurrence of colorectal cancer (Ryuk JP et al., 2014).

New emerging protein biomarkers in colorectal cancer

With the limited clinical applicability of CEA and CA19-9, additional candidate proteins have been proposed as CRC diagnostic protein markers. A single protein marker, TIMP-1, is currently being tested in a large prospective study, detecting CRC with 95% specificity (Holten-Andersen MN et al., 2002). The detection of circulating tumor-associated auto-antigens and the use of commercial protein arrays have facilitated the identification of proteins that are differentially expressed and circulating in CRC patient sera. Babel I et al., (2009) reported 43 proteins that could distinguish between CRC patients and healthy controls, developing a diagnostic ELISA using two of these proteins, MAPKAPK3 and ACVR2B. Three additional colon-specific antigens, CCSA-2, CCSA-3, and CCSA-4, were identified by proteomic analysis of structural proteins. Other putative diagnostic markers that have been evaluated are the matrix MMP 9, S100A8, and S100A9 (Kim MS et al., 2009; Hurst NG et al., 2007).

A number of recent genome-wide (GW) gene expression studies have successfully identified several distinct subtypes of CRC that exhibit heterogeneous biological and clinical behaviours (Cancer Genome Atlas Network, 2012; Marisa L et al., 2013; Sadanandam A et al., 2013), implying that there may be several prognostic signatures for CRC, each of which corresponds to different tumour behaviour. Unfortunately, few surrogate signatures have been shown to be clinically feasible, particularly as prognostic markers.

Recently colorectal adenomas, in particular, villous and tubulovillous adenomas as well as cancers, have been reported to show CIMP (Takayama T et al., 2006). Cancers demonstrating methylation and silencing of multiple genes are described as CIMP positive. The most frequent genes target of hypermethylation and silencing in human colorectal cancers are hMLH1 gene (which leads to the MSI-H phenotype), $p16^{INK4A}$, MGMT, estrogen receptor (ER), APC, and COX-2.

In addition to the predictive and prognostic biomarkers recently recommended and published by the European group for Tumor Markers (EGTM) for use in CRC, some of these biomarkers for CRC are considered to be "*emerging biomarkers*" (*Fig. 22*), such as K-*ras G13D* gene mutation, B-raf murine sarcoma viral oncogene homolog B (*B-raf*), *V600E* gene mutation, cycloxygenase 2 (COX–2), VEGF, microRNAs, besides microsatellite instability (MSI), CpG island methylator phenotype (CIMP) and chromosomal instability (CIN), which were already discussed previously (Kalia M, 2015). These are currently used such criteria clearly need to be further consolidated for efficient responses to individualized chemotherapy (Marisa L et al., 2013; Oh DY et al., 2012).

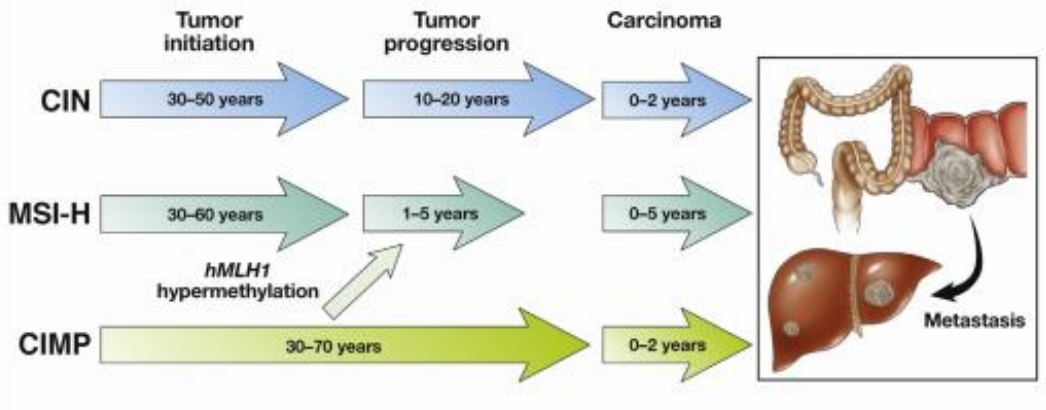

Figure 22. Timeline for sporadic CRC pathogenesis based on the mean age of CRC for each type.

✓ The **K-*ras*** protooncogene encodes a small G protein (guanosine triphosphate/guanosine diphosphate binding protein) downstream of EGFR in the PI3K/PTEN/AKT and RAF/MEK/ERK signaling pathways, transducing extracellular signals from the EGFR to the nucleus. Detection of K-*ras* mutations is currently the most utilized predictive marker for response to the anti-EGFR antibody-based therapies in colorectal cancer. Approximately 40% of colon cancers are positive for mutations in K-*ras* in codons 12, 13, 61 and are resistant to anti-EGFR monoclonal antibodies (cetuximab and panitumumab). A diagnostic kit was recently approved to determine whether patients with advanced colorectal cancer have a wild K-*ras* gene, indicating whether they would respond to cetuximab or pantiumumab (Chung C and Christianson M, 2014). Recent studies have reported persuasive evidence that, in addition to K-*ras*, mutations in N-*ras* predict nonresponse to anti-EGFR therapy. These studies support the use of extended RAS (K-*ras* and N-*ras*) mutational analyses as negative predictive markers for anti-EGFR therapy in metastatic CRC (mCRC).

✓ **B-raf** is considered an emerging biomarker of negative response to K-*ras* and a prognostic biomarker for poor prognosis in patients in initial therapy. It belongs to the family serine/threonine kinase and it is the immediate downstream effector of K-*ras* in the Ras/Raf/MAPK signaling pathway. Mutations in the B-raf gene have been associated with CRC development and found in 10-20% of colorectal cancers.

✓ **COX** is a key enzyme in the conversion of arachidonic acid to prostaglandins, and two isoforms of COX, namely COX-1 and COX-2, have been identified. COX-2, in particular, is induced by a variety of agents including cytokines, hormones, growth factors, and tumour promoters, and its expression is elevated in inflammatory cells and sites of inflammation (Xie W and Herschman HR, 1995). Recently multiple studies have shown that COX- 2 is expressed at high levels in 80–90% of colorectal adenocarcinomas. Another recent report demonstrated

that human colon cancer (Caco-2) cells permanently transfected with a COX-2 expression vector, acquired increased invasiveness, with amplified activation of matrix metalloproteinase-2 (MMP-2) and increased RNA level of membrane-type matrix metalloproteinase-1. COX-2 overexpression in colorectal cancer did not correlate with venous permeation, but with increased haematogenous metastasis formation (Tomozawa S et al., 2000).

✓ **VEGF** (vascular endothelial growth factor) is the predominant angiogenic factor in CRC. VEGFs are soluble growth factors that can be secreted by tumor cells. The VEGF family of growth factors is composed of seven members (VEGF-A,B,C,D,E, placental growth factor PlGF-1 and 2), with VEGF-A being the most prominent mediator of tumor angiogenesis. The intracellular domain of VEGFR contains catalytic tyrosine kinase domains that, when activated, initiate a signaling cascade that results in endothelial cell survival, proliferation, migration, differentiation, and increased vascular permeability.

✓ Various dysregulated **miRNAs** are associated with CRC development, progression and therapeutic response. Studies examining miRNA expression in CRC have shown a total of 362 differentially expressed miRNAs when compared to noncancerous tissue; 242 were upregulated and 120 were downregulated (Ma Y et al., 2011). Evidence suggests that plasma and faecal miRNAs could potentially serve as non-invasive markers for CRC detection. One study reported that a 69-gene miRNA signature panel in plasma could differentiate between CRC and healthy patients (Chen X et al., 2008) and another study reported that a panel of eight miRNAs (miR-532-3p, miR-331, miR-331, miR195, miR-17, miR142-3p, miR15b, miR532, and miR-652) could accurately detect polyps. Moreover, the expression levels of miR21 has been examined in several studies: miR21 correlates with disease recurrence and mortality suggesting that it could be evaluated as a prognostic marker in the future (Menéndez P et al., 2013). To determine if miRNA markers can be implemented as screening, diagnostic, and/or prognostic tools in the future, it is necessary to evaluate in many independent studies, new miRNA candidate markers, both individually and in panels.

New markers of metastasis

In the invasion and metastasis steps of colorectal cancers, many gene alterations have been identified as being involved in proteolysis of the local extracellular matrix (ECM), adhesion, angiogenesis, dissemination and cell growth. The introduction of new cytotoxic and targeted agents for patients with metastatic CRC (mCRC) has improved overall survival (OS) rates. Many potential predictive biomarkers for mCRC have been reported using a variety of molecular data types (*Tab. 2*). Other prognostic markers include the expression levels of Thymidylate Synthase (**TS**) and Excision Repair Cross-Complementation Group 1 (**ERCC1**); however, their demonstrated clinical value has been limited. TS is an enzyme responsible for the generation of deoxythymidine triphosphate (dTMP), which is needed for the formation of the nucleic acid thymine; ERCC1 is involved in the nucleotide excision and repair pathway, a part of the cellular response to DNA damage. ERCC1 and TS expression levels have been previously described as potentially promising biomarkers in mCRC (Shirota Y et al., 2001), identifing a population with poor prognosis (high ERCC1/TS expression) as well as a population with a remarkably high response rate to FOLFOX chemotherapy (low ERCC1/TS expression). According to the authors, ERCC1 and TS profiling could help physicians better manage patients with metastatic colorectal cancer, individualizing and optimizing therapy for subsequent interventions such as surgical removal of metastatic tumors.

Genes	Characters of gene products
Genes for proteolysis	
MMP-7 (matrylisin)	Digestion of fibronectin, laminin, collagen IV, and protoglycans
MMP-2, -9 (gelatinases)	Digestion of gelatins and collagen IV
MMP-1, -8, -13 (collagenases)	Digestion of collagens I, II, III, IV, VI, IX, X, and XI
MMP-3 (stromelysin-1)	Digestion of fibronectin and laminin
TIMP-1	Tissue inhibitors of MMP
uPAR	Activation of plasmin-plasminogen system
Genes for adhesion	
Integrins	Binding to laminin, collagen, fibronectin, and vitronectin
Cadherins	Cell–cell adhesion
CD44	Binding to hyaluronan
CEA	Binding to a receptor on Kupffer cells
Genes for angiogenesis	
VEGF	Angiogenesis, MMP-9 induction
PD-ECGF	Angiogenesis
Genes for cell survival and others	
TRAIL-R	Binding to TRAIL to induce apoptosis
CXCR4	Binding to SDF-1 to enhance migration and invasiveness
Drg-1	Cell differentiation
c-Met	Binding to HGF to enhance motility and invasiveness

Table 2. Genes related to invasion and metastasis in colorectal cancers. (Takayama T et al., 2006).

Currently, it was found as a possible marker of metastasis the expression of **Cathepsin D** (CATD). CATD is a lysosomal aspartyl endopeptidase, present in most mammalian cells and essential for regulating cell growth and tissue homeostasis of colon epithelium. Overexpression of this acid protease has been associated with the progression of many human cancers, including gastric cancer, melanoma and ovarian cancer and with poor prognosis in breast cancer patients.

Cathepsin D degrades many intracellular and endocytosed proteins as well as ECM (extracellular matrix) proteins and proteins of the basal epithelium. Cathepsin D can participate in limited proteolysis and it activates cysteine procathepsins B and L and also degrades and makes inactive their active forms. It has been shown that human cathepsin D stimulates tumour growth by acting – directly or indirectly – as a mitogenic factor on cancer cells independently of its catalytic activity (Berchem G et al., 2002). In normal cells, these cathepsins are regulated at every level of their biosynthesis, including transcription, posttranscriptional processing, translation, post-translational processing and trafficking, thus maintaining their normal function in cell metabolism. In tumour cells, misregulation of this cathepsin at one or more of these levels results in increased mRNA and protein expression, increased activity and altered intracellular distribution. However, the correlation between CATD expression in CRCA and specific clinicopathologic factors is controversial. In the majority of the investigations, CATD expression was not correlated with stage. Alternatively, CATD expression in tumor stromal cells has been reported to be significantly correlated with lymphatic invasion and lymph node metastasis (Kirana C et al., 2012). Recently some authors have reported using laser microdissection that the expression of cathepsin D in colorectal cancer in the liver metastasis is greater than the region of the invasion front, which in turn presents a greater expression of cathepsin D respect to the heart of the tumor. Moreover, CATD was correlated with a poor prognosis in terms of the cancer-free survival and the colorectal cancer specific survival. Patients with cathepsin D positivity had a poorer outcome than patients who were cathepsin D-negative. Thus, cathepsin D may provide an indicator for appropriate intensive follow-up and adjuvant chemotherapy.

The proteomic approach: an emerging technology for cancer

Proteomics is the science that analyzes the proteome, i.e. the set of protein complement expressed from the genome in a biological system at a given point in time. The term "proteome" was coined in 1994 by MR Wilkins to define the protein complement encoded by a genome. Proteome is in a constant state of dynamic space-time: the cells of the same organism, distributed in different tissues, are characterized by distinct proteomic assets, rising from differential gene transcription; and proteomic profiles undergo modulations over time in response to stimuli from particular physiological or pathological conditions. Now proteomics is advised as a multidisciplinary integration of all biochemical, bioanalytical and bioinformatics methods, used for the study of the proteome (Wasinger VC et al., 1995; Wilkins MR et al., 1996) and it quickly became the object of ambitious international initiatives, including those undertaken by the HUPO (Human Proteome Organization), founded in 2001. Proteomic analysis can complement the information obtained from the genetic sequence and from the study of the transcriptome. The determination of the gene sequence, in fact, does not allow the identification of post-translational modifications to which the proteins undergo, much less protein interactions through which each protein performs its function. The study of the transcriptome, by contrast, provides direct information on the levels of gene expression, but does not provide information on the instant in which a particular protein is synthesized, since not all mRNAs are translated synchronously. Finally, the levels of each mRNA present in the cell are not always proportional to the content and/or activity of the corresponding protein. The characterization of the proteome of different cell types is therefore a key step to understanding both the functioning of the genome, since the mechanisms by which the alteration of genomic cause the occurrence of pathological states, including cancer. Is clear then the importance of a comprehensive approach that allow to correlate the presence, absence or the different level of expression of a protein to a particular time or physiological condition.

There are two types of proteomic approach: expression proteomics and functional proteomics. The *expression proteomics* is the study of the qualitative and quantitative proteomic profile of a cell at a given time, in order to characterize the phenotype, making it possible, for example, the comparison between the proteome of healthy and cancerous cells and the identification of diagnostic, prognostic and therapeutic markers. The *functional proteomics*, however, studies the functions of expressed proteins, the signal transduction pathways in which the expressed proteins are involved and includes the study of interactions between proteins (*interactomics*), the study of interactions between a protein and its substrates (*metabolomics*) and the study of

specific functions of proteins. The rapid development of proteomics has depended upon substantial technological advances in many specific areas including gel-based or gel-free protein separation and identification techniques (shotgun proteomics), protein chips (SELDI-MS, protein/tissue/antibody arrays), mass spectrometry (MS), and bioinformatics. Currently, large scale studies of protein complexes are emerging that show how the cell organizes to deliver function at the molecular level (system biology).

Intelligent therapeutic systems

Although scientific research in oncology has undergone a considerable evolution in the study of novel tumor markers, it is still difficult to associate a specific marker to a type of cancer cell and then it can be used in screening for different types of cancers; moreover it is clear what the difficulties found today in treating cancer with chemotherapy, drugs that, although they may kill cancer cells, because of their low specificity, generally also damage healthy tissue, with severe side effects that affect the patient.

For these reasons, in recent years, controlled **drug delivery systems** (DDS) have attracted increasing attention (Qiu Y and Park K, 2001; Jeong B et al., 2002) and numerous drugs designed to target various cellular processes have emerged, creating a demand for the development of intelligent drug delivery systems that can sense and respond directly to pathophysiological conditions. Drug delivery is an emerging field focused on targeting drugs or genes to a desirable group of cells and its goal is to transport proper amounts of drugs to the desirable sites (mainly tumors cells) while minimizing unwanted side effects of the drugs on other tissues (Tran PA et al., 2009). Use of smart drug delivery systems such as micro- and nanoparticles, could allow to maximize the efficacy of therapeutic treatments for their ability to act directly on target cells. To meet these necessities, researchers must be able to interface synthetic and hybrid materials with dynamic biological systems on the micro- and nano-length scale. Stimuli responsive biomaterials are very promising carriers for the development of advanced intelligent therapeutics (Moore MC and Peppas NA, 2009).

Metal nanoparticles (MeNPs) have been used in various biomedical applications including probes for electron microscopy to visualize cellular components, drug delivery (vehicle for delivering drugs, proteins, peptides, plasmids, DNAs, etc.), detection, diagnosis and therapy (targeted and non-targeted) (Bhattacharya R and Mukherjee P, 2008; Goldman ER et al., 2004; Alivisatos AP et al., 2005; Adeli M et al., 2011).

The NPs can be linked simultaneously to anticancer drugs and molecules able to function as receptor ligands. Through the interaction of these ligands with the receptors of the cell membrane, NPs can enter specifically in certain cell populations without hitting undesirable districts. It has been shown that even in the absence of receptor-ligand interactions, neoplastic cells internalize in greater quantity the nanoparticles, thanks to the presence of pores and/or defects on their membrane. Metal nanoparticles such as with **silver** have many optical and electronic properties, derived from their size and composition (Jana NR et al., 2001). To be

considered as such, the metal nanoparticles should have dimensions between 5 nm and 500 nm (Loo C et al., 2005).

The scientific literature points to the wide use of silver in numerous applications. Historically, silver compounds and ions have been extensively used for both hygienic and healing purposes (Chen X and Schluesener HJ, 2008). However, over time, the use of silver compounds and ions has faded as an anti-infection agent due to the advent of antibiotics and other disinfectants and the poorly understood mechanisms of their toxic effects.

It is well established that silver nanoparticles are known for their strong antibacterial effects for a wide array of organisms (e.g., viruses, bacteria, fungi). Therefore, silver nanoparticles in the nanometer range have been routinely used to prevent the attack of a broad spectrum of microorganisms in medical devices and supplies such as wound dressings, scaffold, skin donation, recipient sites, sterilized materials in hospitals, medical catheters, contraceptive devices, surgical instruments, bone prostheses, artificial teeth, and bone coating. Silver particles are also used in medicine to reduce infection in burn treatment, arthroplasty, etc. One can also observe their wide use in consumer products such as cosmetics, lotions, creams, toothpastes, laundry detergents, soaps, surface cleaners, room sprays, toys, antimicrobial paints, home appliances (e.g., washing machines, air and water filters), automotive upholstery, shoe insoles, brooms, food storage containers, and textiles (Navaladian S et al, 2008; Thomas CD et al., 2006).

In general, silver nanoparticles are synthesized using various techniques resulting in different shapes and sizes for use in numerous applications. The synthesis techniques are categorized into top-down and bottom-up approaches (del Rocío Balaguera-Gelves M et al, 2006). Silver nanoparticles are often synthesized via reduction of AgNO3, dissolution in water, and utilization of reductants also acting as capping or stabilizing agents for the control of particle size to ensure a relatively stable suspension. The solvents and reducing agents used in these processes affect the physical and morphological characteristics of manufactured silver nanoparticles. In turn, these specific characteristics will influence the fate, transport and toxicity of nanoparticles in the environment. The commonly used synthesis methods usually produce negatively charged silver nanoparticles; for example, the use of sodium citrate as a reducing agent generates a negatively charged silver nanoparticle which may behave differently than a positively charged silver nanoparticle generated via branched polyethyleneimine (BPEI) (Tan S et al., 2007).

It has been shown that silver nanoparticles with 15 nm diameters had the highest toxic effect on rats'alveolar macrophages in comparison to larger nanoparticles (i.e., 30 to 55 nm) (Cataleya C, 2006). This trend is most likely the result of increased surface reactive area of silver nanoparticles and the comparable size of particle to protein in biological cells. Silver nanoparticles with 1-10 nm size demonstrated interaction with HIV by inhibiting the virus from binding to the host cells. Silver nanoparticles may attach to the surface of the cell membrane and disturb its permeability properties, possibly affecting respiration in aerobes. The binding of the particles to bacteria may depend on the surface area available for interaction. Smaller particles, possessing larger surface area to volume ratio, will be more bactericidal than larger particles (Tolaymata TM et al., 2010).

Globally, AgNPs exhibit low toxicity to mammalian cells and the safety and efficacy of using metal nanoparticles is debatable among scientists. For example, recently, it was shown that alga-mediated synthesis of metal nanoparticles may be considered to develop innovative, safety, and low-cost tools in the fight against the dengue virus, serotype DEN-2, and its vector *A. aegypti*, with little cytotoxicity on mammalian cells (Murugan K et al., 2015). In another study, it was investigated the metabolic behavior and toxicity of AgNPs in comparison to silver nitrate (AgNO3) both in vivo and in vitro (Arai Y et al., 2015), injecting into the mouse lung AgNPs (20 nm diameter) suspended in 1% albumin solution or $AgNO_3$ solution. It was found that 4h after administration, less than 1% of the initial dose of AgNPs and more than 7% of the initial dose of $AgNO_3$ was recovered in the liver, suggesting that the ionic form of silver was absorbed by the lung tissue and entered the systemic circulation more efficiently than AgNPs. In the in vitro study, $AgNO_3$ was more cytotoxic than 20, 60, or 100 nm diameter AgNPs in a mouse macrophage cell line (J774.1), suggesting that AgNPs gradually dissolved in the macrophages with insignificant inflammatory stimulation in the mouse lung compared to $AgNO_3$. Nowadays, several microorganisms have been explored as potential cell-factories for both intra- and extracellular synthesis of nanoparticles of various metals.

Production of AgNPs-EPS

In this work, silver nanoparticles (AgNPs) were previously biosynthesized by Klebsiella oxytoca DSM29614 (KO), ex BAS-10, isolated from a mining area rich in toxic metals. Klebsiella oxytoca is a ubiquitous Gram negative, facultative anaerobic. This strain can ferment Fe(III)-citrate under anaerobic conditions, in addition to usual Na-citrate, giving acetic acid and CO_2 and producing a specific exopolysaccharide (EPS), which binds Fe (III) (*Fig. 23*).

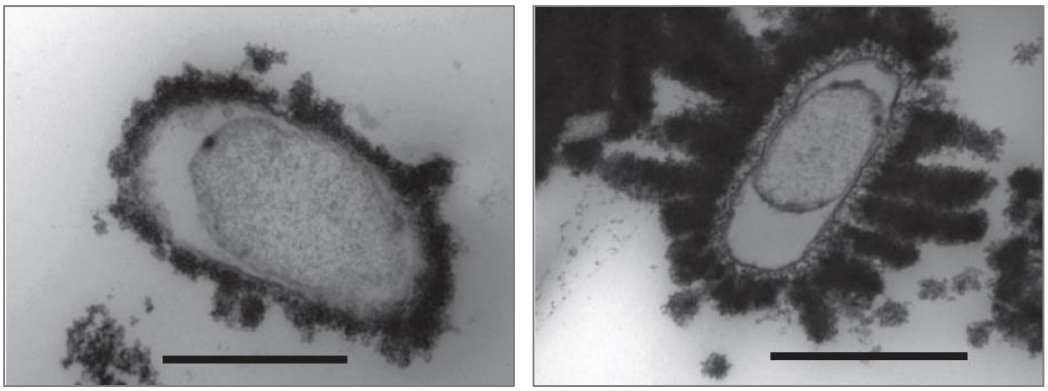

Figure 23. TEM observations of KO growing anaerobically in FeC medium, with electron dense extrusion from wall. Bar 1µm.

The production of Fe (III)-EPS under anaerobic conditions is a strategy for the strain to survive in pyrite mine drainages and other acidic conditions (Baldi F et al., 2009). KO-EPSs are high-molecular-weight sugar polymers produced by bacterial cells, with a peculiar sugar composition containing glucuronic acid (28.6%), galactose (14.3%) e high amounts of rhamnose (57.1%), able to bind metals and protect cells from environmental stress. The strong Fe (III) binding of EPS and its sugar composition suggests several applications in all fields were iron-ligands are used.

Recently, Battistel D et al. (2015), treating KO cultures with $AgNO_3$ under aerobic or anaerobic, produced silver nanoparticles embedded in EPS (AgNPs-EPS), containing different amounts of Ag(0) and Ag(1) forms (*Fig. 24)*. The metal binding properties of KO-EPS suggest a potential role as antibacterial and in cancer therapy; in fact, metal ion up-taking into bacterial cells usually causes generation of reactive oxygen species and negatively affects proliferation. Concerning tumor suppression, although different metals can promote solid tumors, on the other hand several evidences prove possible applications of metal ions in solid tumors as inhibitory chemotherapeutics. In addition, metal-EPSs could be used for drug delivery as nanoparticles able to limit the cytotoxicity.

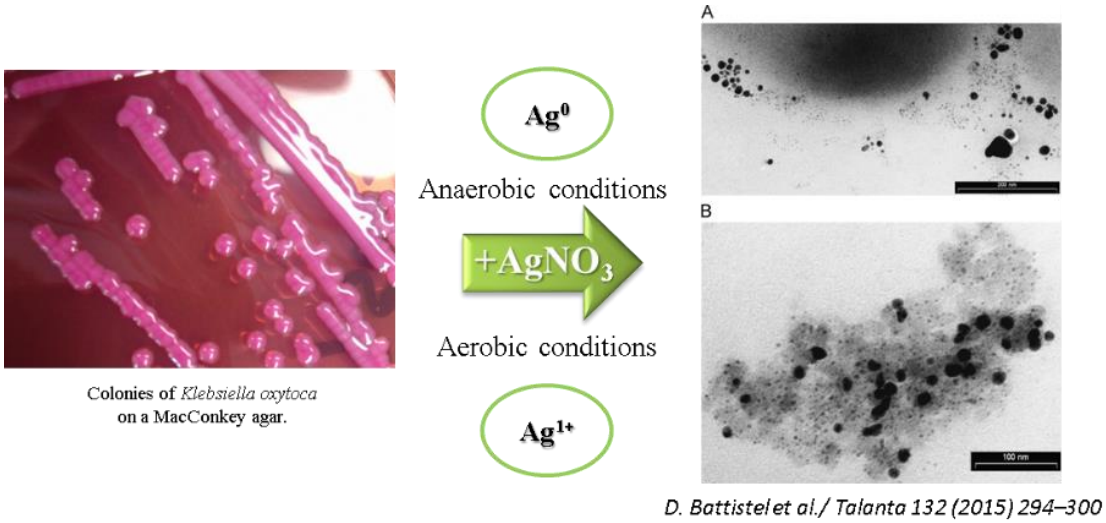

Figure 24. Schematized view of the AgNPs production and TEM micrographs in aerobic and anaerobic conditions.

Aerobic and anaerobic AgNPs-EPS were prepared from a suspension containing KO cells in glycerol and nutrient broth, and then inoculated in a chloride-free NAC medium. The chloride-free NAC medium pH 7.6, used for cell cultures, contained sodium hydrogen carbonate, ammonium nitrate, magnesium sulphate heptahydrate, sodium di hydrogen phosphate, potassium acetate and sodium citrate (Baldi F et al., 2011). The KO cultures were grown both in aerobic and anaerobic conditions, at a controlled temperature of 30°C. Aerobic conditions were ensured by stirring the cultures with an orbital stirrer under air-exposed media. For the anaerobic growth, the cultures were placed in a Pyrex bottle that had been previously saturated with nitrogen, then sealed and maintained under nitrogen blanket. At stationary phase of growth, $AgNO_3$ was added to both types of KO cultures. These were left for 24-48 hours, till the metal-enriched polysaccharide flocculated in the bottom of the flask. AgNPs-EPS, obtained in both aerobic and anaerobic conditions, were separated by centrifugation and treated with cooled ethanol (kept at 5°C overnight). Then the colloidal materials were dried out under vacuum and grinded in a mortar. Investigations on the AgNPs-EPS size and shape were made by transmission electron microscopy (TEM), while the relative abundance of Ag(0) or Ag(1) into AgNPs-EPS was established by scanning electrochemical microscopy (SECM) and voltammetric experiments.

AIM OF THE STUDY

Proteomics represent an attractive approach to study complex diseases, including cancer. The purposes of studying the proteome in relation to cancer can be several, but there are two main starting points: to better understanding cancer biology and to identify cancer biomarkers. Clinical proteomics has focused on diagnostic, prognostic and predictive biomarker discovery. The analysis, comparison, and quantification of protein modulations is particularly useful because the signaling pathways mediated by proteins control the majority of cellular events.

The aim of this thesis was to perform extensive studies on cancer specimens (breast and colon), in order to generate a different signature able to distinguish between cancer and cancer-free patients and able to give important prognostic information's.

Moreover, we tested the cytotoxic effects of Silver nanoparticles, embedded into EPS of Klebsiella oxytoca on breast cancer cell line.

The result sections were separated into 4 part and at the beginning of each part, a brief synopsis of the state of the art and aim was reported.

MATERIALS AND METHODS

Clinical specimens

The present study was conducted on 27 surgical tissues of colorectal cancer and 24 breast cancer selected by tissue *criobanking* available at the Maddalena Hospital, and stored at -80°C until use. Research was carried out in compliance with the Helsinki declaration with the patients'written consent and with the approval of the Institutional Review'Board (n°515/2008). The analyzed samples include tissues (colon and breast cancer with matched normal adjacent tissues) and sera. The colon data set contains moreover one liver metastasis and the breast data set contains moreover other 87 tumor samples. Sera were used with a dilution of 1:25.

Protein extraction from biopsies

The frozen tissue samples were washed several times with PBS and homogenized with a rotating pestle (Polytron) on ice using in 50mM Tris-HCl pH 7.5. The extraction was carried out overnight at 4°C with the same buffer. The total cellular lysate was centrifuged at 10500 rpm for 20 minutes (x3), at 4°C, to remove tissue debris and the collected supernatant used for zymographic analysis. For proteomic analysis, the protein extract was dialysed against ultrapure distillate water, lyophilized and solubilized in DIGE buffer or in ISOT buffer. The total protein concentration was determined by the Bradford method using bovine serum albumin as a standard and stored at -80°C until use.

Saggio di Bradford

The Bradford assay is a colorimetric method used to quantify the protein, based on the use of a dye, *Bradford reagent*, constituted by Coomassie Brilliant Blue G-250 0.01%, 5% Ethanol and 10% Phosphoric Acid (solution is filtered and stored at 4°C). Coomassie Brilliant Blue G-250 binds to proteins in the residues of arginine, tryptophan, tyrosine, histidine and phenylalanine, in anionic form, with a maximum absorbance adjustable at 595 nm (blue). Unknown protein samples, blank tube. 5 ml of Bradford reagent was added to each tube, mixed and incubated at room temperature (RT) for at least 5 min and no more than 1 h. Absorbance was reader at 595 nm.

SDS-Page and Gelatin Zymography

The polyacrylamide gels were prepared according to the procedure described by Laemli (1970). The separating gel was prepared with 30% Acrylamide, 0.8% Bis-acrylamide, 1.5M Tris/HCl pH 8.8, 10% SDS (sodium dodecyl sulfate), 10% APS and TEMED (tetramethyl-ethylene-diamine). The gel concentration of 4% differs from the previous for the presence of 1M Tris/HCl pH 6.8. A particular application of the SDS-PAGE is the zymography, which allows to highlight the enzymatic activities present in the sample, such as the activity of MMP-2 and MMP-9. The method is based on the possibility to incorporate the substrate in the meshes of polyacrylamide gel and to let the enzyme act after the run. The substrate used was gelatin to a final concentration of 0.1%. Gels were prepared at a final concentration of acrylamide of 12% for SDS-Page and 7.5% for zymography.

The samples (tissue samples: 18 µg for zymography, 20 µg for SDS-Page; serum samples: 10 µl for zymography), were suspended in a buffer containing 0.5M Tris/HCl pH 6.8, 10% SDS, 100% glycerol, 0.05% bromophenol blue. The run was performed at 150V for approximately 1 hour. Running buffer was constituted by 0.25M Tris, 1.92M glycine, 1% SDS. After the run, the gel was washed for one hour with a rinaturating buffer containing 2.5% Triton X-100, 50mM Tris/HCl pH 7.5 and incubated at 37°C for 18 hours in an activation buffer, consisting of 150mM NaCl, 10mM $CaCl_2$ and 50mM Tris/HCl pH 7.5. The gel was finally stained for 30 minutes with a solution consisting of 0.2% Coomassie blue, 40% methanol, 10% acetic acid and destained in Ultrapure MQ water. Areas of enzymatic activity appeared as clear bands over the dark background. Quantification on lytic bands were performed with *Image J* or with *Image Master 2D Platinum 7* software.

Two Dimensional Gel Electrophoresis

The proteins extracted from colon cancer tumor tissue (CCTT), normal adjacent tissue (CCNT) and metastatic tissue (CCTM) were solubilised in ISOT buffer containing 4% CHAPS, 40 mM Tris, 65 mM DTE in 8 M urea. Aliquots of 450 µg (analytical gels) or 1.5 mg (preparative gels) of total proteins were separately mixed with 350 µL of rehydration solution containing 8 M urea, 2% CHAPS, 10 mM DTE and 0.5% carrier anpholytes (Resolyte 3.5-10), and applied for IEF using commercial sigmoidal IPG strips, 18 cm long with pH range 3.0-10. The second dimension was carried out on 9-16% linear gradient polyacrylamide gels (SDS-PAGE), and the separated proteins were visualized by ammoniacal silver staining. Stained gels were digitized using a computing densitometer and analyzed with Image Master Software (Amersham Biosciences, Sweden). Gel calibration was carried out using an internal standard and the support

of the ExPaSy molecular biology server, as described (Pucci-Minafra I et al., 2002).

Proteomic Analysis: 2D-DIGE

Pool of colon cancer samples and paired normal tissues were prepared combining equal amount (100 µg) of each protein extract. Colon cancer pooled tissues and paired normal pooled tissues were labeled with the CyDyes minimal labeling method (GE Healthcare, UK), according to the manufacturer's instructions. Fifty µg of proteins were used for each sample and labeled with Cy3 and with Cy5. The internal standard was constituted by an equal fraction of each sample included in the experiment in order to correct the quantification of the proteins for potential uneven loading and electrophoretic conditions, and labeled with Cy2 (for the internal standard). Briefly, each sample plus internal standard were individually labeled for 1 h on ice in the dark with 400 pmol of either Cy3, Cy5 or Cy2. Labeling reaction was stopped by the addition of 1 µL 10 mM lysine solution and incubation for 15 min on ice in the dark. Labeled samples were pooled such that each pool contained an equal ratio of proteins marked with Cy2, Cy3, and Cy5 The final volume was adjusted to 350 µL of a rehydration solution containing 8M Urea, 4% Chaps, 1% DTE, 0.75% of IPG Buffer pH 3-10 NL and 1% of Blue Bromophenol and applied for IEF using commercial sigmoidal IPG strips, 18 cm long with pH range 3.0-10. First dimension separation was carried out on *EttanTM IPGphor™3* (GE Healthcare), at 20°C, with a voltage at 30V for 10 hours, 200 V for one hour, 300V for 30 minutes and 3500V for 3 hours; then for 8 hours at voltage stabilized at 8000V, for a total of about 23,5 hours. Subsequently, the strips were subjected to equilibration for 12 minutes in a *Solution* consisting of 6M Urea, 30% glycerol, 2% SDS, 0.05M Tris-HCl pH6.8 and 2% DTE and then for 5 minutes in a *Solution* in which the DTE was replaced with 2.5% of Iodoacetamide and trace amounts of Bromophenol Blue. The second dimension was carried out on 9-16% linear gradient polyacrylamide gels (SDS-PAGE), The strips were placed into the glass plates and fixed with a solution of 0.5% agarose, dissolved in Running Buffer consisting of 0.125M Tris, 0.96M Glycine and 1% SDS. The SDS-PAGE electrophoretic run was carried out with *GE Healthcare Ettan™ DALT six Large Vertical System* at 10°C, with a constant current of 20mÅ/gel until the Bromophenol Blue come out from the gel plates. The 2D-gels were scanned with a *Typhoon FLA 9500* (GE Healthcare), according to manufacturer's instructions. Differential gel analysis was performed semi-automatically by using the *Image Master 2D Platinum 7* software (GE Healthcare). Protein spots were automatically detected and then matched. Individual spot abundance was automatically calculated from quadruplicated 2D-gels as mean spot volume, i.e. integration of optical density over spot area, and normalized to

the Cy2-labeled internal pooled protein standard. Protein spots showing more than 1.2 fold change in spot volume (increased for up-regulation or decreased for down-regulation), with a statistically significant ANOVA value ($P \leq 0.05$), were considered differentially represented and further identified by MS analysis. After the acquisition, each gel was stained with an ammoniac solution of silver nitrate. It consists of a series of steps by means of which cause the oxidation of the proteins, their bond with silver ions and therefore the reduction of these ions to metallic silver using a citric acid solution containing formaldehyde.

In-gel digestion

For peptide mass fingerprinting (PMF) spots of interest with different intensity levels ≥ of 1.2 fold and anova ≤ 0.05 were destained with mixture of the two destaining reagents $K_3[Fe(CN)_6]$ and $Na_2S_2O_3$ dissolved in water as given above. Then, the gel particles were washed with 200 mM Ammonium bicarbonate for 15 minutes at 55°C and contracted with 100% Acetonitrile and vacuum dried. Spots were rehydrated with 0.02 µg/µl trypsin (Boehringer Mannhein sequencing grade) and incubated overnight at 37°C. The supernatants were collected and pooled with three additional extractions, two using 50% Acetonitrile/5% TFA and one with 50% Acetonitrile. Pooled extracts were vacuum stored at -80°C until used.

MS analysis of tryptic digests

For cleaning samples prior to analyzing them by MALDI is using the ZipTip™ pipette tips, with a bed of resin fixed at the end, useful for concentrating, desalting and fractionating picomole amounts of peptide, protein or oligonucleotide samples. Samples are aspirated and dispensed through the tip to bind, wash and elute the analyte(s) of interest. The concentrated, purified sample is eluted in 3µl di eluent. Then the peptides were eluted in 1 µL of matrix solution 5mg/1mL of α-cyano-4-hydroxycinnamic acid (Sigma Aldrich, St. Louis, USA), dissolved in 30% Acetonitrile and 0.1% TFA, directly onto the MALDI target plate (Bruker Daltonics GmbH, Bremen, Germany). A peptide calibration standard was spotted separately onto the MALDI target plate. Mass spectra were obtained using an Ultraflex MALDI-TOF mass spectrometer in reflection mode (Bruker Daltonics, Bremen, Germany). Using the software dedicated *Flex Control,* for each sample it obtains a spectrometric profile that then it can be identified based on the Mascot scores of the peptide subjected to MS Analysis.

Western Blotting

After the electrophoretic run on polyacrylamide gel under denaturing conditions by SDS-PAGE, the gel is incubated in Transfer Buffer (25mM Tris, 190mM Glycine and 20%

Methanol) for 5 minutes, and so also the nitrocellulose membrane (Hybond ECL, Amersham), after a rapid wash in distilled H_2O; then the sandwich was assembled in the presence of ice and it is carried out for one hour at 100V and 400mA constant. Before proceeding to immunodetection with a specific antibody, the membranes were stained for 3 minutes with a solution of 0.2% Ponceau Red S (Sigma) in 3% Trichloroacetic Acid. The membranes were then incubated for one hour at room temperature with gentle stirring in blocking solution (TBS pH 7.6: 20mM Tris and 137mM NaCl with 0.05% Tween 20 and 5% milk) and then incubated overnight at 4°C with one of the following antibodies diluted in 1% milk/T-TBS 0.05%: Akt-1 (Santacruz), 1:1000, IgG1 mouse monoclonal; pAkt (Santacruz), 1:1000, rabbit polyclonal; ACTIN beta (Calbiochem), 1:20000, IgM mouse monoclonal; IGF-1R (Santacruz), 1:500, mouse monoclonal; CATD (Santacruz), 1:1000, IgG1 mouse monoclonal.

After six washes for 5 minutes in T-TBS 0.05%, the membranes were incubated for one hour at room temperature under gentle agitation with the secondary antibody, also diluted in 1% milk (Goat Anti-Mouse (Santacruz), 1:2000, for Akt-1; Anti-Rabbit (Santacruz), 1:5000, for p-Akt; Goat Anti-Mouse (Amersham), 1:10000, for Actin; Goat Anti-Mouse (Amersham), 1:3000, for IGF-1R and Goat Anti-Mouse (Santacruz), 1:3000, for CATD). After 6 washes for 5 minutes in T-TBS 0.5% tween, the reaction was revealed by the ECL detection system, using high performance films (Hyperfilm ECL, Amersham). The relative amount of each protein analyzed was determined by the use of the software *Image Master 2D Platinum 7* which, through the application of specific algorithms, allows to transform the digital signal in the relative intensity of each band shown on the photographic plate. For WB was calculated Volume (integration of area and optical density).

Statistical Analysis

The data were presented as the means ± SD. Statistical analyses were performed. For statistical analyses Ms Excel and Graph Pad Prism 4 software were used. Differences and correlations among groups were calculates using the Student's t-test or Pearson correlation test. In all cases, $p<0.05$ was considered significant (*), $p<0.01$ highly significant (**) and $p<0.001$ very highly significant (***).

Microarray Data Analysis

The microarray data source (series accession number GSE28702) was obtained from the Gene Expression Omnibus (GEO). The data set was not subjected to any additional normalization. In the GSE28702 study, 83 patients with unresectable CRC, including 56 patients with primary CRC and 27 patients with metastatic lesions in the liver (23 tumors), lungs (1 tumor), and

peritoneum (3 tumors), were recruited from April 2007 to December 2010 at Teikyo University Hospital and Gifu University Hospital. 26 all CRC samples were obtained before mFOLFOX6 therapy. We analyzed the expression of TAGL and CATD.

Cell culture and treatments

Human cancer cell lines SKBR-3, 8701-BC, HT-29 and HCT-116, were cultured in RPMI 1640 media (Gibco), supplemented with 10% heat-inactivated fetal bovine serum and 100 µg/ml penicillin/streptomycin (Sigma Aldrich). All culture cells were maintained at 37°C and 5% CO_2. Cells were seeded at cell density of $2x10^4/cm^2$, and to 70% confluence they were treated with different concentrations of Ag^0NPs-EPS, Ag^{+1}1NPs-EPS and NaNPs-EPS (produced in absence of metal), for 24 hours for all experiments. Where not expressed, the cells were treated with 5 µg/ml of NPs-EPS, corresponding to IC50 of Ag^{+1}1NPs-EPS.

Protein extraction from cell line SKBR-3 and conditioned medium (CM) preparation

After the AgNPs-EPS treatments, SKBR-3 cells were washed twice with PBS and recovered from the plate with the aid of a scraper and centrifuged in PBS at 1000 rpm for 5 minutes (x3). Protein extraction was performed in DIGE lysis Buffer (7M Urea, 2M Thiourea, 4% CHAPS, 30mM Tris-HCl pH 8.5) on ice for 30 minutes, and then centrifuged at 12000 g for 10 minutes at 4°C. Supernatant was recovered in clean tubes. The cellular lysates obtained were quantized by the Bradford. For zymography, confluent cultures of SKBR-3 were treated for 24 hours with AgNPs-EPS and NANP-EPS in serum free medium. The conditioned medium (CM) of each well was transferred to a clean tube, centrifuged at 1000 rpm for 5 minutes and dialyzed, lyophilized, resuspended in Ultrapure and quantized by Bradford assay. The cellular lysates were subjected to SDS-Page (10 µg) and CM to zymography (2, 5 and 5 µg for line).

Cell Proliferation Assay

SKBR-3 cells were cultured in a 96-well plate at cell density of $5x10^3$ cells/well. After 24 hours, cells were incubated with appropriate concentrations of AgNPs-EPS (from 500-to 0.05µg/µl) at 37°C for 24h and then cell viability was determined by MTT assay. Cells were treated with CellTiter 96® Aqueous One Solution Cell Proliferation Assay, that contains tetrazolium salt, MTS [3-(4,5-dimethylthiazol-2-yl)-5-(3-carboxymethoxyphenyl)-2-(4-sulfophenyl)-2H tetrazolium, inner salt], and a reagent (phenazine ethosulfate) with the capacity of "electron–coupling" (final concentration, 0.5 mg/ml) for 1-4h at 37°C in 96-well plates.

The complex (also called "Owen's reagent"), is produced by cells in Formazan, colored product that is soluble in the culture medium. The quantity of formazan which originated as product of

the described enzymatic reaction is measured by spectrophotometry at 490 nm through the reader *BioTrak Microplate Reader* (Amersham Bioscience) and is directly proportional to the number of viable cells present in culture. Percentage of cell viability was calculated by using the following formula:

$$\text{Percentage of cell viability} = \frac{\text{OD value of experimental sample (AgNPs-EPS)}}{\text{OD value of experimental control (untreated)}} \text{ X } 100$$

Colony formation assay

Cells are harvested from a stock culture and plated at appropriate dilutions into (cluster) dishes (6-well plate at density of 200, 400 and 800 cells). After attachment of the cells to the dishes, which generally takes 2 h, the cells were treated for 1h and for 24h with 50 and 5 μg of AgNPs-EPS. The dishes are washed carefully and placed in an incubator and left there for a time equivalent to at least six potential cell divisions (10 days). This method is often used for a quick screening of the sensitivity of cells to different treatments. Colonies were fixed and stained with a mixture of 6.0% glutaraldehyde and 0.5% crystal violet and then counted microscopically using 10× high power fields. Clonogenic index was then calculated as the ratio of plating efficiency of treated cells on wells divided by the number of cells in the control wells (PE is the rate of number of cell colony on wells containing nanoparticles divided by the number of cells in the control wells).

Morphological Analysis: Hoechst 33342 Staining

Hoechst labeling of cells was used to detect apoptotic nuclei by the evaluation of nuclear morphology. Briefly, SKBR-3 cells were incubated in a 12-well plate at cell density of $1x10^5$ cells/well and after 24h treated with μg AgNPs-EPS for 24h. Then cells were stained with Hoechst 33342 at final concentration of 1 mg/ml for 10 minutes. After being washed with PBS, the cells were observed under an *Axio Observer.A1* fluorescence microscope (*Carl Zeiss*).

Morphological Analysis: AO/EB Staining

AO/EB double staining was used to detect the apoptosis of SKBR-3 cells, which were incubated in glasses, placed in a 12-well plate, at cell density of $1x10^5$ cells/well and after 24 hours treated with 5μg/ml of AgNPs-EPS for 24 hours. Cells were washed with PBS and stained with EB/AO dye mix and observed under an *Axio Observer.A1* fluorescence microscope (*Carl Zeiss*).

Scratch Assay

The scratch-wound assay is a simple, reproducible assay commonly used to measure basic cell migration parameters such as speed, persistence, and polarity. SKBR-3 cells were grown to confluence in a 12-well plate and a thin "wound" introduced by scratching with a pipette tip. Then, cells were treated with 5µg/ml of AgNPs-EPS for 24 hours. Wound closure was monitored at different time points (0, 6 hours, 24 hours). Percentage of wound closure was then calculated with *Image Master 2D Platinum*.

Transmission Electron microscopy (TEM) analysis

SKBR-3 cells were grown to confluence in a 12-well plate and treated with 50-5µg/ml of AgNPs-EPS for 24 hours; then cells were recovered in PBS through a scraper and centrifugated at 1000 rpm for 5 minutes (x3) and immediately fixed in Karnovsky buffer (2% Paraformaldehyde/2.5% Glutaraldehyde in 0.1 M phosphate or cacodylate buffer), for 30 min. Cells were dehydratated using increasing concentrations of ethanol (10%, 35%, 50%, 70%, 95% and 100%) in water, for 5 minutes each at room temperature and send to University of Siena for TEM analysis.

Nuclear, cytosolic and mitochondrial isolation

SKBR-3 cells were grown to confluence in 75 cm^2 flasks and treated with 5µg/ml of AgNPs-EPS for 24 hours.; then cells were recovered in PBS through a scraper and centrifugated at 1000 rpm for 5 minutes (x3); the cell pellet was resuspended by gentle pipetting in Sucrose buffer (5mM Tris-HCl pH 7.4, 0.32M Sucrose and 0.001 mg/mL Protease/phosphatase inhibitor). Nuclei were pelleted by centrifugation at 1000 g for 20 minutes; mitochondria from the post-nuclear supernatants were recovered by centrifugation at 8500 g for 30 minutes; lysosome by centrifugation at 20000 g for 30 minutes and mycrosome by centrifugation at 105000 g for 90 minutes. In a second nuclear and mitochondrial isolation, the cell pellet (resuspended in sucrose buffer) were centrifugated respectively only at 1000 and 8500 g. Recovered fractions were send to University of Venice for voltammetry analysis.

Proteomic Analysis: 2D-DIGE

The cellular lysates were subjected to 2D DIGE. Samples were separately labeled with different CyDyes (Cy2, Cy3, and Cy5), as already described. The ratio of protein to CyDye was maintained at 50 µg/400 pmol. 2D-DIGE gel analysis and protein identification have already been described previously.

Kaplan-Meier curves

The correlation between the expression of S100 genes and prognosis of breast cancer patients was analyzed using an online Kaplan-Meier plotter (http://kmplot.com/analysis/). The Kaplan-Meier plotter is a competent tool for assessing the effect of any gene or gene combination on survival in breast, lung, ovarian and gastric cancer patients using 10,188 cancer samples. The datasets include gene expression and survival data from Gene Expression Omnibus (GEO) and The Cancer Genome Atlas (TCGA) (Affymetrix HG-U133A, HG-U133A 2.0, and HG-U133 Plus 2.0 microarrays). To analyze the prognostic value of the probe, the samples were split into two groups according to the median expression of the probe (auto select best cutoff). The two patient groups (higher and lower expression of genes) were compared using a Kaplan-Meier survival plot. The hazard ratios (HRs) with 95% confidence intervals, and the log rank p value was calculated using a default algorithm. We analyzed the best specific probes (JetSet probes) that recognized genes which maps to Affymetrix probe sets by selecting the best probe set for this analysis.

RESULTS PART I

Background and aim

Colorectal cancer (CRC) is a leading cause of cancer death worldwide. Pathological staging is the gold standard for prognosis, but frequently fails to accurately predict recurrence in patients undergoing curative surgery for locally advanced CRC. In addition, tumors with similar histopathological appearances often manifest significantly different clinical behavior. A large number of CRC patients relapse after complete surgical resection. The most common site of recurrence in CRC is the liver (Cunningham D et al., 2010). Otherwise, it is critical to understand the molecular heterogeneity associated with different outcome between individual patients. This scenario emphasizes the need to identify multiparametric biological markers for more accurate cancer detection and management. The proteomic approach, based on 2-DE combined with MS spectrometry, is one of the most promising techniques for the identification of protein species related to malignancy, and has provided powerful analytical tools for identifying the differentially expressed and/or post-translationally modified proteins as potential biomarkers in tumors. Previous studies performed by our group successfully applied proteomic approach for biomarkers discovery in breast cancer in vitro (Pucci-Minafra I et al., 2002) and ex vivo on breast tissues (Pucci-Minafra I et al., 2007). In the latter study, comparative proteomic profile of 13 breast cancer tissues and their matched non-tumoral tissues (*Fig. 25*), demonstrated qualitative and quantitative differences between the two groups. The differentially expressed proteins, according to the Student's t-test, were grouped into seven functional categories (cytoskeleton and associated proteins; metabolic enzymes; molecular chaperones; proliferation and differentiation regulators; detoxification and redox proteins; protein degradation; serum proteins).

In the present study, we firstly perform a comparative proteomic profile of pooled colon cancer tissues paired with adjacent non-tumoral mucosa, to investigate potential target proteins correlated with carcinogenesis. After that, we used a three-step approach to compare normal-colon cancer and liver metastasis from the same patient, in order to identify putative proteomic signatures for CRC occurrence and metastasis. We selected unique and common proteins involved in tumorigenesis (normal versus tumoral) and metastasis (tumoral versus metastasis). The differentially expressed proteins, functionally classified, have been suggested to act at multiple tumor progression steps, affecting cell proliferation, apoptosis, metabolic pathways, oxidative stress, cell motility and invasion. Interestingly, in the present study we able to identified Transgelin (four different isoforms), a 22 kDa actin-binding protein, as a possible

tumor suppressor and biomarker for CRC, and cathepsin D (two different isoforms), a lysosomal aspartyl endopeptidase, differentially expressed between tumor and metastatic tissue.

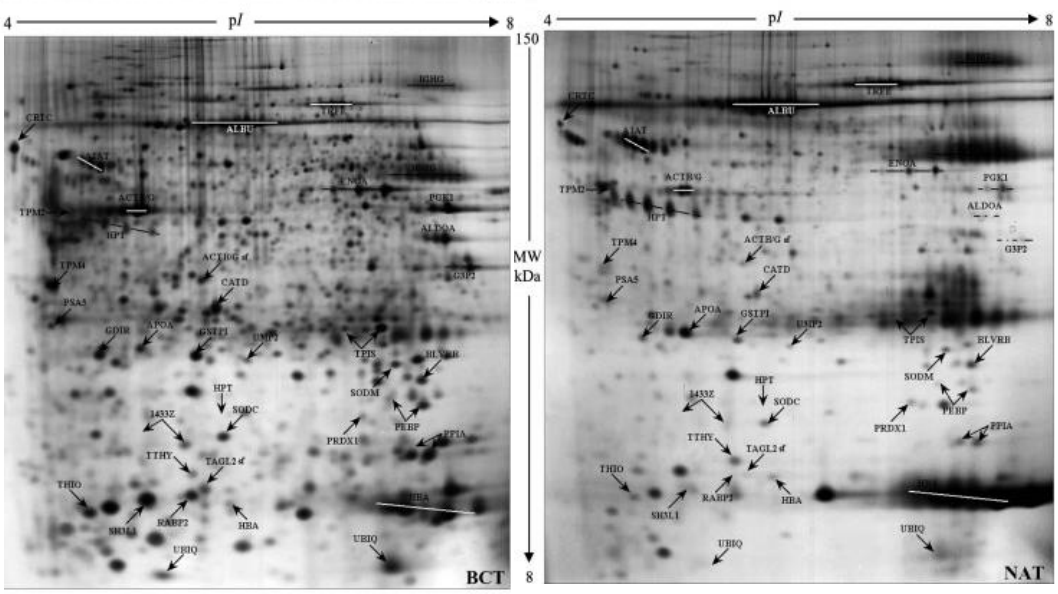

Figure 25. Representative proteomic maps of matched breast cancer tissue (BCT) and normal adjacent tissue (NAT), random selected among the 13 analyzed patients. It is possible to observe that the cancer derived proteomics display a far higher level of complexity than non tumor tissues, probably because the differentiated healthy mammary gland contains a reduced amount of parenchyma with respect to the surrounding stroma, if compared to tumor tissue.

Pooling of samples for proteomics experiments

The pooling of samples in proteomics work is a valid and potentially valuable procedure because is a strategy that can be used to reduce the biological variance (Diz AP et al., 2009; Karp NA et al., 2009). The underlying assumption is that the measurements taken on the pool are equal to the average of the measurements taken on the individuals samples. The comparative proteomic analysis was performed on colon cancer pooled tissues and paired normal pooled tissues, both to minimize the variability within each group, both to reduce the patient-related differences not associated to cancer. For this study we used 52 surgical samples obtained from 26 patients with colon cancer, identified with a progressive number. All clinical parameters were blinded. For each patient the tumor tissue (CT), the adjacent healthy tissue (NT) and serum (S) were available. Before pooling the two groups (normal adjacent and colon cancer), qualitative and quantitative check of protein extracts (20 µg) were done by SDS-PAGE electrophoresis (*Fig. 26*). The two different pools of colon tumor tissue and adjacent healthy tissue were generated by mixing equal amounts in terms of protein concentration of individual samples.

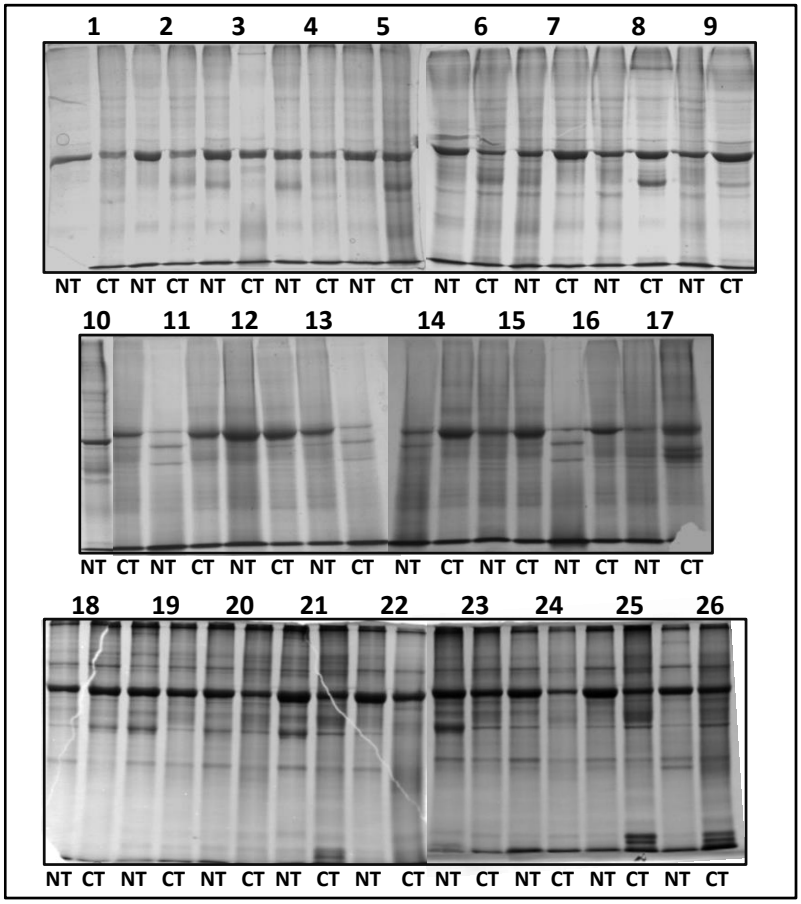

Figure 26: SDS-PAGE electrophoresis of protein extracts from 26 colon cancer tissues (CT) and paired normal tissues (NT) stained with Blue Coomassie.

Comparative proteomic analysis between pooled colon cancer (CT) and paired normal tissues (NT)

To determine a colon cancer genesis-specific protein expression pattern, comparative proteomic analysis of pooled colon cancer tissues and paired normal tissues was performed by 2D-DIGE. Briefly, an equal amount of the protein samples was covalently labeled with the Cy3 and Cy5 dyes, respectively, and then the samples were mixed in 1:1 ratio and loaded on a 2D gel system. The Cy2 dye was used to label the internal standard, obtained by mixing an equal amount of all samples, allowing a significant quantitative comparison of proteomic variations. A total of three gels were run to achieve a statistically significant measure of the differences in protein expression between the two groups (*Fig. 27*). In the dedicated software analysis, all protein spots were quantified, normalized and inter-gel matched. 143 protein spots from colon cancer tissues showed a significant difference in intensity when compared with the normal tissues (*Fig. 28*). The protein expression changes were considered significant only when their values exceeded the threshold settings (fold change ≥ 1.2, $p < 0.05$). Among the differentially expressed spots, 79 spots were up-regulated and 64 down-regulated in CT (*Fig. 29*). The significant spots were picked manually and submitted to trypsin in-gel digestion. The peptides recovered from the gel were subjected to MALDI TOF-MS/MS analysis, and the MS data analyzed with MASCOT database: We successfully identified 111 protein spot, corresponding to 68 proteins (supplementary *Tab. 1*). Several proteins were found in different isoforms and then detected in multiple spots. The identified proteins were submitted to a functional annotation cluster analysis by David functional annotation database (https://david.ncifcrf.gov/home.jsp), and grouped into eight functional categories namely: cytoskeleton, serum proteins, response to oxidative stress, biosynthesis and degradation/chaperones, cell growth and proliferation, metabolic enzymes, *ras* protein signal transduction, regulation of apoptosis. *Fig. 30* shows the histograms of the identified proteins, sorted into functional classes and plotted as log of fold change (pooled colon cancer versus paired normal tissues).

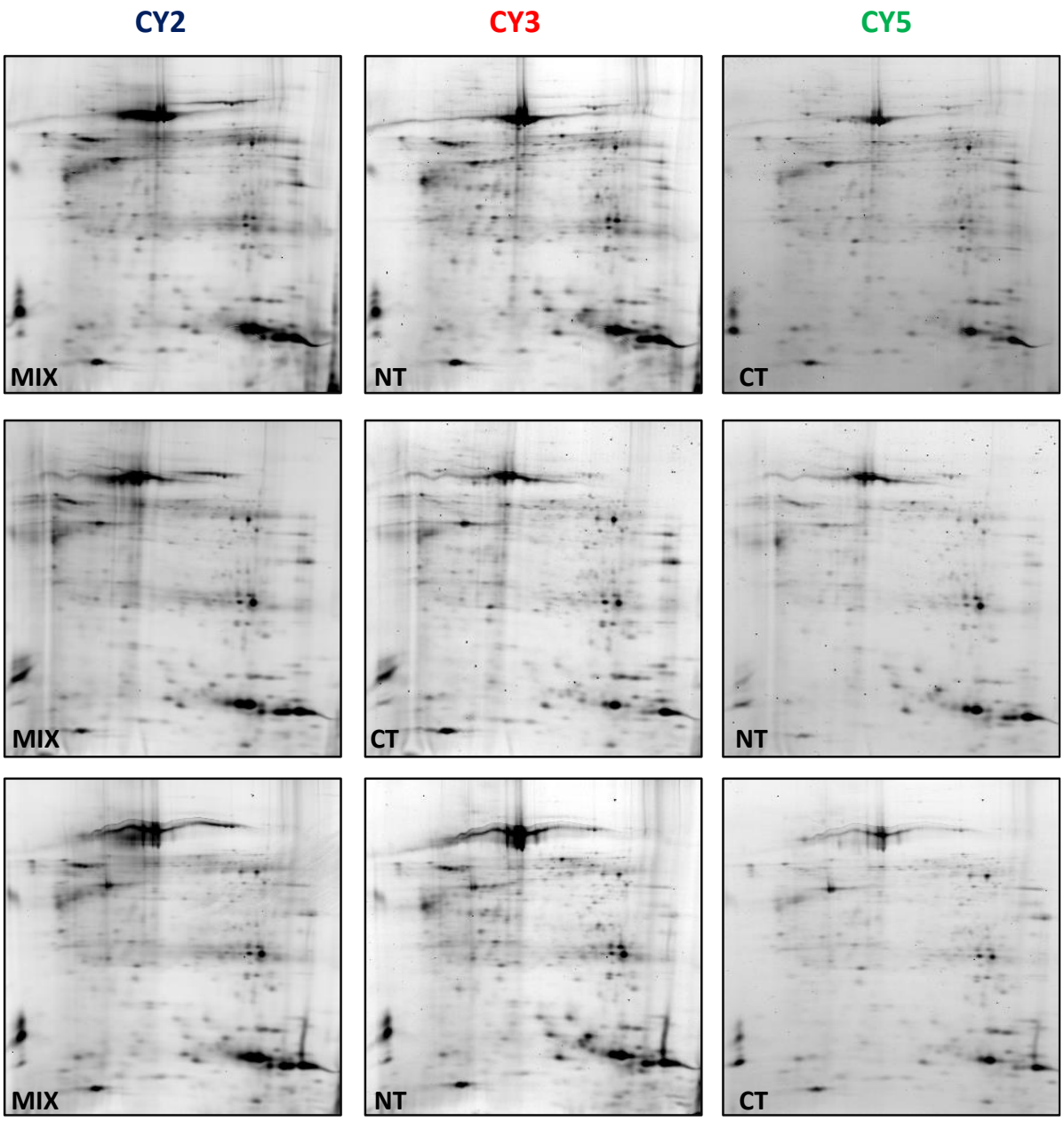

Figure 27. Panel showing the miniatures of the 2D-DIGE maps from NT and CT pools. Equal amounts of Cy2 (standard with equally mixed samples), Cy3 and Cy5 labeled samples were mixed and then separated on analytical 2D-DIGE.

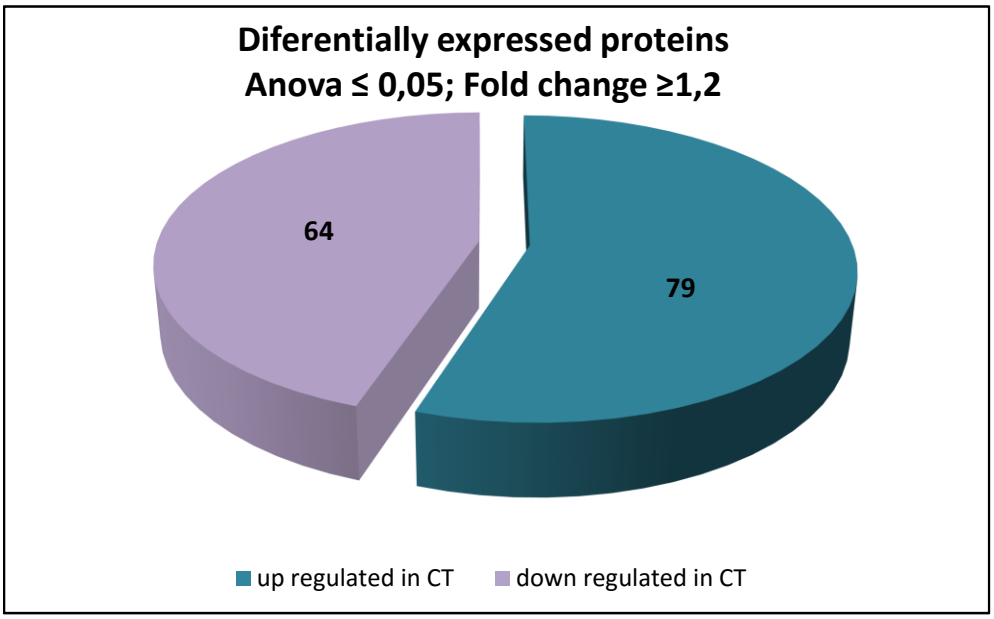

Figure 28. Differentially expressed proteins were selected on the basis of the threshold settings (fold change ≥1.2, $p < 0.05$). 79 spots were up-regulated and 64 down-regulated in colon cancer tissues compared to paired normal tissues.

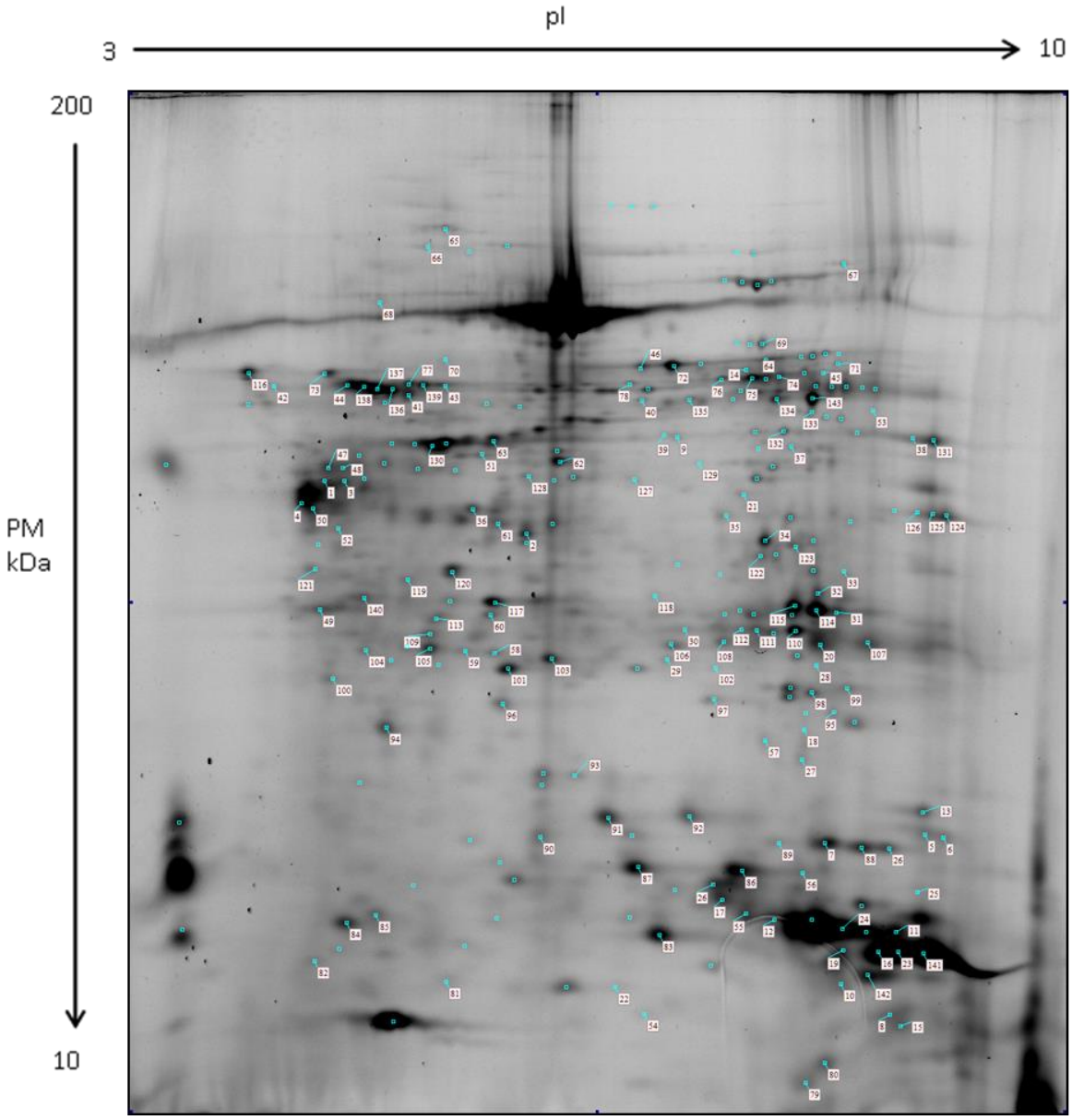

Figure 29. Representative two-dimensional differential in gel electrophoresis (2D-DIGE) images of pooled colon cancer and normal adjacent tissues. The differential proteins are marked with a label corresponding to the number of spots.

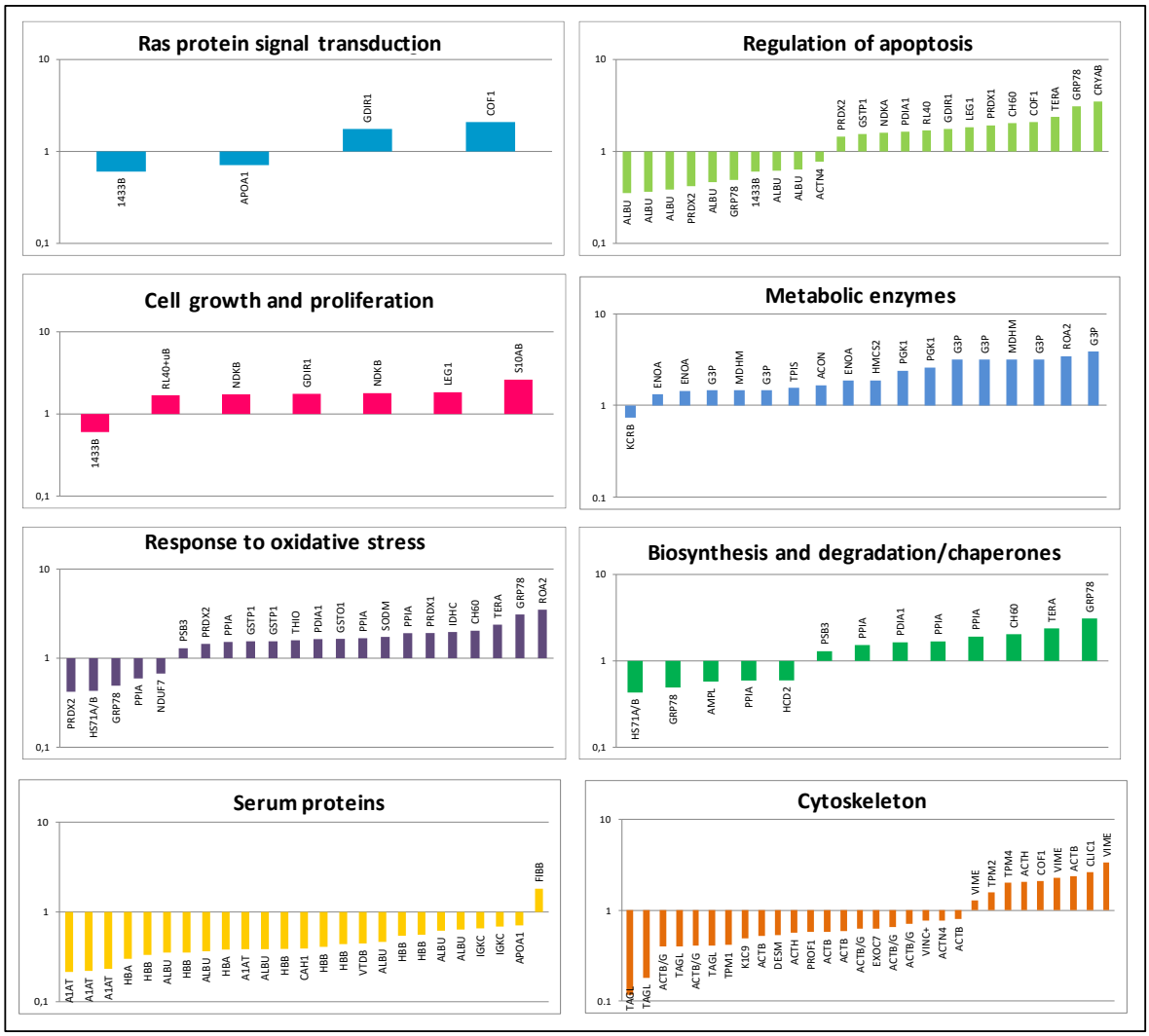

Figure 30. Histograms of the identified proteins, sorted into functional classes and plotted as log of fold change (pooled colon cancer versus paired normal tissues).

Ras protein signal transduction

The cluster of proteins involved in signal transduction mechanisms mediated by *ras* represents a specific cluster related to colon cancer genesis, and strengthens the true involvement of the other differentially expressed proteins in colon carcinogenesis.

Regulation of apoptosis

Apoptosis is a programmed cell death mechanism activated by a variety of stimuli and physiological stress factors, including oncogenes signaling and DNA damage. Tumor cells do not respond to apoptotic signals through different strategies that include the inactivation of tumor suppressor genes, such as p53 or the altered expression of pro and anti-apoptotic genes

or by altering the survival signals. Among the identified proteins, GRP78 plays important antiapoptotic functions, but is also induced during acquisition of chemoresistance.

Cell growth and proliferation

The most identified protein within this class were upregulated in pooled colon cancer tissues compared to adjacent normal tissues, testifying the deregulation of cell proliferation usually find during neoplastic transformation.

14-3-3 protein beta/alpha (**1433B**) is an adapter protein implicated in the regulation of a large spectrum of both general and specialized signaling pathways. 1433B binds to a large number of partners, usually by recognition of a phosphoserine or phosphothreonine motif. Binding will generally result in the modulation of the activity of the binding partner.

S100AB, or calgizzarin is implicated in cell cycle regulation, differentiation, growth and metabolic control. These activities are mediated via interactions with target proteins such as annexins and cytosolic phospholipase A2. Several authors reported S100AB as highly expressed in CRC and correlated with progression and lymph node metastasis (Wang G et al., 2008; Meding S et al., 2012).

Metabolic enzymes

Collectively, glycolytic enzymes are mostly expressed in the tumor pool. Our finding is in agreement with the anaerobic shift of the metabolism of cancer cells, already described by Warburg and named the *Warburg effect*. It is a common phenomenon during the development of tumors and seems to be a key step for tumor progression (Vander Heiden MG et al., 2009).

Response to oxidative stress

Peroxiredoxin 2 (**PRDX2**), 2 isoforms was found differentially modulated: an isoform was up-regulated in CRC tissues compared with the matched normal tissues, while the other was down-regulated. Peroxiredoxin 2 is a member of the peroxiredoxin family, which is responsible for neutralizing reactive oxygen species. It has been found to be elevated in several human cancer cells and tissues, including colorectal cancer (CRC), and it influences diverse cellular processes involving cells' survival, proliferation, and apoptosis. Lu W et al. (2014) found PRDX2 overexpressed in CRC tissues and associated with the development of metastases.

The **ROA2** protein (hnRNPB1) is a nuclear RNA-binding protein involved in the splicing of mRNA and its subsequent transport from the nucleus to the cytoplasm. Our results are in agreement with literature data showing an overexpression of the protein in CRC. Ushigome M

and collaborators (2005) have reported that cytoplasmic localization of ROA2 correlates with the progression of CRC. The overexpression and cytoplasmatic localization of hnRNPK correlated with advancement of colorectal cancer. In normal colon, K protein was detected only in the nucleus, whereas in tumor tissues the protein was observed both in the cytoplasm and in the nucleus (Carpenter B et al., 2006).

The protein chaperone **GRP78**, found up regulated in pooled colon cancer, is a key regulator of the endoplasmic reticulum stress and its overexpression has been correlated with tumor aggressiveness. Even for this protein there are conflicting literature: Chang YJ and colleagues (2015) recently reported that in the CRC low expression of GRP78 correlates with higher risk of metastasis, while other studies report a better prognosis in patients overexpressing GRP78. Furthermore, it was demonstrated that GRP78 can be translocated to the cell surface, acting as a signaling receptor for a variety of ligands, activating downstream PI3K/AKT and Wnt/β-catenin signaling, which promote colon cancer cell proliferation (Fu R et al., 2014). In contrast, other authors report that the expression of GRP78 on the cell membrane reduces the tumorigenicity of cells (Hardy B et al., 2012).

Serum proteins

Collectively, the serum proteins are down regulated, except for fibrinogen (FIBB), an acute phase protein whose concentration differs significantly in response to inflammatory processes. In tumors, which usually show significant inflammation response, was found high levels of fibrinogen. Fibrinogen is considered a major determinant of the metastatic potential of circulating tumor cells. (Palumbo JS et al., 2000).

Cytoskeleton

Cytoskeleton represents a structural support but also a functional system for the cell. It is responsible for cell shape, motility and signaling. Among the identified protein within this category, Vimentin (3 isoforms), Chloride intracellular channel 1 (CLIC1), and ACTH were significantly up-regulated in colon cancer tissues compared to normal tissues. **VIME** is a type III intermediate filament protein involved in cell attachment, migration and signaling. It is a biomarker for mesenchymal phenotype and for ETM, an important process required for tumor invasion. The overexpression of vimentin in gastric cancers (Otsuki S et al., 2011), as well as in the stroma of CRC tumors (Ngan CY et al., 2007) was associated with a high risk of progression.

Several studies reported **CLIC protein 1** as an overexpressed protein in CRC (Wang P et al., 2012, 2014). CLIC1 is able to control colon cancer cell migration and invasion through ROS/ERK pathway, probably through the regulation of MMP-2 and MMP-9 (Petrova DT et al., 2008).

Of particular relevance was the overexpression of **ACTH** protein, or the γ actin; because ACTH, by determining the cytoskeleton remodeling, can increase migratory and invasive capacity of colon cells (Simiczyjew A et al., 2014).

The most down regulated protein is **TAGL** (4 isoforms), a 23 kDa actin binding protein. Literature data report several roles for this protein. A few in vivo studies report TAGL as a negative prognostic factor overexpressed in tumor tissues (Zhang Y et al., 2010; Lin Y et al., 2009); in vitro studies on CRC cell lines have also shown that TAGL promotes the invasion and survival and when localized into the nucleus may regulate the transcriptional program involved in epithelial-mesenchymal transition (Petrova DT et al., 2008). On the contrary several in vitro studies showed that TAGL suppresses the 92-kDa type IV collagenase (MMP-9), affecting cell migration (Nair RR et al., 2006). It is demonstrated also that TAGL is down-regulated by the Ras pathway representing an important early event in tumor progression (Shields JM et al., 2002). Moreover, both in breast and colon cancer, TAGL is silenced through epigenetic mechanisms involving promoter hypermethylation (Sayar N et al., 2015; Zhao L et al., 2009), associated with poor prognosis.

Spectrometric analysis of TAGL isoforms

To the best of our knowledge, this is the first proteomic study which reports 4 different isoforms of TAGL, collectively down-regulated in colon cancer tissues. The *Fig. 31* reports the spectrometric characterization of TAGL isoforms by MALDI-TOF MS. Transgelin is a 23 kDa protein, composed of 201 aa. Spot number 86 and 87 show a lower molecular weight compared to the spot number 91 and 92, identifying two different short forms of transgelin in the C-terminal end. As shown, the peptide mass fingerprinting covers the protein sequence from N-terminal end up to the residue number 172 only for the spot number 91 and 92, with two specific matched peptides (m/z value corresponding to 1451.7 and 1295.6) covering the protein sequence from 162 to 172 aa residues. Interestingly, this portion contains two different phoshoserine residues. It is reasonable to believe that these isoforms may exert diversified functions in the cell. We believe that this is an important contribution to the knowledge of TAGL isoforms and represents an open intriguing question, which deserves further investigation.

A)

spot n°	Abbreviated Protein name	Entry	Protein name	Gene name	Score	number of peptide matched/searched	Coverage	Molecular weight (Da)	Theoretical pI
86	TAGL	Q01995	Transgelin	TAGLN	134	20/86	58%	22610.9	8.87
87	TAGL	Q01995	Transgelin	TAGLN	110	14/49	54%	22610.9	8.87
91	TAGL	Q01995	Transgelin	TAGLN	100	18/122	59%	22610.9	8.87
92	TAGL	Q01995	Transgelin	TAGLN	85	14/49	39%	22610.9	8.87

B)

```
 1 MANKGPSYGM SREVQSKIEK KYDEELEERL VEWIIVQCGP DVGRPDRGRL
51 GFQVWLKNGV ILSKLVNSLY PDGSKPVKVP ENPPSMVFKQ MEQVAQFLKA
101 AEDYGVIKTD MFQTVDLFEG KDMAAVQRTL MALGSLAVTK NDGHYRGDPN
151 WFMKKAQEHK REFTESQLQE GKHVIGLQMG SNRGASQAGM TGYGRPRQII
201 S                                                SPOT 86

 1 MANKGPSYGM SREVQSKIEK KYDEELEERL VEWIIVQCGP DVGRPDRGRL
51 GFQVWLKNGV ILSKLVNSLY PDGSKPVKVP ENPPSMVFKQ MEQVAQFLKA
101 AEDYGVIKTD MFQTVDLFEG KDMAAVQRTL MALGSLAVTK NDGHYRGDPN
151 WFMKKAQEHK REFTESQLQE GKHVIGLQMG SNRGASQAGM TGYGRPRQII
201 S                                                SPOT 87

 1 MANKGPSYGM SREVQSKIEK KYDEELEERL VEWIIVQCGP DVGRPDRGRL
51 GFQVWLKNGV ILSKLVNSLY PDGSKPVKVP ENPPSMVFKQ MEQVAQFLKA
101 AEDYGVIKTD MFQTVDLFEG KDMAAVQRTL MALGSLAVTK NDGHYRGDPN
151 WFMKKAQEHK REFTESQLQE GKHVIGLQMG SNRGASQAGM TGYGRPRQII
201 S                                                SPOT 91

 1 MANKGPSYGM SREVQSKIEK KYDEELEERL VEWIIVQCGP DVGRPDRGRL
51 GFQVWLKNGV ILSKLVNSLY PDGSKPVKVP ENPPSMVFKQ MEQVAQFLKA
101 AEDYGVIKTD MFQTVDLFEG KDMAAVQRTL MALGSLAVTK NDGHYRGDPN
151 WFMKKAQEHK REFTESQLQE GKHVIGLQMG SNRGASQAGM TGYGRPRQII
201 S                                                SPOT 92
```

C)

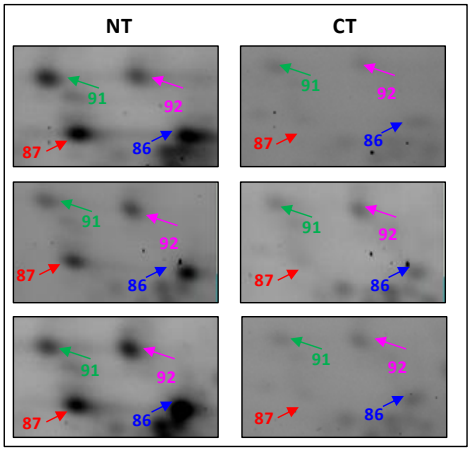

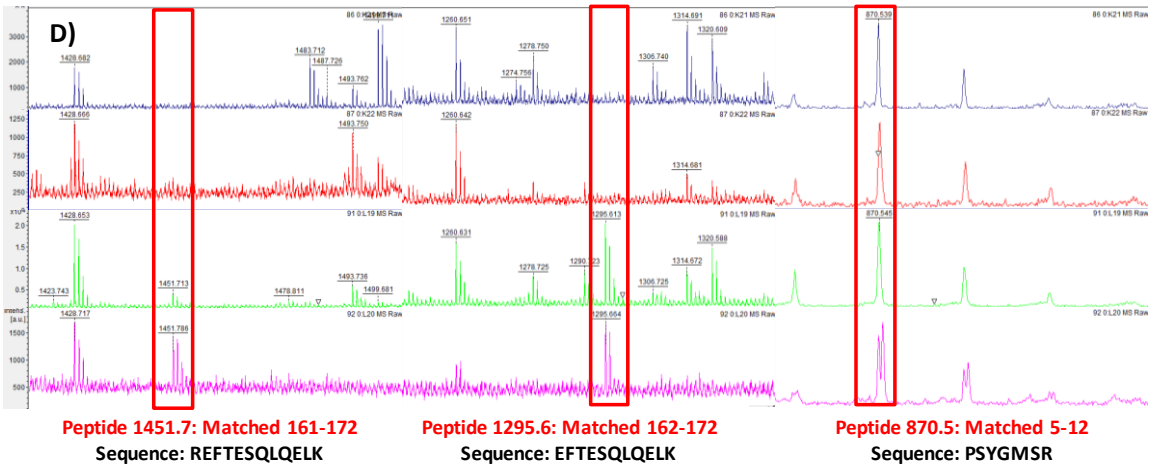

Figure 31. Spectrometric analysis of TAGL isoforms: A) Table reporting the data of MALDI-TOF/MS identification. B) Sequence coverage of the matched Peptides; C) Sperimental window of 2D-DIGE to show the down-regulation of transgelin in pooled colon cancer tissues; D) Analysis of the depicted peptides spectra in all 4 protein spots.

Comparative proteomic analysis of primary metastatic colon cancer tissue and its metastasis to liver

Approximately 50% of patients with colon cancer, develop liver metastasis, the main cause of death from advanced stage of colon cancer. Therefore, it is crucial to elucidate the biological mechanisms underlying liver metastasis of colon cancer and accelerate the development of new treatment strategies. Moreover, the high clinical heterogeneity of this disease and the great difference seen in outcome between individual patients, emphasized the clear requirement to new validating biomarkers useful to classify and stratify colon cancer patients. With this aim, we perform a comparative proteomic profile of colon cancer tissue (CCTT) paired with adjacent non-tumoral tissue (CCNT) and with liver metastasis (CCTM) from the same patient. The selected sample set (normal-tumor-liver metastatic tissue) provides some important advantages: firstly it allows to evaluate the different key step of tumor progression in a comparative manner. Moreover, taking advantage from our previous comparative screening performed on pooled colon cancer tissues and paired normal tissues, we may select new potential prognostic biomarkers, able to predict, at molecular level, the metastatic propensity of the tumor. *Fig. 32* shows the miniatures of the 2D-gels from CCNT, CCTT e CCTM, carried out in duplicate and stained with silver nitrate. Using a three-step approach, we selected unique and common proteins involved in tumorigenesis and metastasis. Firstly, the comparative analysis was performed between CCTT *versus* CCNT. This analysis revealed 169 differentially expressed spots. Among them, 100 spots were up-regulated and 69 down-regulated in CCTT (*Fig. 33*). Functional classification of the identified proteins fully overlaps with our previous classification performed on pooled samples. These findings support the importance of the identified pathways to sustain colon cancer tumorigenesis, which remain unchanged even if some proteins are different. Excluding the differentially expressed proteins already identified in the pooled tissues and/o already identified in breast cancer proteomics (Pucci-Minafra I et al., 2008), only 11 proteins (CMPK1, EVA1C, COLEC10, CLTA, PFDN5, PDXK, IMPDH2, RALB, AGR2, ALKBH5, ARL5B, TAGL) were selected among the identified in this study. We believe that in this group of proteins it is possible to check potential prognostic biomarkers (*Fig. 34A*).

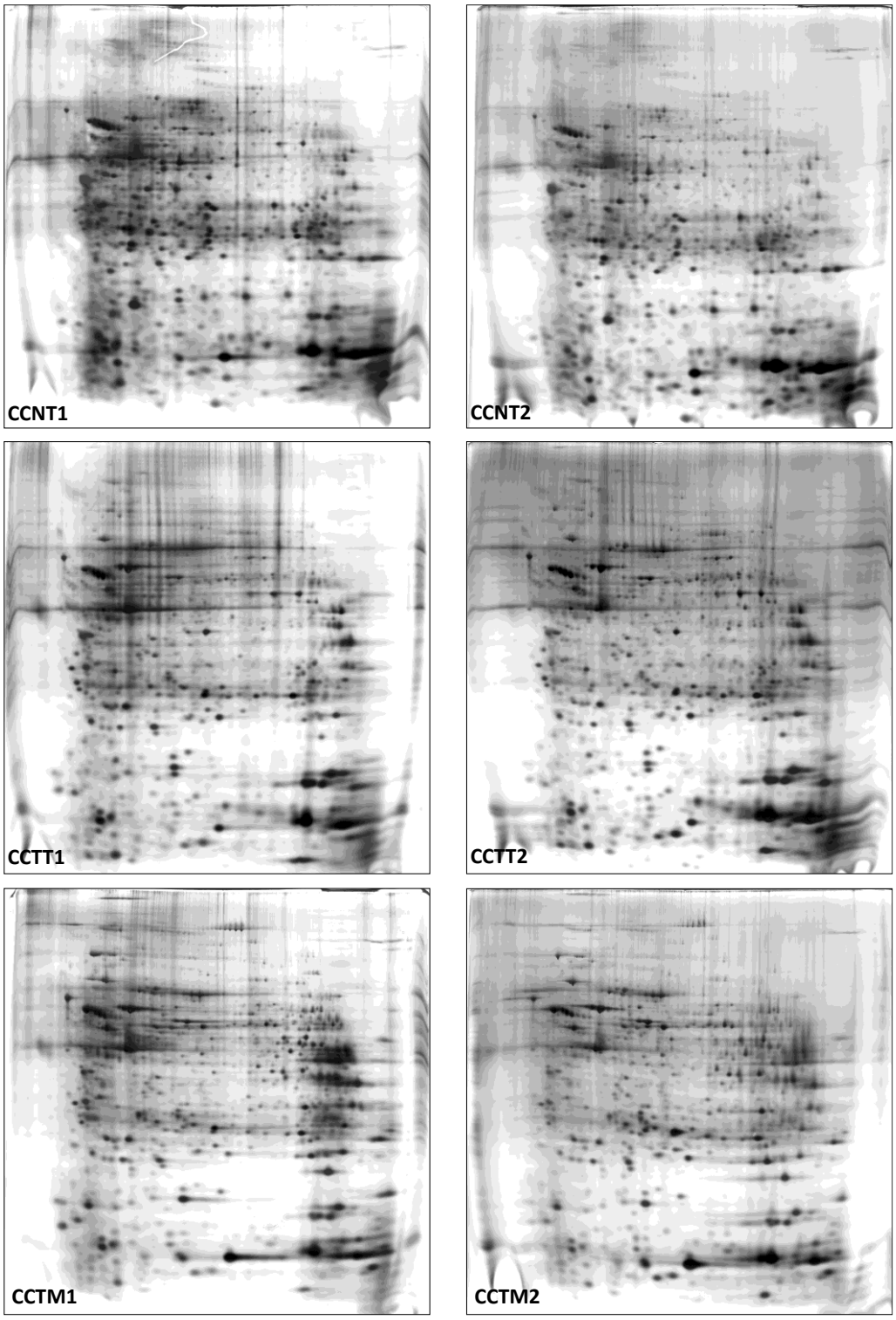

Figure 32. Miniatures of the 2D-gels from CCNT, CCTT and CCTM, carried out in duplicate and stained with silver nitrate.

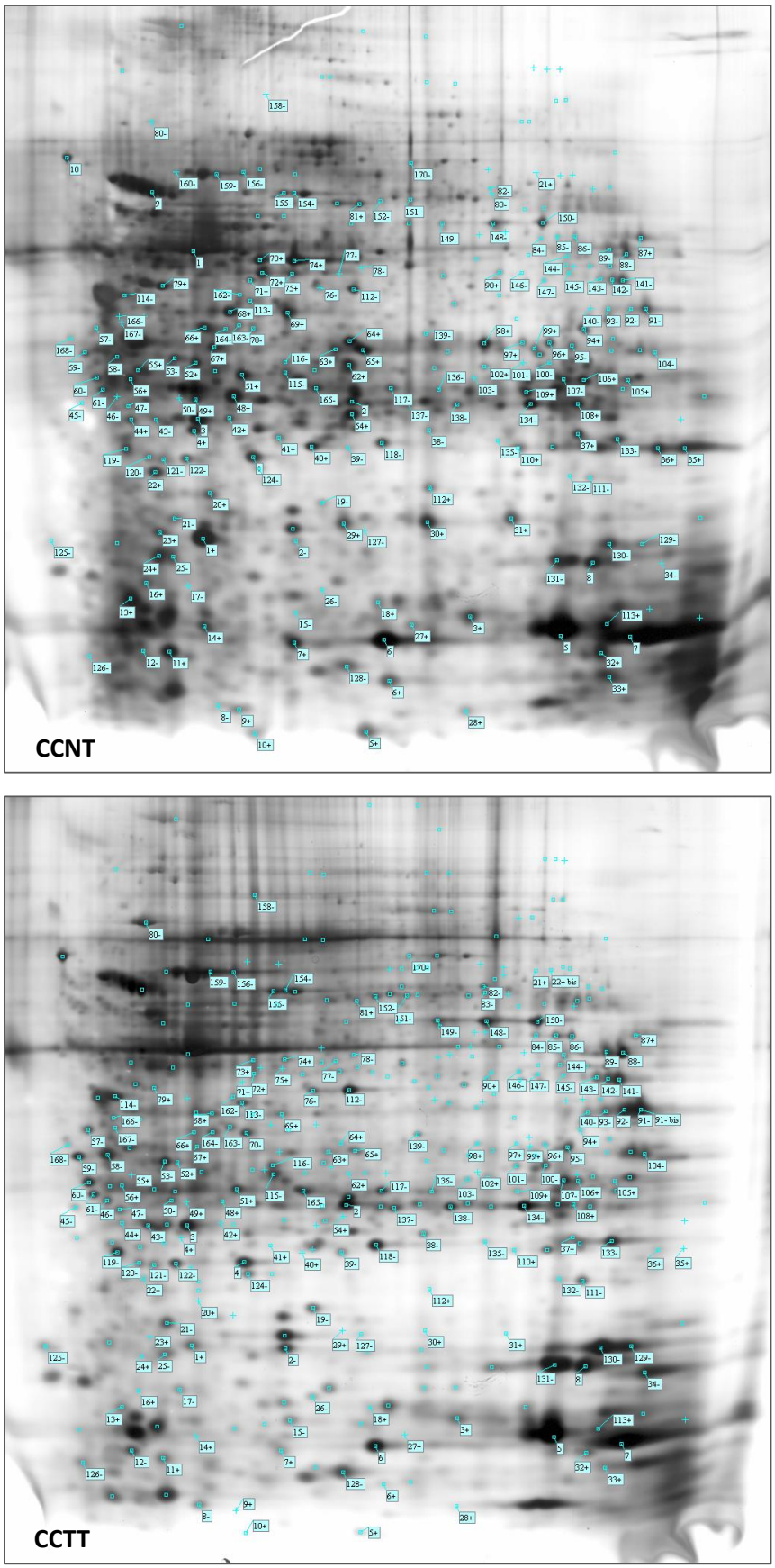

Figure 33. 2D-gels from CCNT and CCTT with the differentially expressed proteins.

Functionally, some proteins are involved in biosynthesis of nucleotides (PDXK, KCY, MDH2), in heterotrimeric G-protein signaling pathway (RALB, ARL5B, EVA1C), and some proteins were identified in colon cancer vesicles (CLTA, ARL5B, PDF5). STRING analyses for protein interactions resulted in a network of proteins containing two connected clusters around vesiculation and proliferation; however some proteins remained unconnected (*Fig. 34B*). Some of the identified proteins was already described as important proteins involved in key step of tumorigenesis:

AGR2, anterior gradient 2 homolog (Xenopus laevis), is required for MUC2 post-transcriptional synthesis and secretion, acting as a protein disulfide isomerase-like molecule. It is a proto-oncogene that plays an important role in cell migration, cell differentiation and cell growth; in fact, a recent study demonstrates that AGR2 induces the expression of the growth-promoting EGFR ligand amphiregulin in human adenocarcinomas (Verma S et al., 2012). Moreover, AGR2 functions at the tumor cell surface to induce cell adhesion in cancer development and metastasis and to affect patient survival (Patel P et al., 2013). Finally, AGR2 mRNA was significantly elevated in the blood of patients with CRC compared to controls.

RALB, is a multifunctional GTPase involved in a variety of cellular processes including gene expression, cell migration, cell proliferation, oncogenic transformation and membrane trafficking. RALB activity was found critical for Matrigel invasion in vitro and lung colonization metastasis in vivo. In experimental models of pancreas, colon, lung, prostate and bladder cancer, the expression of RALB promotes proliferation, survival, and metastasis. Importantly, most cancers with mutational activation of Ras genes also have activation of RAL, since RAL GTPases are, in addition to Raf and PI3K, canonical downstream effectors of Ras. Therefore, it is expected that 95% of pancreatic, 25% of lung and 30% of colon cancers with K-*Ras* mutations, are also RAL dependent (Martin TD, Der CJ, 2012; Martin TD et al., 2011).

IMPDH2, IMP (inosine 5'-monophosphate) dehydrogenase 2, catalyzes the conversion of inosine 5'-phosphate (IMP) to xanthosine 5'-phosphate (XMP), the first step in the de novo synthesis of guanine nucleotides, and therefore plays an important role in the regulation of cell growth. Could also have a single-stranded nucleic acid-binding activity and could play a role in RNA and/or DNA metabolism. It also has a role in the development of malignancy and the growth progression of some tumors.

ALKBH5, is a mammalian RNA demethylase that impacts RNA metabolism (Zheng G et al., 2013).

CLTA, **ARL5B** and **PDF 5** were found in extracellular vesicles derived from human primary and metastatic colorectal cancer cells (Choi DS et al., 2012; Hong BS et al., 2009).

PDXK, pyridoxal (pyridoxine, vitamin B6) kinase is required for synthesis of pyridoxal-5-phosphate from vitamin B6 (312 aa).

COLEC10, collectin sub-family member 10 (C-type lectin), is a lectin-binding protein with specific roles in initial host defense on the cell surface of microorganisms through their carbohydrate recognition domain.

PFDN5, prefoldin subunit 5, binds specifically to cytosolic chaperonin and transfers target proteins to it. It was reported that represses the transcriptional activity of MYC.

CMPK1, cytidine monophosphate (UMP-CMP) kinase 1, plays an important role in de novo pyrimidine nucleotide biosynthesis.

EVAC1, was expressed in stem cell initiating cells of Glioblastoma and is involved in maintaining of pluripotency. It binds heparin (441 aa) ARL5B, ADP-ribosylation factor-like 5B; binds and exchanges GTP and GDP (179 aa). This demethylation activity of ALKBH5 significantly affects mRNA export and RNA metabolism as well as the assembly of mRNA processing factors in nuclear speckles (Zheng G et al., 2013).

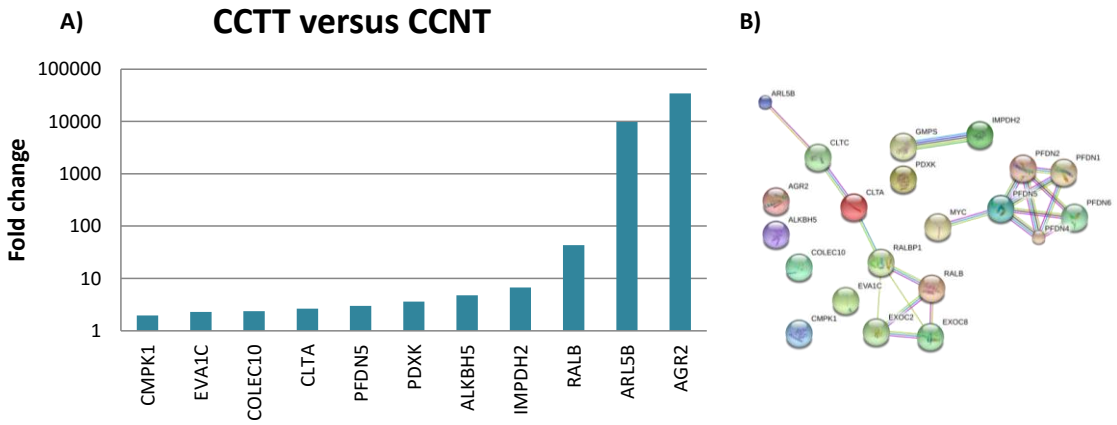

Figure 34. A) Histogram of the identified proteins, differentially expressed between CCTT and CCNT and plotted as log of fold change; B) Analysis of protein-protein interaction of the proteins performed by STRING database.

Subsequently the comparative analysis was extended between CCMT versus CCTT. 57 spots were found overexpressed in metastatic tissue compared to tumor tissue (*Fig. 35*). Intentionally, matching with the reference proteomics map of normal liver, available on ExPASy database, was performed in order to exclude the liver proteins. The 39 up-regulated spots corresponding to 30 proteins, were mainly involved in several biological processes including response to oxidative stress, glucose metabolism and proteolysis (*Fig. 36A*); consequently, they are

principally localized in mitochondria and in extracellular matrix. STRING analyses resulted in a loose network of proteins connected around glycolitic pathway (*Fig. 36B*).

The role of mitochondria in cancer progression/metastasis includes alteration of glycolysis, regulation of ROS and suppression of intrinsic apoptosis. Moreover, the mitochondria of cancer cells are involved not only in providing in part the necessary energy (ATP) to fuel their growth, but also to spread from their site of origin to other body locations. While for the mitochondrial proteins is not easy to define the specific contribution to the metastatic phenotype, a strong and specific involvement in metastatic process it is recognized for proteolytic enzymes, in fact, recently, Naba and collegues reported a different ECM signatures of human primary metastatic colon cancers and their metastases to liver (Naba A et al., 2014).

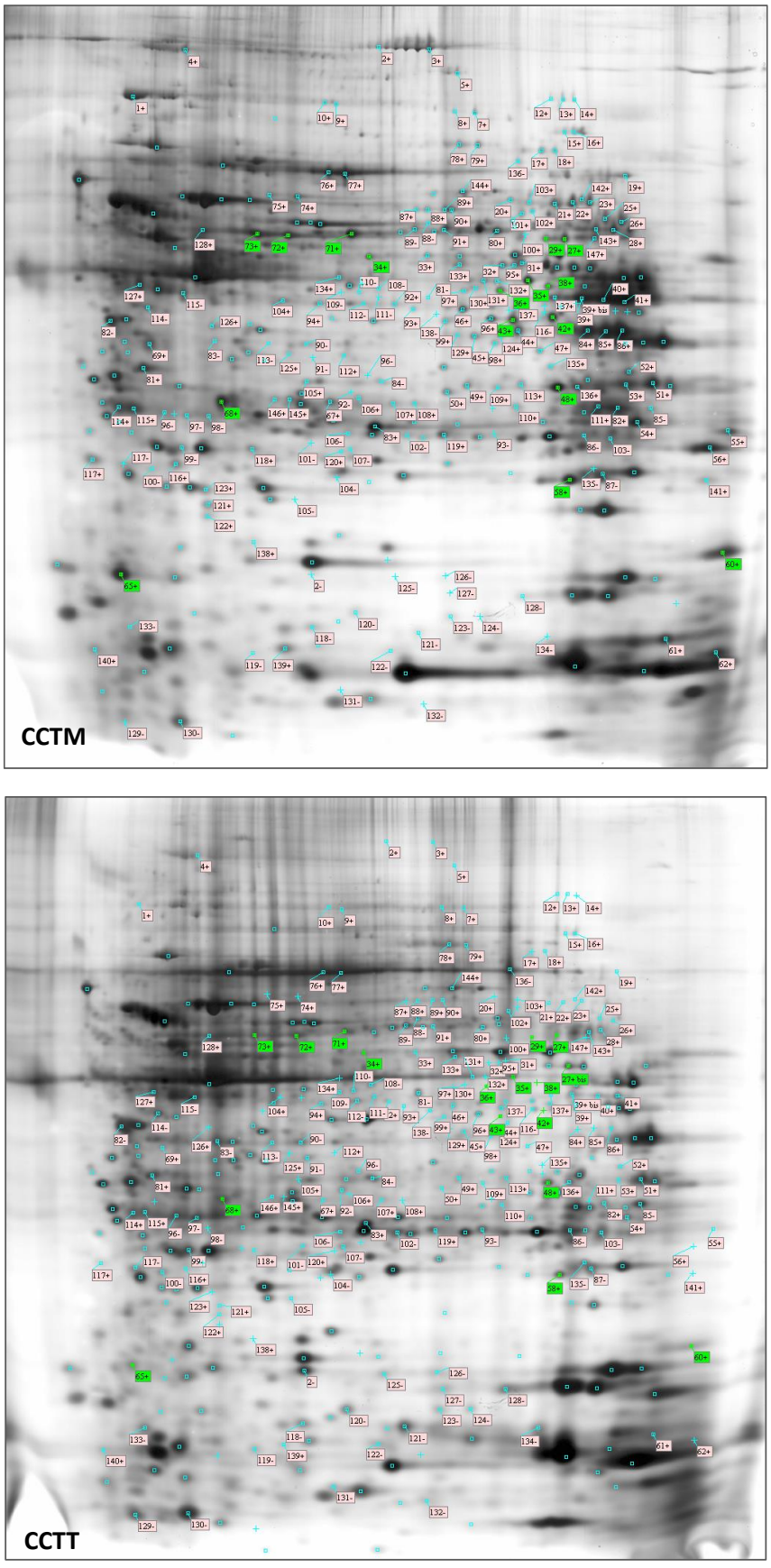

Figure 35. 2D-gels from CCTT and CCTM with the differentially expressed proteins; the liver proteins are shown with green labels.

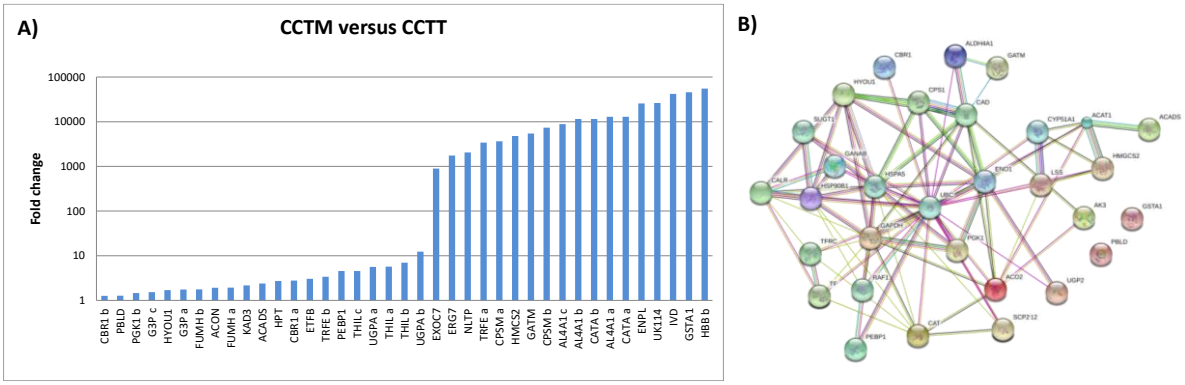

Figure 36. A) Histogram of the identified proteins, differentially expressed between CCMT and CCTT and plotted as log of log of fold change; B) Analysis of protein-protein interaction of the proteins performed by STRING database.

Among the identified proteins, a particular remark should be reserved to cathepsin D, for at least two reasons: the first is that CATD represents one of the most overexpressed proteins in CCMT compared to CCTT; the second reason is that also for CATD we found different isoforms (*Fig. 37*).

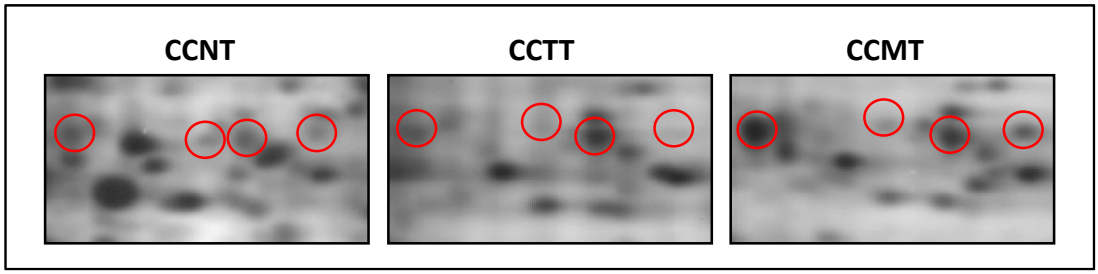

Figure 37. Sperimental window of 2D gels showing the different isoforms of CATD identified as differentially expressed between CCNT/CCTT/CCMT.

The human cathepsin D gene is located on the short arm of chromosome 11 in region p15 in the vicinity of the H-ras oncogene. Overexpression of this protease has been associated with the progression of several human cancers including gastric carcinoma, melanoma, and ovarian cancer (Saku T et al., 1990). Cathepsin D promotes tumor growth directly by acting to degrade and remodels the basement membrane and interstitial stroma surrounding the primary tumor and indirectly by stimulation of other enzymes or in cooperation with other cathepsins in the proteolysis process (Tan GJ et al., 2014). In breast cancer, cathepsin D is closely correlated with poor prognosis (Jacobson-Raber G et al., 2011). In CRC, the information's are limited, and results are contradictory with respect to the association between cathepsin D expression or activity and prognosis of CRC: some authors have described a significant relationship between overexpression of cathepsin D and a trend towards advanced tumor stages, other studies have demonstrated the opposite (Kuester D et al., 2008). Recently it was reported that cathepsin D

expression was significantly greater in cells from invasive front (IF) area and liver metastasis (LM) than those from main tumor body (MTB). Moreover, cathepsin D expression in cells from the MTB was highly elevated in late stage CRC and showed significant correlation with subsequent distant metastasis and shorter cancer-specific survival (Kirana C el al., 2012). This result is in agreement with our finding and suggests the possible role of cathepsin D as prognostic biomarkers in colon cancer. Subsequently, a western blot analysis was performed on a subset of colon and paired normal tissues (n = 17), in order to detect cathepsin D expression (*Fig. 38***)**.

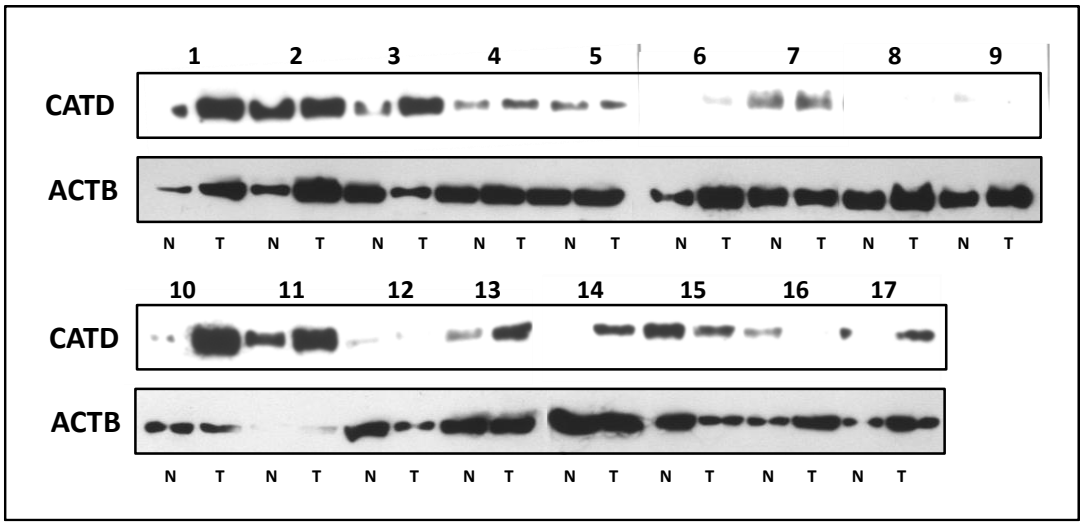

Figure 38. Western blot analysis of cathepsin performed on a subset of colon and paired normal tissues (n = 17). Expression of Actin B was used as loading control.

The cathepsin expression is almost variable among the analyzed paired samples. A general up-regulation of cathepsin D expression was observed in colon cancer tissue compared to the normal adjacent tissue, even if in some cases no difference or a decrement was observed. Other authors have reported differential regulation of cathepsin D expression by mutant versus wild-type p53 may contribute to variable cathepsin D levels in colorectal cancers (Iacobuzio-Donahue C et al., 2004).

Confirmation of Transgelin and Cathepsin expression in CRC with microarray data set

To further validate our data, we analyzed public microarray data sets from GEO. As expected, the analysis (*Fig. 39*) showed that the expression level of TAGL was down-regulated, while the expression level of CATD was up-regulated significantly in metastatic CRC ($p < 0.05$).

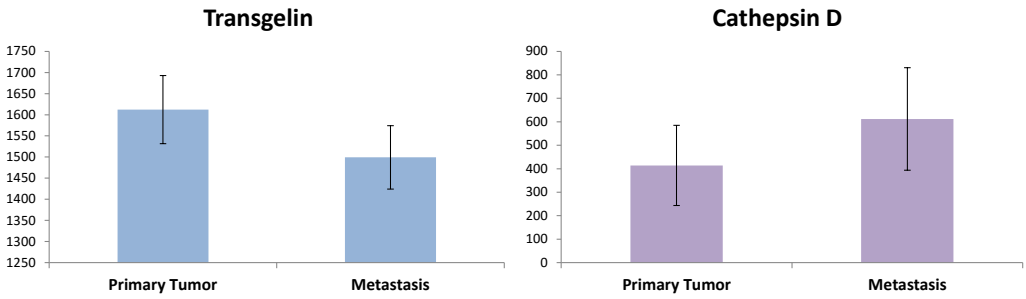

Figure 39. Publicly available microarray data set (GSE28702) for validation. Low expression of TAGL and high expression of CATD was associated with CRC metastasis.

Conclusion

Differential proteomics allow us to identify candidate biomarkers for colon cancer detection and prognosis. The first proposed biomarker is TAGL, identified as a down-regulated protein in colon cancer tissues compared to the normal adjacent tissues. The second proposed biomarker is CATD, identified as up regulated protein in liver metastasis compared to colon cancer tissue.

RESULTS PART II

Background and aim

MMP-2 and/or MMP-9 are overexpressed in many carcinomas, by virtue of their important role in tumor invasion and metastasis. Several studies have already evaluated the diagnostic and prognostic value of circulating MMP-2 and MMP-9. Elevated levels of both MMP-2 and MMP-9 have been found in blood from breast cancer patients and repeatedly associated with advanced stage, lymph node metastasis and poor prognosis (Coskun U et al., 2007). In serum of colon cancer patients it was demonstrated that Pro-MMP-9, but not Pro-MMP-2, is significantly higher compared to the normal sera (Pucci-Minafra I et al., 2001). In addition, several oligomeric circulating and tissue forms of MMP-9 are preferentially found in the oncologic samples, both in mono- and second-dimension zymograms. The aim of this part of thesis was to assess the levels of MMP-2 and MMP-9 in cancer tissues from breast and colon cancer patients, and paired normal tissues. Our investigations were performed in a cohort of 24 patients with ductal breast cancer and 26 patients with colorectal cancer.

Gelatin Zymography in tissue extracts

MMP-2 and/or MMP-9 are overexpressed in many carcinomas, by virtue of their important role in tumor invasion and metastasis. Several studies have already evaluated the diagnostic and prognostic value of circulating MMP-2 and MMP-9. Elevated levels of both MMP-2 and MMP-9 have been found in blood from breast cancer patients and repeatedly associated with advanced stage, lymph node metastasis and poor prognosis (Coskun U et al., 2007). In serum of colon cancer patients it was demonstrated that Pro-MMP-9, but not Pro-MMP-2, is significantly higher compared to the normal sera (Pucci-Minafra I et al., 2001). In addition, several oligomeric circulating and tissue forms of MMP-9 are preferentially found in the oncologic samples, both in mono- and second-dimension zymograms.

The aim of this part of thesis was to assess the levels of MMP-2 and MMP-9 in cancer tissues from breast and colon cancer patients, and paired normal tissues. Our investigations were performed in a cohort of 24 patients with ductal breast cancer and 26 patients with colorectal cancer. The *Fig. 40* shows the zymograms relative to the matched samples in the two classes of patients.

In general, the zymographic analysis showed the presence of higher lytic activity in the tumor extract compared to normal counterpart, although with different enzymatic profile changes between patients. The observed lytic bands correspond to Pro-MMP-9 (92 kDa) and Pro-MMP-

2 (72 kDa), with high levels of significance compared to normal tissues and with greater expression of the Pro-MMP-9 with respect to Pro-MMP-2, both in breast and colon patients. Further, bands belonging to the activated enzymatic forms are distinguished (MMP-9 83 kDa and 67 kDa MMMP-2), which are undetected in paired normal breast tissues, and expressed in some normal colon tissues. Finally, some tumor samples show bands of high molecular weight, correspondent to complexes formed between gelatinases and inhibitors. In particular, the band of 200 kDa corresponds to Pro-MMP-9 dimers, while the band of 116 kDa corresponds toPro-MMP-9- TIMP-1 complexes. In particular, the levels of Pro-MMP-9 and Pro-MMP-2 are higher in tissues extracted from colorectal cancer compared to tissues of breast cancer, while the activated forms are more expressed in breast tumor tissue. Lytic bands were quantified by three different experiments and comparative analysis between the expression of MMPs in normal and pathological tissue samples (breast and colon) was performed using t-test (*Fig. 41*). Statistical significant differences were found both in breast and colon for all detected MMPs between normal and cancer tissues ($p<0.05$). Moreover, a higher level of expression was detected for Pro-MMP-9 in colon cancer tissues compared to breast cancer tissues.

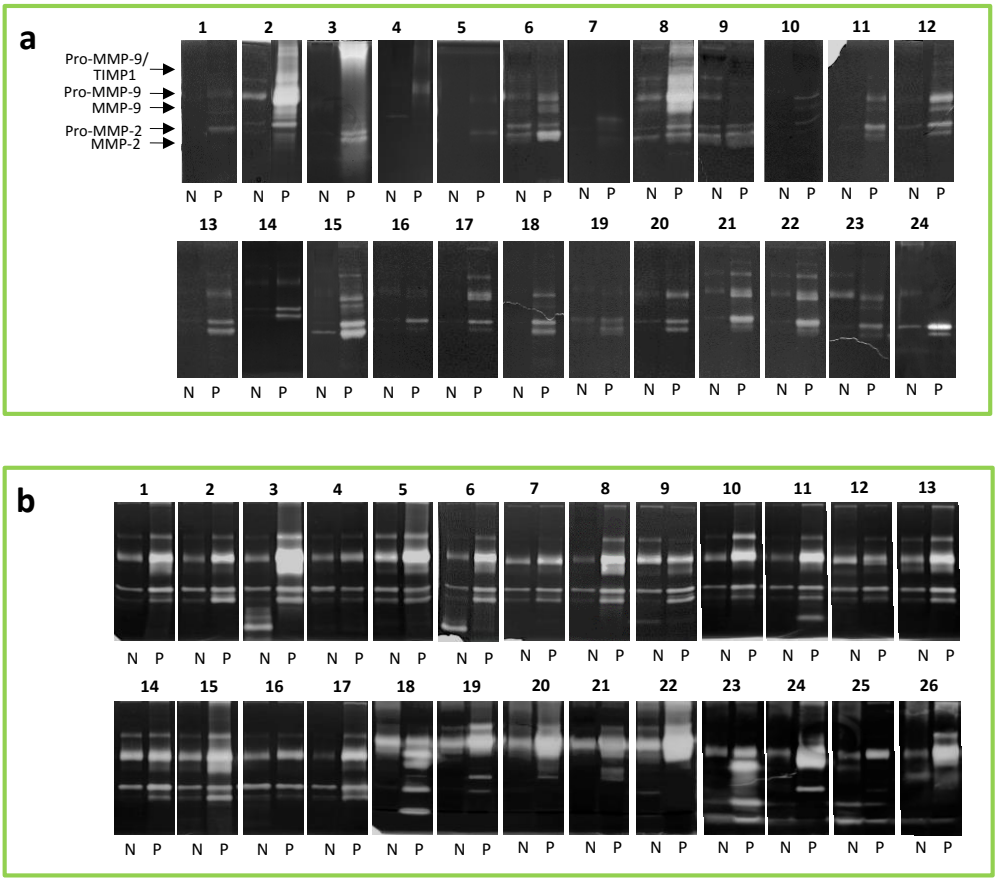

Figure 40. Representative gelatin zymograms (7.5% SDS-PAGE) of tissue extracts from breast (a) and colon carcinoma (b). Pathological tissues are indicated with P and paired normal tissues with N.

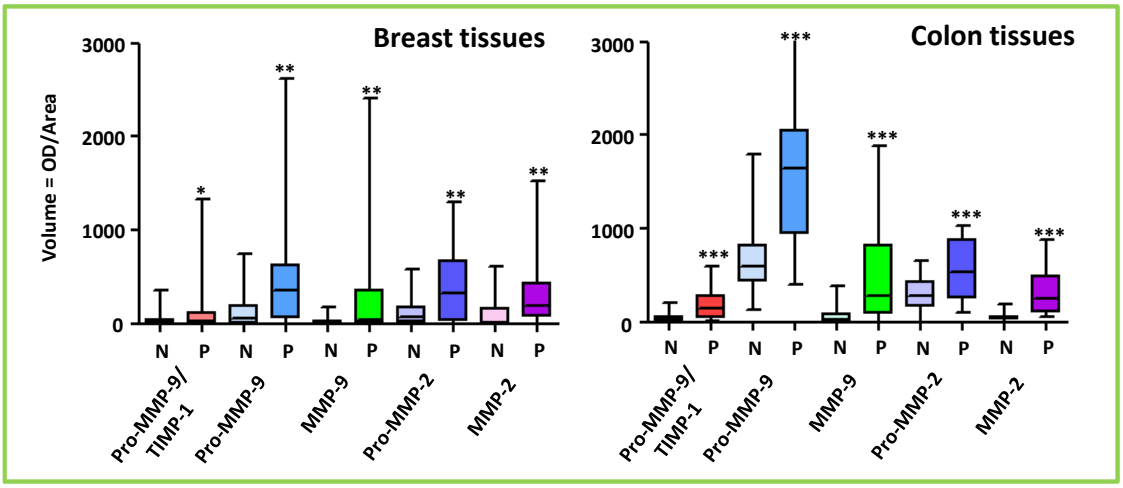

Figure 41. Quantitative analysis of MMPs expression, given as box-plot graphs in breast and colon cancer tissues (P) and paired normal adjacent tissues (N). Quantification was performed using Image Master Software. Statistical significance was assessed by the Students't-test.

Gelatin Zymography in serum samples

We also evaluated the expression levels of gelatinase in serum samples of patients previously analyzed. Therefore, we tested sera of 24 patients with ductal breast cancer (*Fig. 42a*) and sera from 26 patients with colorectal carcinoma (*Fig.42b*).

As expected in sera samples are not detectable the active forms of MMP-9 and MMP-2. Both in breast and colon sera, MMP-9 is almost variable than MMP-2. In order to detect if the circulating MMPs correlate with tissues'expression we performed a correlation analysis using Pearson test (*Fig. 43*). Unfortunately, no significant correlation was found between the sera and tissues MMPs expression, suggesting a complex regulation of MMPs in different tissues.

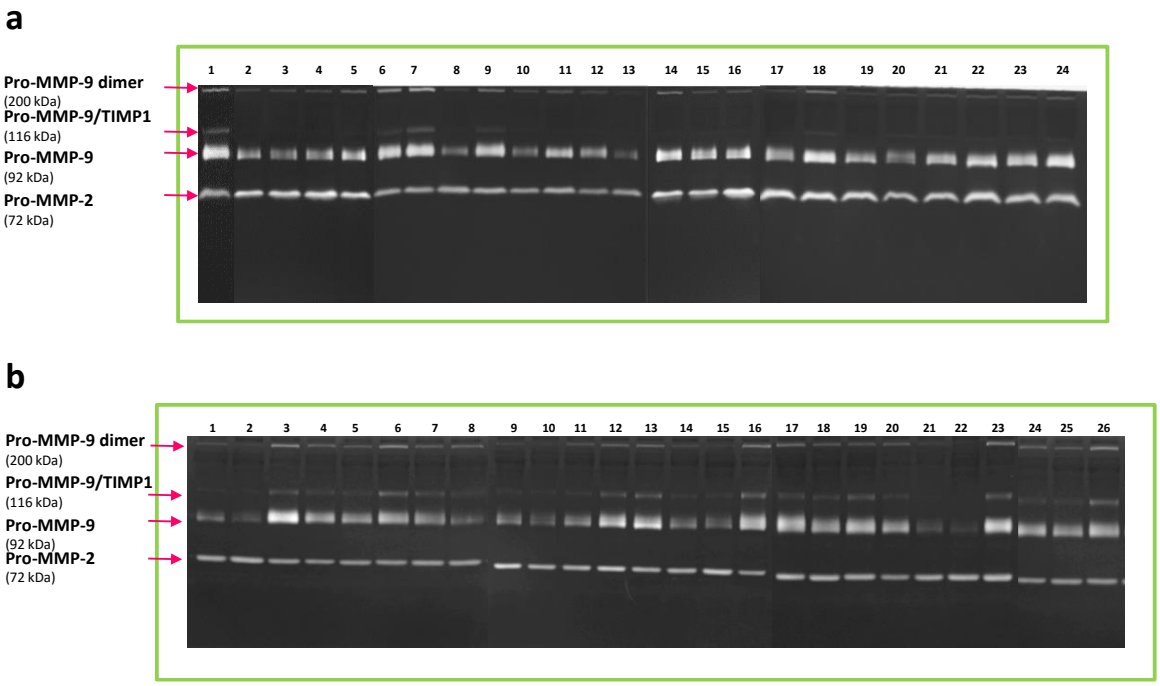

Figure 42. Gelatin zymography performed on 24 serum samples of patients with breast carcinoma (a) and 26 serum samples of patients with colorectal carcinoma (b).

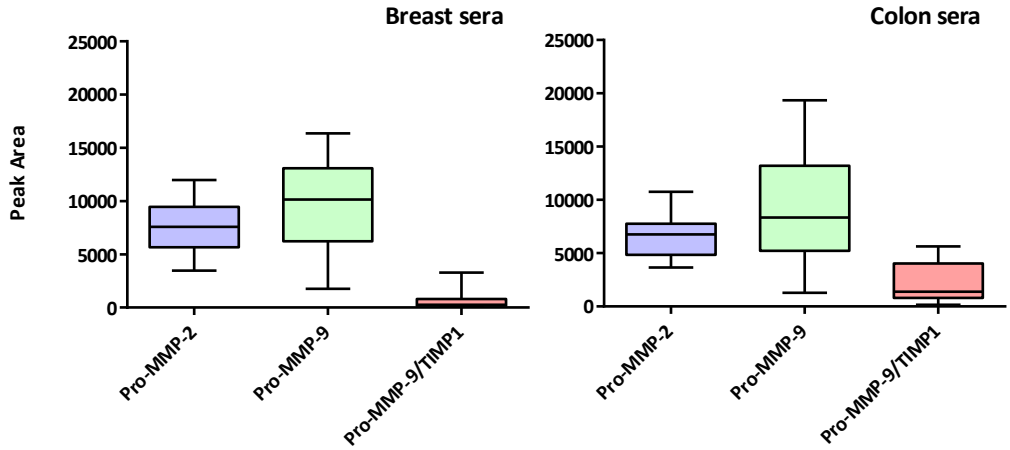

Figure 43. Quantitative analysis of MMPs expression, given as box-plot graphs, in 24 breast cancer sera and 26 colon cancer sera. Quantification was performed using Image J. Statistical correlation with MMPs expressed in pathological tissues was analyzed by the Pearson correlation.

RESULTS PART III

Background and aim

Attempts to reduce morbidity and mortality in breast cancer is based on efforts to identify novel biomarkers to support prognosis and therapeutic choices. One class of proteins that is emerging as a potentially important group of markers in cancer development and progression is the S100 family. The association between S100 family members and tumors may be explained by several observations: firstly, the region of human chromosome 1q21, where most of S100 genes are clustered, is prone to genomic rearrangements, likely supporting the tumor progression; secondly, several S100 members show altered expression levels in cancer cells compared to normal cells and are differentially expressed in various malignancies, according to types and stages of cancer. Finally, a number of S100 proteins have been shown to interact with and to regulate various proteins involved in cancer and exert different effects on p53 activity. Moreover, S100 proteins possess a wide range of biological functions that can alter and regulate the major phenotypic features of cancer, including proliferation, apoptosis, metastasis, tumor microenvironment and cancer stem cells (*Fig. 44*)

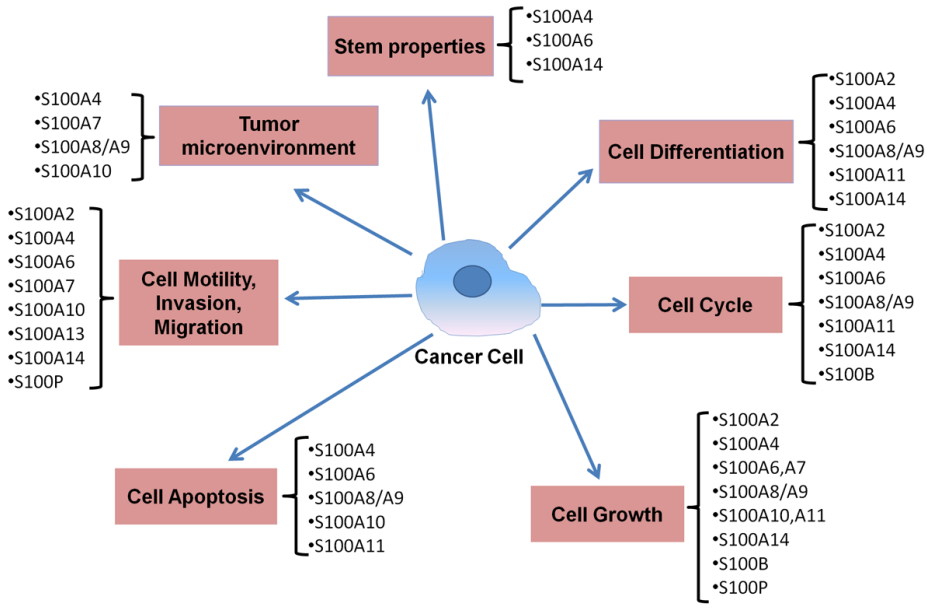

Figure 44. Different roles of S100 proteins during key steps of tumorigenic process. S100 proteins are involved in many aspects of phenotypic features of cancer including regulation of cell differentiation, cell cycle progression, cell proliferation, cell apoptosis, cell motility, invasion and migration, tumor microenvironment and cancer stem cells.

A large-scale proteomic investigation performed on breast cancer patients for the screening of multiple forms of S100 proteins (Cancemi P et al., 2010), showed that the majority of S100 proteins were present at very low levels, if not absent, in the non-tumoral tissues adjacent to the

primary tumor. The proteomic screening performed on 100 cryo-preserved breast cancer tissues, showed that some S100 protein members were ubiquitously expressed in almost all patients, while others appeared more sporadic among the same group of patients. Most, if not all, of the detected S100 members appeared reciprocally correlated. More interestingly, patients which developed distant metastases after a three year follow-up showed a general tendency of higher S100 protein expression, compared to the disease-free group. Subsequently, it also investigated the incidence of S100A7 protein in breast cancer patients and its correlation with the collective profile of cancer patients' proteomics (Cancemi P et al., 2012). However, the exact role of S100 proteins in cancer progression as well as the potential molecular mechanism in tumorigenesis still remain obscure. PI3K/AKT signaling pathway is associated with several cellular functions such as cell proliferation, differentiation and intracellular trafficking, all of which are involved in cancer development. Several in vitro studies provided evidence showing that activation of the PI3K/AKT/mTOR signaling pathway is involved in the oncogenic property of some S100 proteins: for example S100A4 (Wang H et al., 2014) and S100A2 (Naz S et al., 2014). Moreover, extracellular S100 proteins, exert their functions bind to RAGE and trigger RAGE-mediated cellular signaling which involves MAP Kinase, NF-κB, and phosphatidylinositol 3-kinase (PI-3K)/AKT signaling pathway. Therefore, in this study, taking advantage from our previous S100 proteomic results, we investigated the possible correlation between AKT signaling and S100 proteins expression. Our analysis was also extended to IGF-1R and MMPs for their prominent involvement in breast cancer progression. Moreover, we aimed to assess the in silico prognostic value of S100 gene expression levels utilizing a breast cancer dataset generated on Affymetrix microarrays technologies.

AKT-1 and p-AKT expression in matched breast cancer tissues (BCT) and non-tumoral adjacent tissues (NAT)

The expression of AKT-1 and its phosphorylated form (p-AKT) was analyzed by western blot, in a group of 24 breast cancer tissues and their matched normal adjacent tissues (*Fig. 45***)**. Although both AKT-1 and p-AKT were generally more expressed in the tumor tissues compared to adjacent normal counterpart, no statistically significant difference was found between the two groups (*Fig. 46).* The expression levels of the proteins analyzed by Western blot were not normalized with the β Actina (ACTB) expression, since, as previously reported, the proteomic profile of non tumoral tissue extracts reveals the almost exclusive presence of serum and blood proteins, consisting mainly of albumin, immunoglubulins, and other globulins,

suggesting that this different pattern is due to the reduced amount of parenchyma in the mammary gland of healthy adult women, opposed to the abundant cell population present in the tumor core.

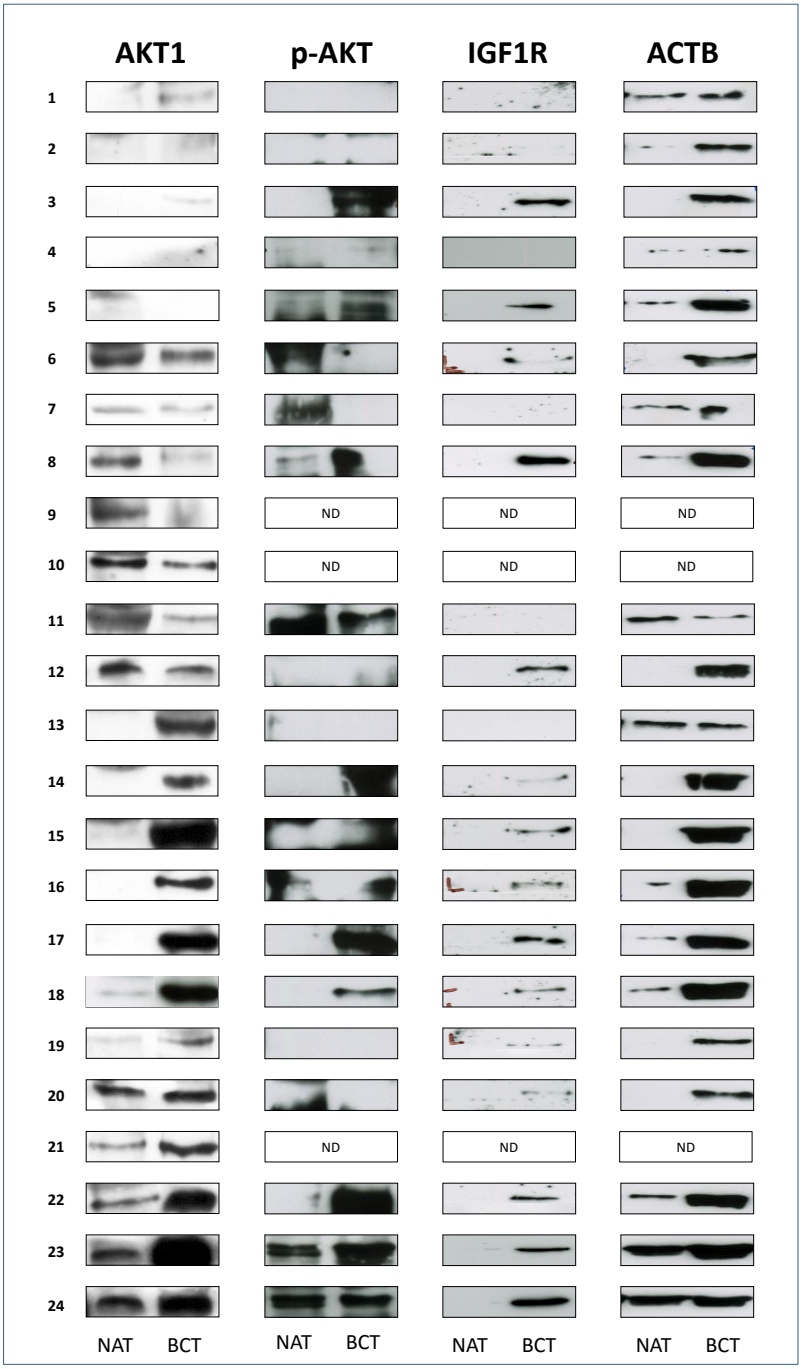

Figure 45. Western blot analysis of AKT-1, p-AKT, IGF-1R and ACTB, in 24 breast cancer tissues (BCT) and matched normal adjacent tissues (NAT); ND = Non detected.

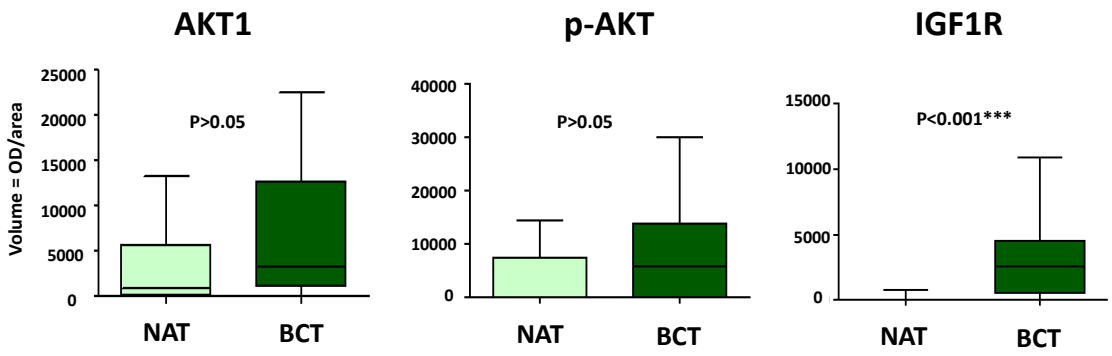

Figure 46. Quantitative analysis of AKT-1, p-AKT and IGF-1R expression, given as box-plot graphs in 24 breast cancer tissues (BCT) and matched normal adjacent tissues (NAT). Quantification was performed using Image Master Software. Statistical significance was analyzed by the Students' t-test.

IGF-1R expression in matched breast cancer tissues (BCT) and non tumoral adjacent tissues (NAT)

The expression of *insulin-like growth factor receptor 1* (IGF-1R) was also analyzed because several studies have shown that it is involved in the activation of the AKT pathway and, on the contrary, its inhibition is associated to a decrease of p-AKT. The antibody recognized only the β subunit of the IGF-1R (containing the intracellular portion with tyrosine kinase residues), with a molecular weight of 97 kDa (*Fig. 45*). IGF-1R was almost exclusively present in the tumor extracts, and statistically significant difference was found between the two groups ($p<0.001$***) (*Fig. 46*).

AKT-1 and p-AKT expression in breast cancer tissues

The expression of AKT-1 and p-AKT proteins was then evaluated in a larger cohort of patients (n=87) (*Fig. 47*). As previously reported, since the cellularity of the tumor biopsy, that is, cell densities within an area of the surgical sample, may be very variable among the different subjects, the expression levels of AKT-1 and p-AKT were normalized to the ACTB.

IGF-1R expression in breast cancer tissues

IGF-1R expression has been evaluated in 48/87 breast cancer tissues examined, to verify the possible correlation between the expression of the receptor and activation of the AKT pathway. Our results (*Fig. 48*) showed that IGF-1R is expressed in almost all samples, although with different levels of intensity. However, no significant correlation was found with AKT-1and p-AKT.

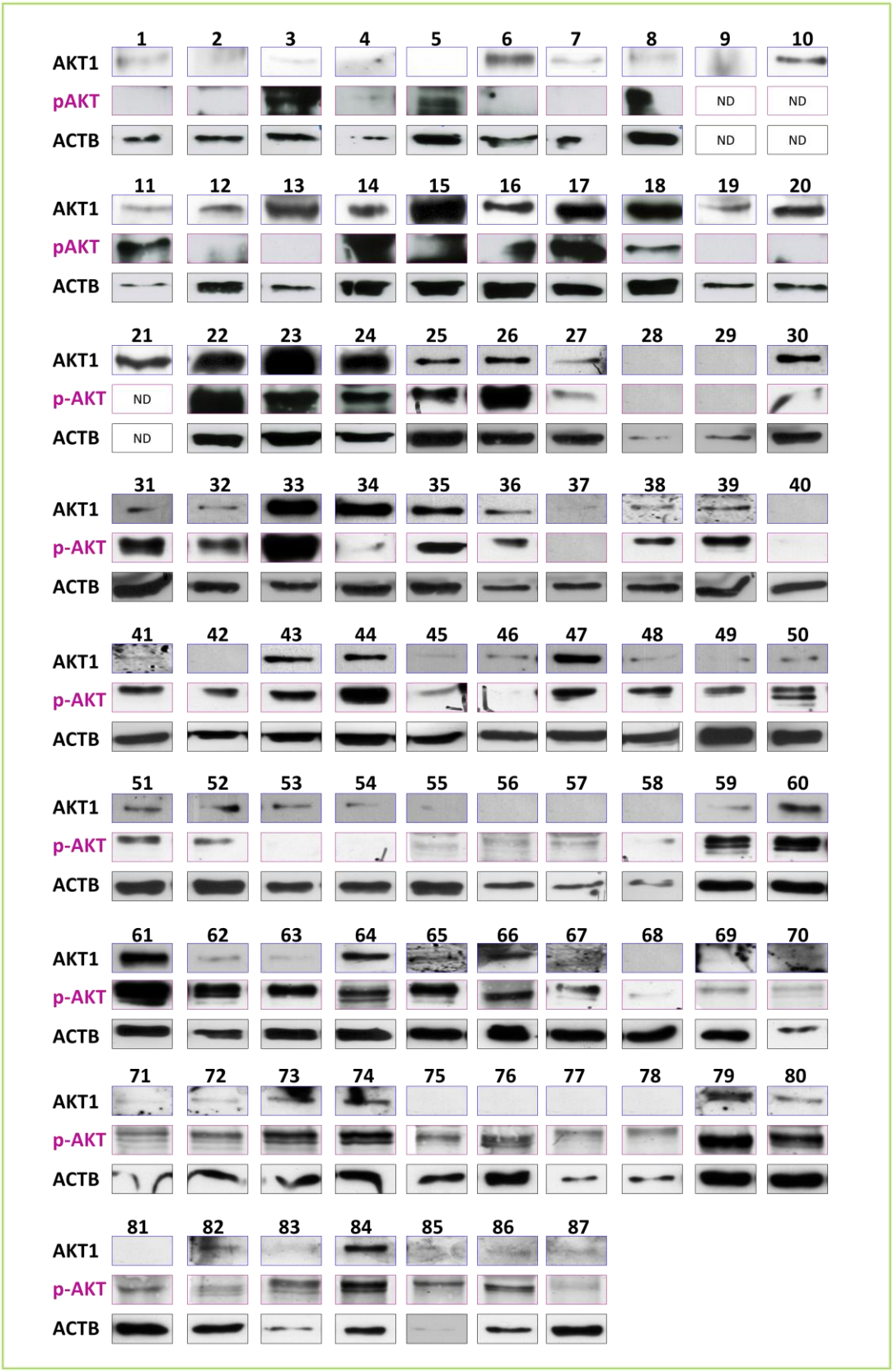

Figure 47. Western blot analysis of AKT-1, p-AKT and ACTB in 87 tissue samples from breast cancer. ND = Non detected.

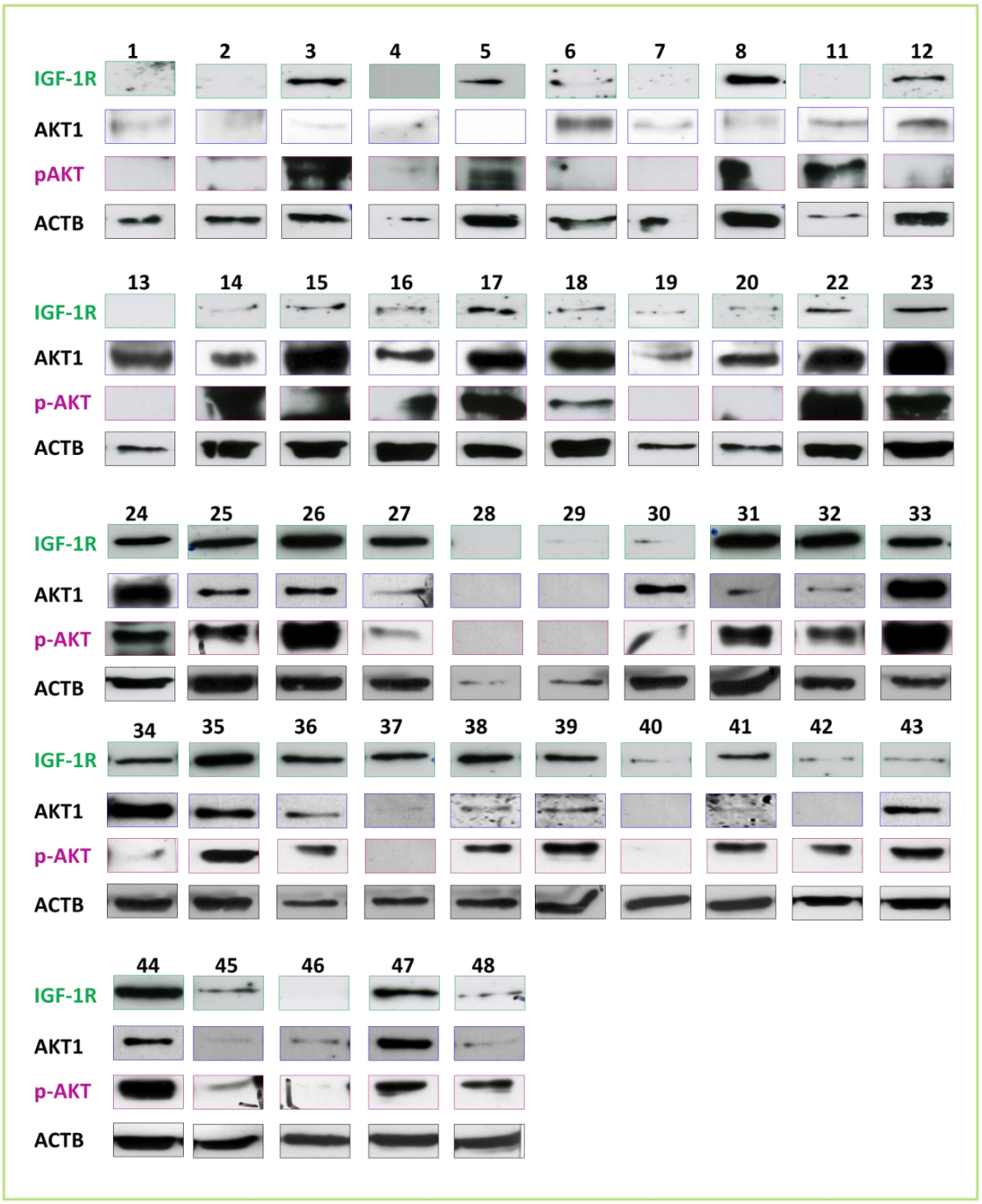

Figure 48. Western blot analysis of IGF-1R in 48 tissue samples from breast cancer.

Zymographic detection of MMP-9 and MMP-2 in breast cancer tissues

The secretion of extracellular proteases plays an important role in tumor invasion and metastasis. Of these proteases, the matrix metalloproteinases (MMPs) have been shown to have increased expression correlated with the progression of various types of tumors. The expression of MMP-2 and MMP-9 has been found to correlate with the metastatic potential of tumor cells. Especially, MMP-9 (gelatinase B/92 kDa type IV collagenase) is expressed in a large variety of malignant cells and degrades collagen, a major component of the ECM and basement membrane. We aimed to investigate the activity levels of MMP-2 and MMP-9 gelatinases in breast cancer tissues by means of zymographic analysis, and to correlate data with AKT-1, p-AKT, IGF-1R and with S100 proteins. *Fig. 49* shows the panel of zymograms from breast cancer tissues. The majority of breast cancer patients shows strong intensity of gelatinolytic bands for both the proenzymatic forms of MMP-2 (72 kDa) and MMP-9 (92 kDa). It is also detectable the active enzymatic forms of MMP-2 and of MMP-9.

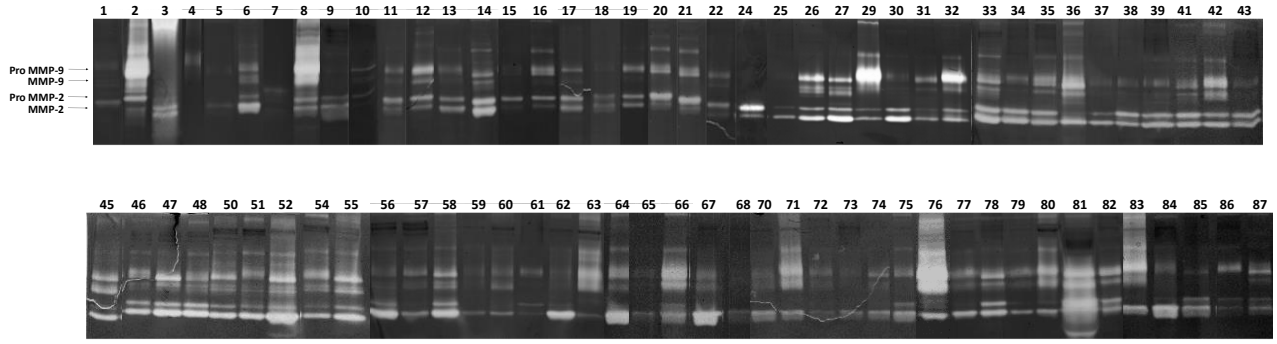

Figure 49. Panel of representative gelatin zymograms of breast cancer tissues.

Proteomic correlations of S100 proteins with AKT-1, p-AKT, IGF-1R and MMPs.

Correlation analyses of the relative expression levels of S100 proteins, identified in the 100 patients'map (Cancemi P et al., 2012) with AKT-1, p-AKT, IGF-1R and MMPs, were performed using Pearson correlation (*Tab. 3*). Surprisingly, no significant correlation was found between the investigated S100 proteins and AKT-1/p-AKT. On the contrary, several correlation were found between S100 proteins and Pro-MMP-9 (S100A7 a, S100A8), MMP-2 (S100A4, S100A8, S100A11 b, S100A11 c) and IGF-1R (S100A6 b, S100A7 a, S100A8). Our results are in agreement with some evidences showing the correlation between several members of S100 protein family and MMPs (Sapkota D et al., 2011; Zhang W et al., 2014; Silva EJ et al., 2014). Although referred to IGF-1R, several reports showed that IGF-1 increases the proteolytic activity and invasive potential of breast cancer cell lines through the activation of MMPs (Walsh LA and Damjanovski S, 2011).

	AKT1	pAKT	IGF1R	Pro MMP-9	MMP-9	Pro MMP-2	MMP-2
S100A2							
S100A4							p= 0.0030**
S100A6 a							
S100A6 b			p= 0.035*				
S100A7 a			p<0.001***	p= 0.005**			
S100A7 b							
S100A8			p=0.002**	p= 0.02*			p= 0.029*
S100A11 a							
S100A11b							p= 0.047*
S100A11 c							p= 0.004**
S100A13							
AKT1		p<0.001***					
pAKT	p<0.001***						
IGF1R				p=0.001**			p=0.03**
Pro MMP-9			p=0.001**		p<0.001***		p= 0.006**
MMP-9				p<0.001***		p= 0.018*	p= 0.005**
Pro MMP-2					p= 0.018*		p= 0.004**
MMP-2			p=0.03	p=0.006**	p=0.006**	p= 0.004**	

Table 3. Association analysis of expression levels of S100 members and AKT-1, p-AKT, IGF-1R and MMPs using Pearson correlation (*p<0.05 was considered as significant; **p<0.01 as highly significant; ***p<0.001 as very highly significant).

Prognostic value of S100 gene expression-based outcome

Our data on differential occurrence of S100 proteins in a large group of breast cancer patients at proteomic levels, strongly support the hypothesis that a significant deregulation of multiple S100 family members is associated with breast cancer progression, and suggest that these proteins might act as potential prognostic factors for patient stratification. However, the prognostic value of individual and/or collective S100 proteins in breast cancer remains elusive. The "*Kaplan–Meier plotter*" (KM plotter) generated survival and gene expression data from 4142 breast cancer patients (as of 2014), from Gene Expression Omnibus (GEO; www. ncbi.nlm.nih.gov/geo/) database. Thus, KM plotter can be utilized for the analysis of individual genes with clinical results to relapse-free survival and total survival of the patients. So far, a number of genes have been identified and/or validated by KM plotter in breast cancer (Zhou X et al; 2015; You Q et al; 2015).

Firstly, we determined the correlation of S100 gene expression of breast cancer patient with survival, utilizing Kaplan Meier Plotter for overall survival (OS), relapse free survival (RFS) and distant metastasis free survival (DMFS). The best specific probes (JetSet probes) that

recognized S100 proteins, selected using the multigene classifier (S100A1, S100A2, S100A3, S100A4, S100A5, S100A6, S100A7, S100A8, S100A9, S100A10, S100A11, S100A12, S100A13, S100A14), and auto select best *cutoff* was chosen in the analysis. As shown in *Fig. 50*, high levels of S100 expression were associated with decreased patient relapse free survival (RFS), overall survival (OS), and distant metastasis free survival (DMFS) (log-rank P<1E-16; 3.5E-5; 1.8E-6, respectively).

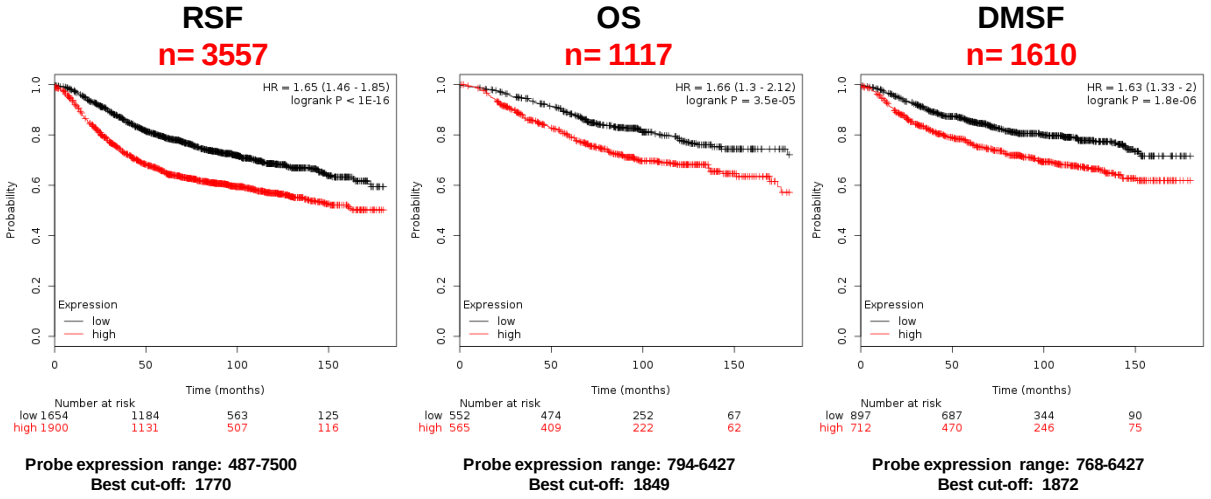

Figure 50. Kaplan-Meier analysis for RSF (relapse free survival), OS (overall survival), and DMFS (distant metastasis free survival in breast cancer patients according to the expression of S100 proteins (n = 3557, 1117 and 1610 respectively). Log-rank P and the hazard ratio (HR) (with 95% confidence intervals) was shown. Query parameters were: RSF, OS, DMSF, split patients by median, auto-select best cut-off and only JetSet best probe set.

Association of S100 gene expression-based outcome with histological and molecular subtypes

Next, we determined the correlation of S100 gene expression with relapse free survival, splitting patients according to ER, PR, lymph node and HER-2 status, histological grade and intrinsic subtype. High levels of S100 expression (*Fig. 51*) were associated with decreased patient relapse free survival (RFS), in all analyzed variables, except for ER^- and PR^+.

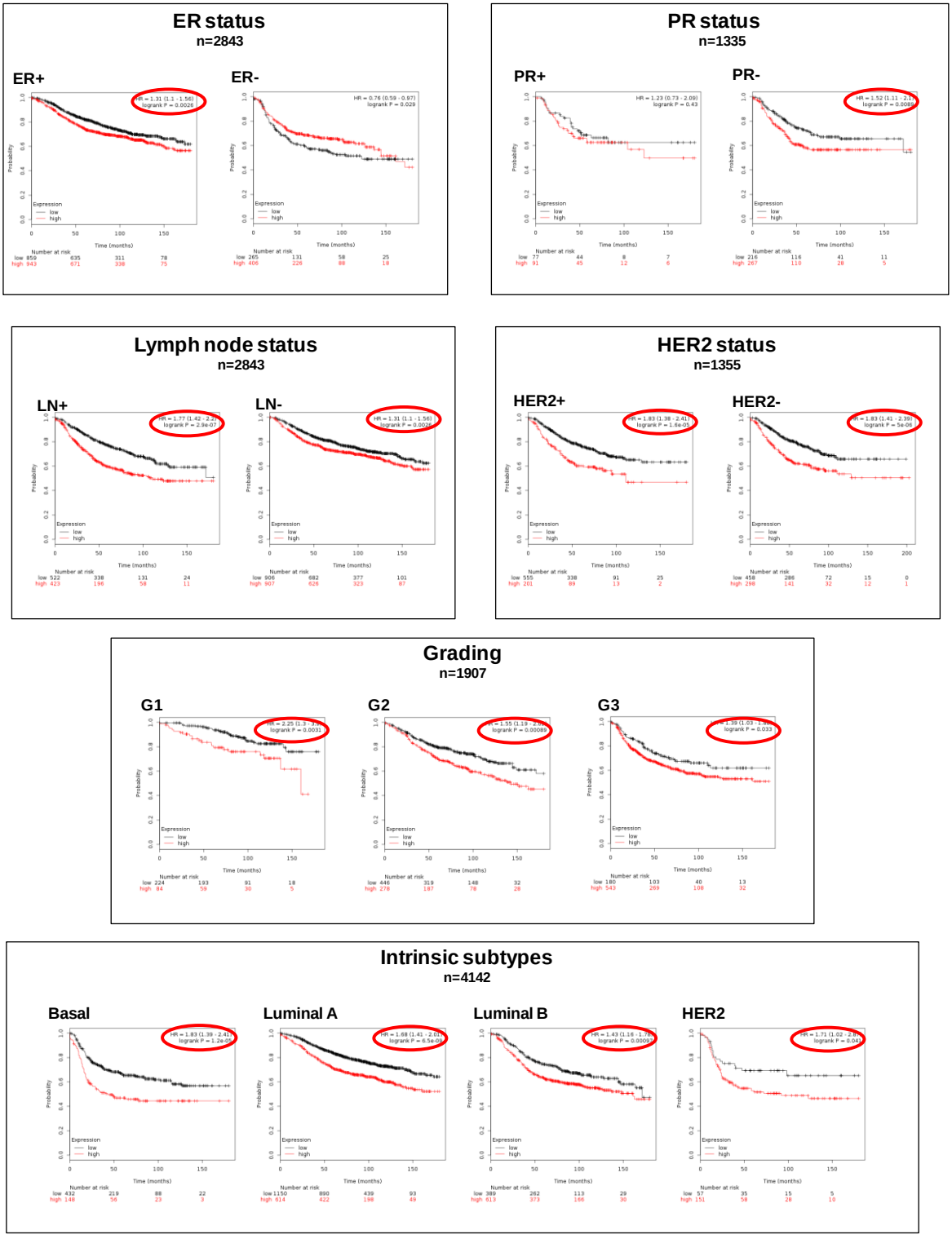

Figure 51. Kaplan-Meier analysis for RSF (relapse free survival), in breast cancer patients according to the expression of S100 proteins. Log-rank P and the hazard ratio (HR) (with 95% confidence intervals) was shown. Patients were stratified based on ER, PR, Lymph node, HER-2 expression, histological tumor grade, or intrinsic subtypes. Query parameters were: RSF, split patients by median, auto-select best cut-off and only JetSet best probe set.

Our results showed for the first time that high levels of S100 proteins may represent an independent predictor of survival in breast cancer.

Finally we want assess if a particular S100 was predictive of outcome. Therefore, we analyzed the correlation of individual S100 gene expression with relapse free survival (RFS) (*Fig. 52*).

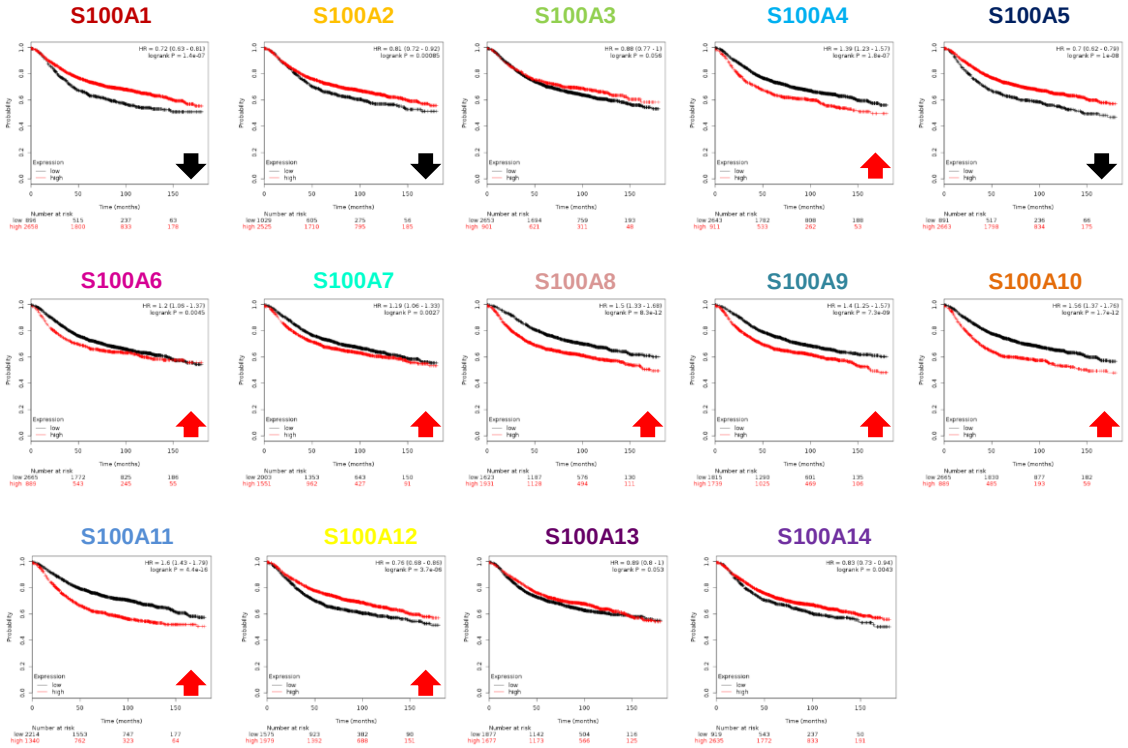

Figure 52. Kaplan-Meier analysis for RSF (relapse free survival), in breast cancer patients according to the expression of individual S100 proteins. Log-rank P and the hazard ratio (HR) (with 95% confidence intervals) was shown. Query parameters were: RSF, split patients by median, auto-select best cut-off and only JetSet best probe set.

Except for S100A3, S100A13 and S100A14, all individual S100 proteins tested were significantly associated with survival. In particular, while high levels of S100A4, S100A6, S100A7, S100A8, S100A9, S100A10, S100A11, S100A12 were negatively associated with relapse free survival, low levels of S100A1, S100A2 and S100A5 increase patient RFS. The complexity of different patterns of alterations implies S100 proteins might act as both friend and foe and exert both pro- and anti- tumorigenic actions in breast cancer.

Conclusion

Here we report for the first time a large proteomic characterization of AKT signaling in breast cancer. It is showed a high variability of AKT-1 and p-AKT in breast cancer tissues and paired normal adjacent tissues. Moreover, no correlations were found between S100 and AKT-1 and

p-AKT, as well as with MMPs, suggesting a more high level of complexity in regulatory mechanisms of this key pathway in breast cancer.

Finally, important correlation between IGF1R and MMPs were found, suggesting a possible link between growth factors signaling and MMPs regulations.

Conclusively, our integrating results obtained by proteomic and trascriptomic analysis of S100 proteins highlight their important involvement in breast cancer progression. Future studies are needed to disclose molecular mechanisms and signaling pathways that define the multiple and specific roles of S100 proteins in breast cancer, providing novel therapeutic targets and biomarkers.

RESULTS PART IV

Background and aim

Nanoscience and nanotechnology has received a great interest over the last few years, due to its potential applications on many scientific areas such as energy, medicine, pharmaceutical industries, electronics, and space industries. In particular, nanoparticles (NPs) showing unique chemical, physical, and biological properties are of extraordinary interest for biomedical such as medical imaging, drug delivery and chemotherapeutics (Salata OV, 2004).

Silver nanoparticles (Ag NPs) exhibit a variety of biological effects, such as antibacterial, antifungal, antiviral, and antinflammatory, and thus are attracting interest for a wide range of biomedical applications, such as molecular imaging, drug delivery, and the development of materials and medical devices with antimicrobial properties (dos Santos CA et al., 2014). In this regard, there is a growing need to develop reliable, nontoxic, clean, ecofriendly, and green experimental protocols for the synthesis of AgNPs (Iravani S et al., 2014). Biological systems for synthesis of NPs are based on natural processes such as use of enzymes, microbial enzymes, vitamins, polysaccharides, biodegradable polymers, microorganisms. Among these, the most promising approach is based on the use of bacteria (Iravani S, 2014). Therefore, a wide number of bacterial species have been used as potential biofactory for the synthesis of metal-NPs, including silver. The mechanism of biological formation of metal-NPs is due to multiple biochemical characteristics or abilities. Among these, the most studied is the capability of biopolymers and, in particular, microbial exopolysaccharides (EPS) to act as metal reducers and/or stabilizers (Kanmani P and Lim ST, 2013). In fact, polysaccharides have hydroxyl groups, a hemiacetal reducing end and other functionalities, that can play important roles in both the reduction and the stabilization of metallic nanoparticles that creates vast opportunities for their utilization and potential mass production.

The EPS of Klebsiella oxytoca DSM 29614 has a peculiar structure consisting of a branched heptasaccharide repeating unit in which sugars are linked by alpha and beta glycosidic bonds and contains: 1 galactose (Gal), 4 rhamnoses (Rha) and 2 glucuronic acids (GlcA), one of which is present in the branch (Baldi F et al., 2001; Leone S et al., 2007; Gallo G et al., 2012). Moreover, the EPS of KO show metal-binding properties, producing metal NPs embedded in this EPS (Baldi F et al. 2010). Silver nanoparticles embedded in the exopolysaccharide of K. oxytoca DSM 29614 differ from other ‘‘Ag-bionanoparticles’’ (Sintubin L et al., 2011), because AgNPs are separated from the cells and are embedded in the extracted EPS. Besides, heavy metal salts are not added to the polysaccharide with the purpose to use it as reducing and

capping agent for Ag^+ (Vigneshwaran N et al., 2006). The capability of K. oxytoca DSM 29614, in synthesizing a specific EPS (Leone S et al., 2007) as a complexing agent for metals, is the result of the environmental adaptation to the acid mine drainages, where the strain was firstly isolated. During the growth, Ag^+ is also partially reduced to Ag^0 and both chemical forms are naturally embedded in the matrix (Baldi F et al., 2011; Battistel D et al., 2015). This characteristic makes these AgNPs unique and different from all the other AgNPs prepared biologically and described so far. It is recently demonstrated that AgNPs-EPS synthesized by Klebsiella oxytoca DSM 29614 cause DNA fragmentation in E. coli cells (Baldi F et al 2016). Silver nanoparticles (AgNPs) were biosynthesised by a Klebsiella oxytoca strain BAS-10, which, during its growth, is known to produce a branched exopolysaccharide (EPS). The produced silver nanoparticles embedded in EPS (AgNPs-EPS) containing different amounts of Ag(0) and Ag(I) forms, established by scanning electrochemical microscopy (SECM).

For these reasons, we aimed to investigate the cytotoxic activity of both AgNPs-EPS, prepared under aerobic and anaerobic conditions, and named as Ag^0 and Ag^{+1} NPs, in breast (SKBR-3 and 8701-BC) and colon cancer (HT-29 and HCT-116) cell lines, and highlight their possible mechanism of action. Since cancer cells have an altered metabolism in the glycolytic direction (Warburg effect), and utilize glucose as an energy font even in the presence of O_2, we believe that they are able to sense the presence of the sugars present in the EPS and to pick it with greater efficiency compared to normal cells.

Cell Proliferation Assay

The potential cytotoxic effects induced by AgNPs-EPS were investigated on two human breast cancer cell lines (SKBR-3 and 8701-BC) and two human colon cancer cell lines (HT-29 and HCT-116) by using the MTT assay. The cells were seeded in a 96-well plate at cell density of $5x10^3$ cells/well and after 24 hours, a series of different doses (racing by 500µg/ml to 0.005µg/ml) of Ag^0NPs-EPS, Ag^{+1}NPs-EPS and NaNPs (produced in the presence of Na-citrate, as a positive control) were used to treat the cells for 24 hours at 37°C.

The in vitro screening of the AgNPs showed potential cytotoxic activity of Ag^{+1}NPs-EPS and not for Na and Ag^0NPs-EPS, against the human breast cancer (SKBR-3 and 8701-BC) cell lines. Less cytotoxicity of synthesized AgNPs against the human colon cancer (HT-29 and HCT-116) cell lines was detected (*Fig. 53*). These results indicate a prominent sensitivity of breast cancer cell lines with respect to the colon cancer cell lines. In particular, SKBR-3 cells proliferation was significantly inhibited by Ag^{+1}NPs with an IC 50 value of 5µg/ml, while an IC 50 value of 7µg/ml was found for 8701-BC cell line. Subsequently, further investigations

were performed on SKBR-3 cell line, utilizing the concentration of treatments equal to 5µg/ml, corresponding to the IC50 value of Ag^{+1}NPs-EPS.

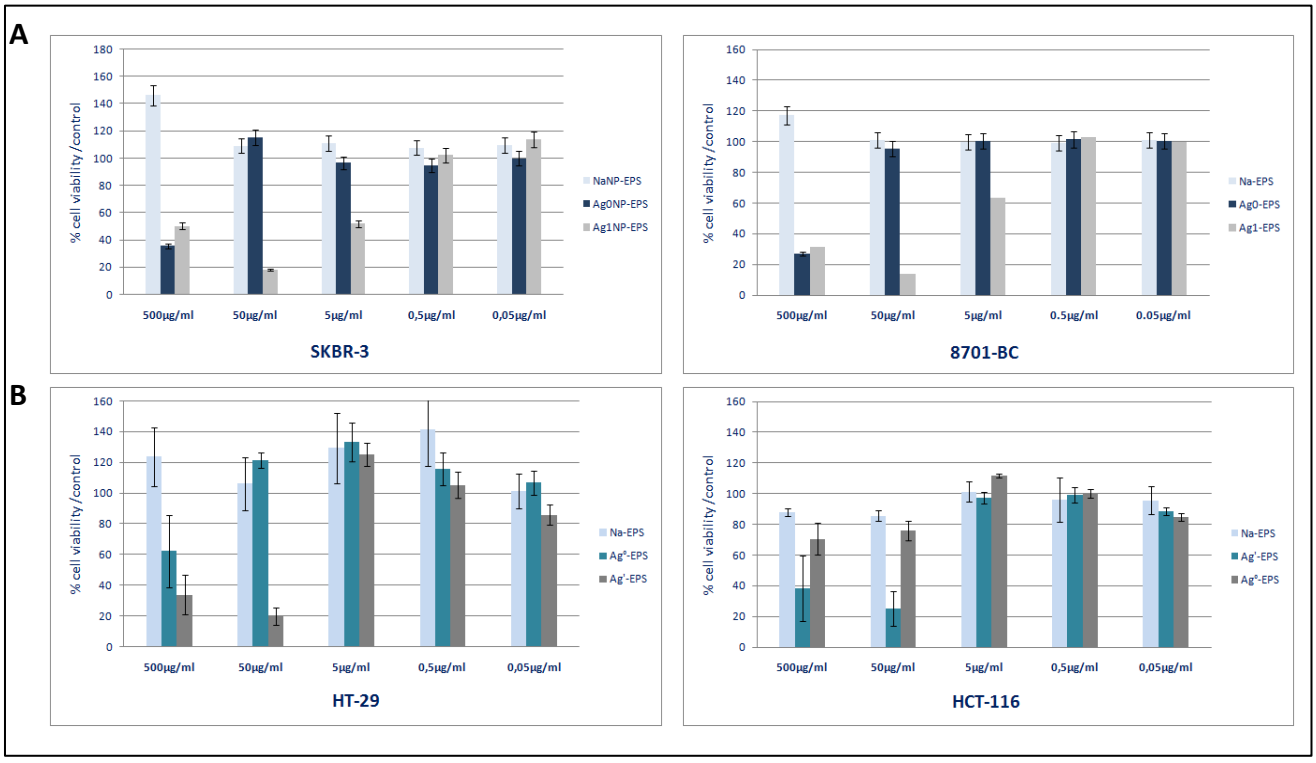

Figure 53. Proliferation assay of human breast cancer cell lines (SKBR-3 and 8701-BC) and human colon cancer cell lines (HT-29 and HCT-116) treated for 24 h with different concentrations of Ag^{0}NP-EPS, Ag^{+1}NP-EPS and NaNP-EPS. Results were expressed as percentage of viable cells with respect to untreated control (100%) as means ± s.d.

Colony-formation assay

In order to assess SKBR-3 cell viability in terms of reproductive capacity after AgNPs-EPS treatment, clonogenic survival assay was performed. The cells were treated with different concentrations (50 and 5µg/ml) for 1 and 24 hours, and then incubate for 10 days. Colonies were counted and quantification was done. (*Fig. 54*). A p value less than 0.05 was considered significant, a p value less than 0.01 was considered high significant and a p value less than 0.001 very high significant. Ag^{+1}NPs-EPS treatment decrease the colony-forming ability of SkBR-3 cells compared to the control cells in a dose and time-dependent manner. The colony-forming ability was not modified after NaNPs-EPS treatment. For Ag^{0}NP-EPS significant results, in term of inhibition of colony formation was observed only for long treatment (24 hours) with higher dose (50µg/ml).These results confirmed the previously obtained with MTT assay.

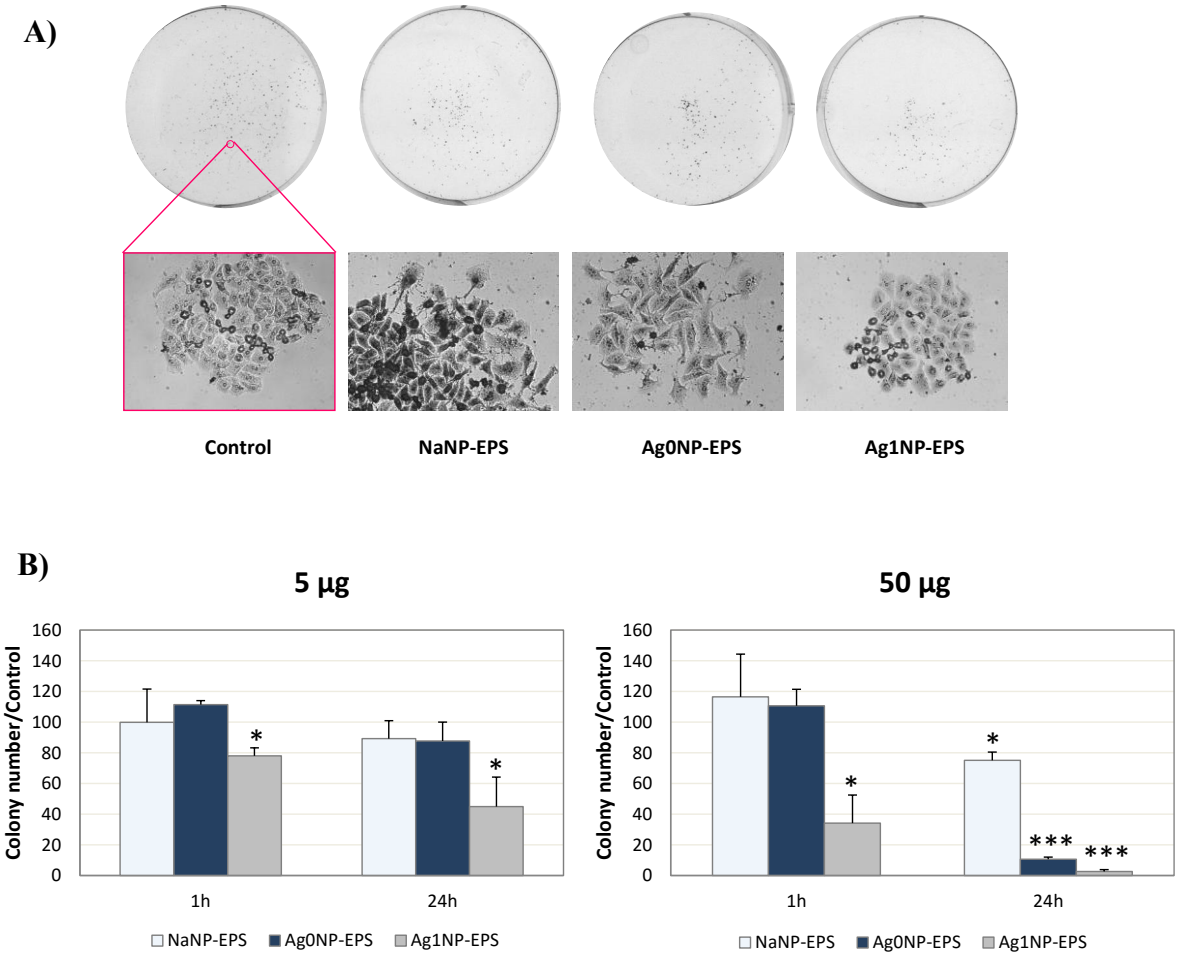

Figure 54. A) Cell colony formation was evaluated by clonogenic assay; B) Statistical results of colony-forming assays presented as surviving colonies (percentage of untreated control).

Morphological assessment of SKBR-3 cells treated with AgNPs-EPS by phase-contrast inverted microscope

Monitoring of 24 hours AgNPs-EPS treated cells under inverted light microscopy showed significant morphological changes compared to control cells. SKBR-3 control cells maintained their original morphology consisted of cuboid, polygonal and polarized cells, with cytoplasmic extensions and large nuclei with prominent nucleoli. The cells treated with NaNPs-EPS show bigger cytoplasmic extensions and numerous cells appear less adherent to the substrate, as marker of imminent cell division. In contrast, Ag^{0}NP-EPS and especially Ag^{+1}NP-EPS treated cells exhibited apoptotic-like characteristics such as shrinkage of rounded up cells and losing contact with neighbouring cells. Moreover, irregularity in shape, cytoplasmic blebbing, intracellular vacuoles, cellular debris and nuclear chromatin condensation were observed, also (*Fig. 55*).

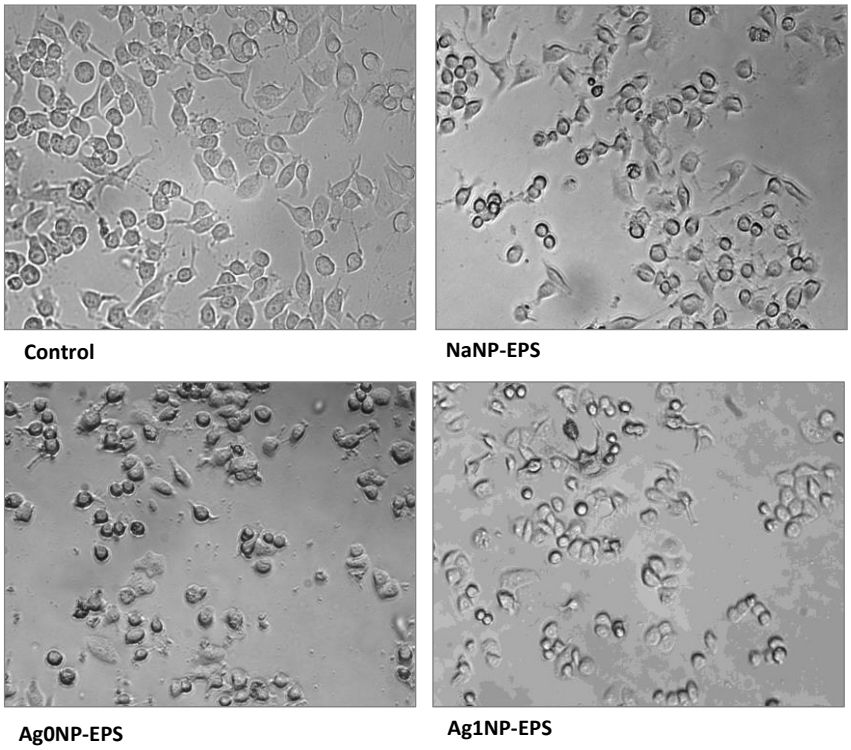

Figure 55. Morphological observation by inverted phase-contrast microscope of SKBR-3 cells after treatment with 5μg/ml of Ag^{0}NP-EPS, Ag^{+1}NP-EPS and Na NP-EPS for 24 hours. Magnification 100X.

Morphological Analysis: AO/EB Staining

The cytotoxic potential of AgNPs-EPS was further analyzed by AO/EB. The cells were treated with 5μg/ml concentration of AgNPs-EPS for 24 h and evaluated for apoptotic changes under fluorescent microscope (*Fig. 56*). AO is a vital dye that stains both live and dead cells as it can penetrate normal cell membrane. On the other hand, EB will stain only cells that have lost membrane integrity. As expected, the control and Na-NPs-EPS cells are vital and emitted green fluorescence due to the permeabilization of a cytoplasmic stain AO. The AgNPs-EPS cells exhibited more reddish orange fluorescence due to the loss in membrane integrity. In particular, cytotoxicity induced by Ag^{+1}NPs-EPS showed a higher number of apoptotic cells with respect to the Ag^{0}NPs-EPS. Quantification of live, necrotic, and apoptotic cells was performed in triplicate (n=3) experiments at 680X magnification *(Fig. 57)*.

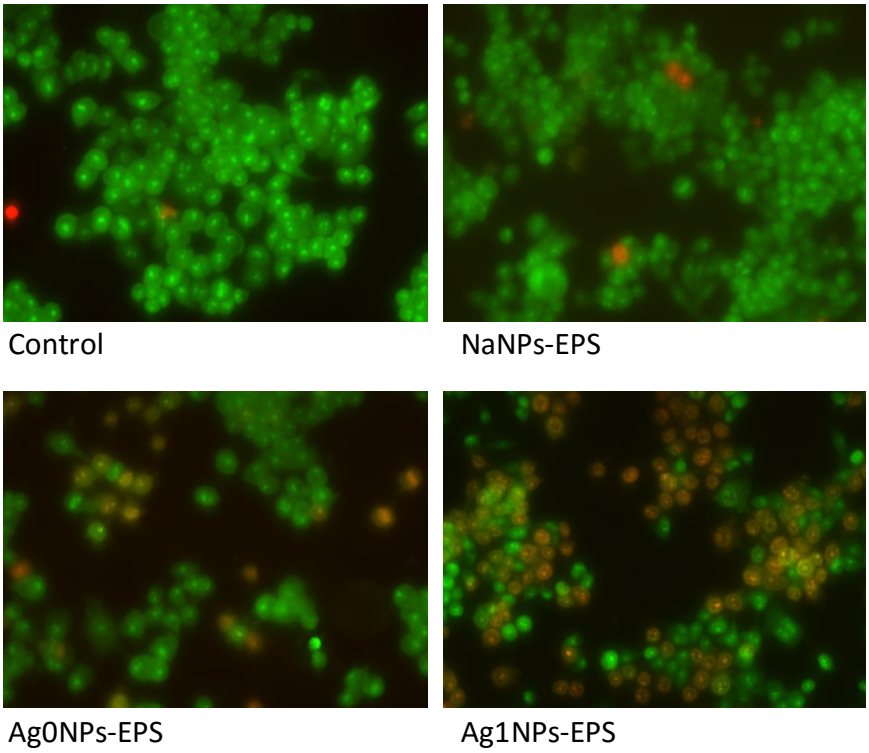

Figure 56. Morphological changes in SKBR-3 cells following treatment with 5µg/ml of AgNPs-EPS for 24 hours and staining by AO/EB. Three types of cells can be recognized under a fluorescence microscope: live cells (green), live apoptotic cells (orange) and dead cells by necrosis (red). Magnification 200X.

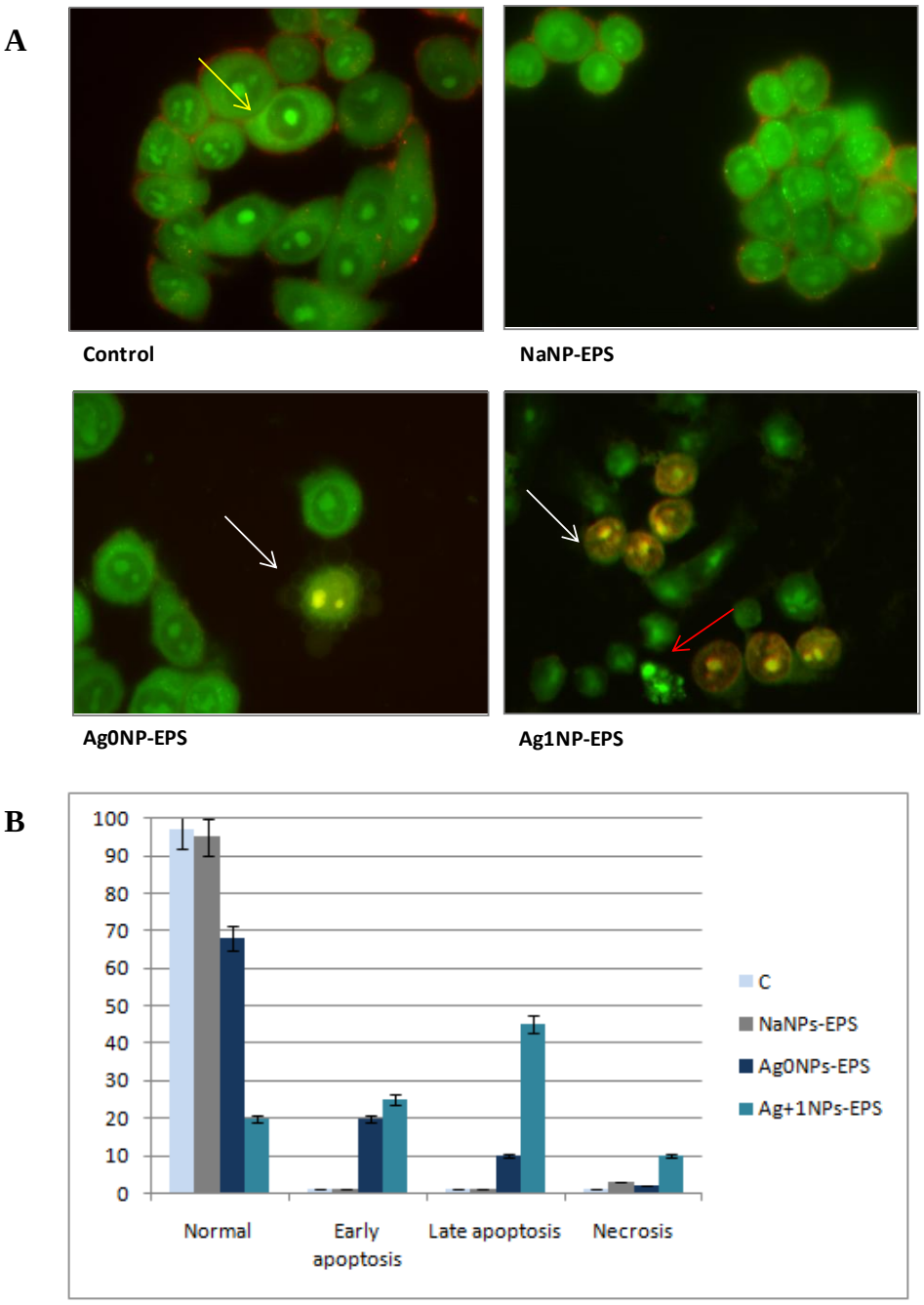

Figure 57. A) Morphological observation with AO/EB double staining by fluorescence microscope. Magnification 680X. Viable cells (yellow arrow), early apoptotic nuclei (red arrow), late apoptotic nuclei (blank arrow). B) Quantification of live, necrotic, and apoptotic cells. Each experiment was performed in triplicate (n=3) and generated similar morphological features.

Morphological Analysis: Hoechst 33342 Staining

To confirm whether the growth inhibitory activity of AgNPs-EPS was related to the induction of apoptosis, we further examined the changes in cell morphology by Hoechst 33342 (*Fig. 58)*. Results showed that Ag^{+1}NPs-EPS-treated cells exhibited chromatin condensation and nuclear fragmentation, which were indicative of apoptosis.

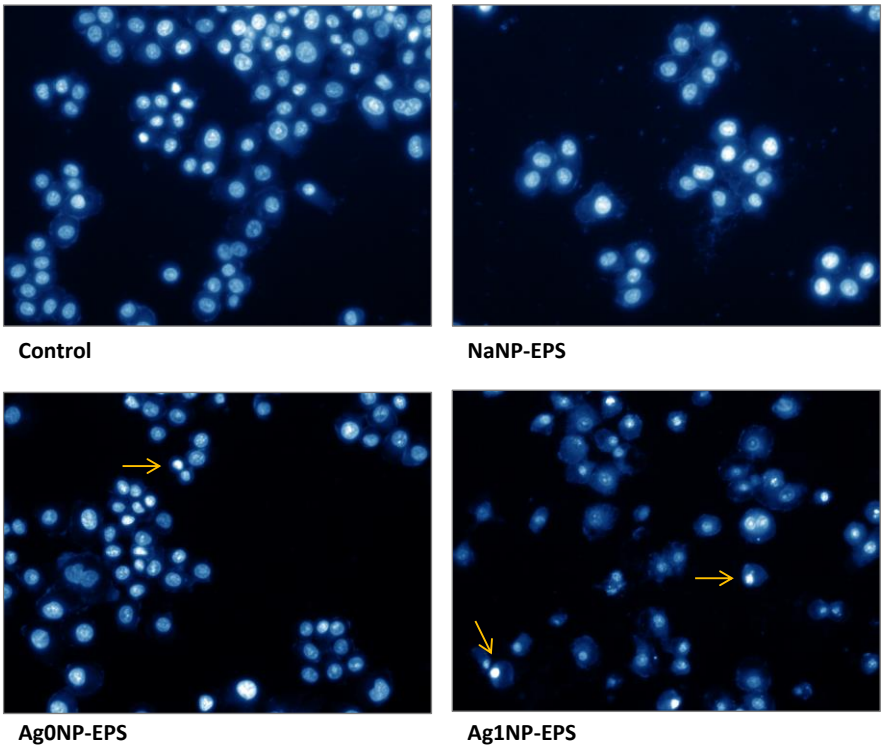

Figure 58. Nuclear changes revealed by Hoechst 33342 in SKBR-3 treated with 5µg/ml of AGNPs-EPS for 24 hours. Magnification 20X. Apoptotic nuclei are indicated with orange arrows. Cells were shrunken and rounded and contained with condensed chromatin.

Morphological Analysis: Transmission electron microscopy

Electron micrographs (*Fig. 59*) revealed structural cell damage at higher concentration of Ag^{+1}NP-EPS. In cells treated with IC50 dose, endosomes containing Ag were observed near the cell membrane, suggesting that NPs enter the cells via endocytosis. Moreover an increase of vesicles and pseudopodia was observed compared to control cells, assuming an entry mediated by endosomal vesicles or the use of ion channels.

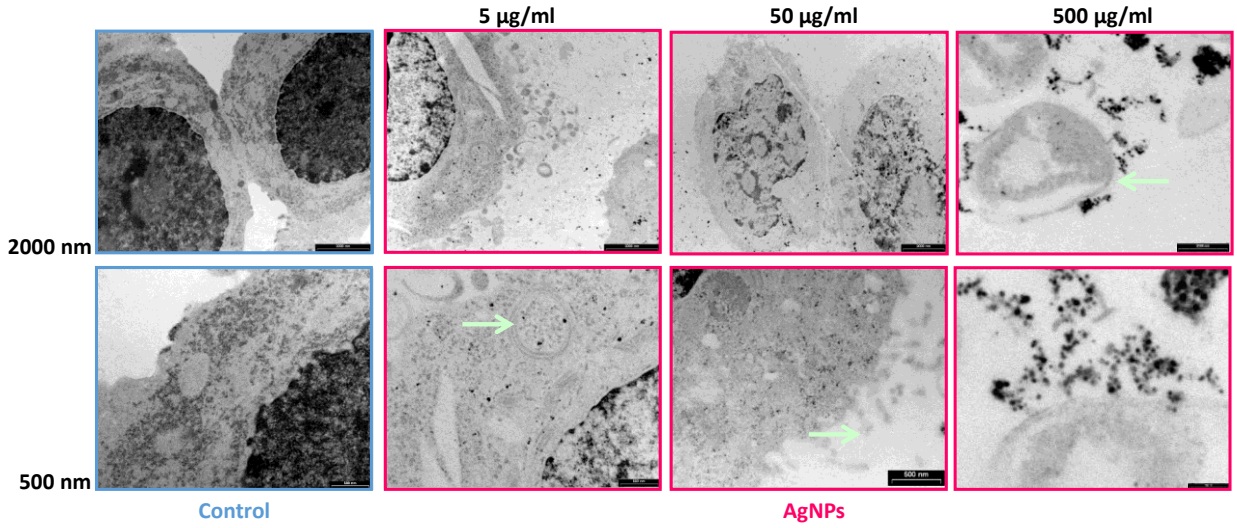

Figure 59. Images by transmission electron microscope of cells SKBR-3 subjected to treatments with AgNPs-EPS. Scale bar 2000 and 500 nm (TEM Images – Dip. Scienze della Vita, University of Siena).

Scratch Assay

To assess if AgNPs-EPS treatments reduce the migratory ability of SKBR-3, a scratch assay was performed. Cells were grown to confluence and a thin "wound" was introduced by scratching with a pipette tip (time point-zero). At the time-point zero, AgNPs-EPS treatments were added and the percentage of wound closure monitored at 6 and 24 hours (*Fig. 60A*). The wound area was calculated by Image Master Software and results reported as percentage of closure with respect to the control at the time point zero (*Fig. 60B*). Results showed a significant decrease of migratory ability at 6 and 24 h in Ag^{+1}NPs-EPS treated cells, also attributable to cell death, induced by treatment.

Gelatin Zymography

Metalloproteases MMP-2 and MMP-9 are involved in the processes of invasion and metastasis, so we aimed to evaluate their expression following treatment with AgNPs-EPS. Serum-free conditioned media (CM) of SKBR-3 cells, recovered after 24 hours of AgNPs-EPS treatments, were subjected to gelatin zymography. The CMs were dialyzed, lyophilized and suspended in 50 mM TrisHCl pH7.5. As expected, a decrease in the expression of Pro-MMP2 and Pro-MMP9 has been observed in Ag^{+1}NPs-EPS treated cells (*Fig. 61*).

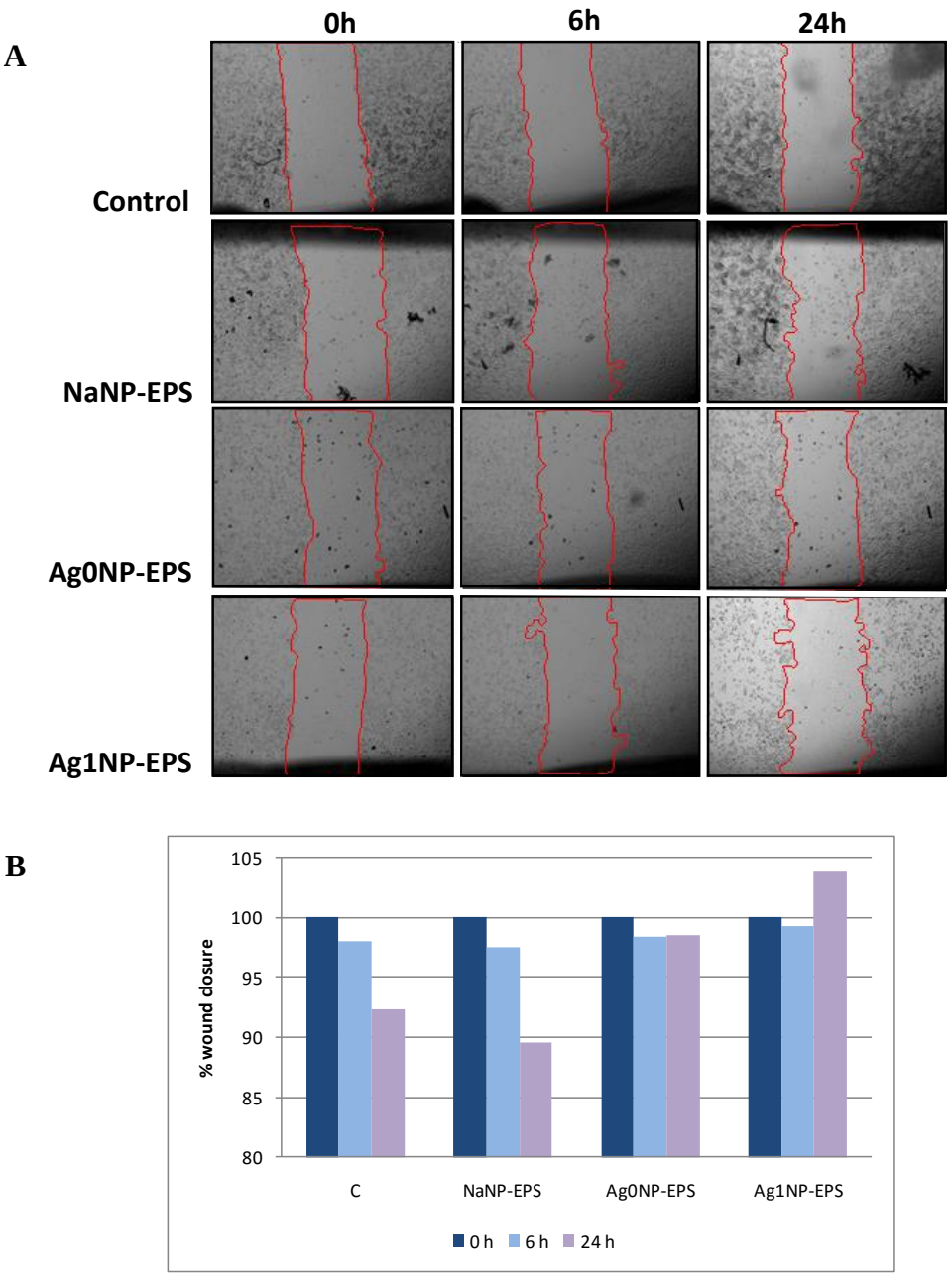

Figure 60. A) Wound-scratch assays performed on SKBR-3 AgNPs-EPS treated cells. Magnification 40X. B) Histograms showing the percentage of closure calculated with respect to control at time point zero.

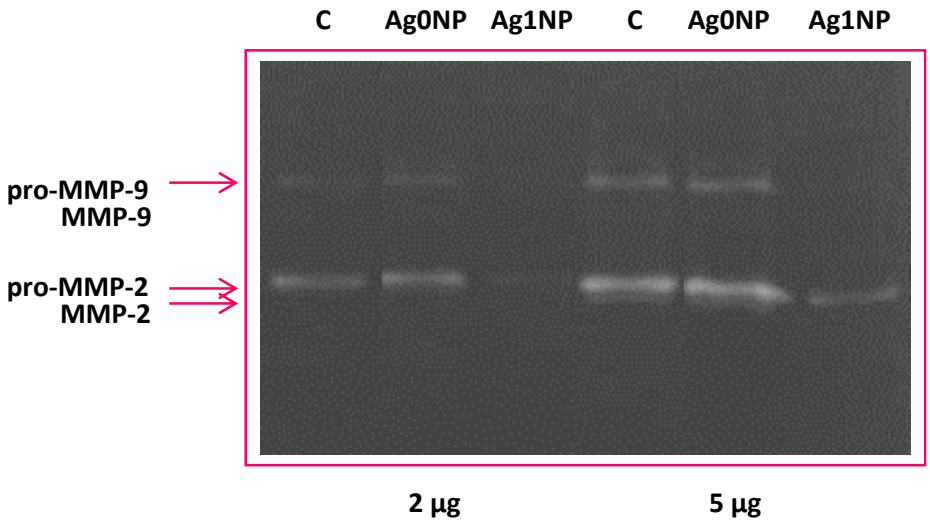

Figure 61. Zymographic analysis of CMs of SKBR-3 treated with AgNPs-EPS. Loaded proteins = 2 and 5µg.

Differential proteomic analysis: 2D-DIGE

Differential proteomic analysis 2D-DIGE was performed to detect protein modulations induced by AgNPs-EPS on SKBR-3 cells, after 24 hours of treatments. Briefly, an equal amount of the protein samples was covalently labeled with the Cy3 and Cy5 dyes, respectively, and then the samples were mixed in 1:1 ratio and loaded on a 2D gel system. The Cy2 dye was used to label the internal standard, obtained by mixing an equal amount of all samples, allowing a significant quantitative comparison of proteomic variations. A total of six gels were run to achieve a statistically significant measure of the differences in protein expression between the analyzed groups (*Fig. 62*). In the dedicated software analysis, all protein spots were quantified, normalized and inter-gel matched. 253 protein spots showed a significant difference (*Fig. 63*). The protein expression changes were considered significant only when their values exceeded the threshold settings (fold change ≥1.2, $p < 0.05$). Among the differentially expressed spots, 202 spots were modulated in Ag^{+1}NPs-EPS, two only in Ag^{0}NPs-EPS and two only in NaNPs-EPS treated cells. Overlapping modulations are showed in *Fig. 64 A.* The trend of up and down regulation of the proteins compared to control cells are showed in *Fig. 64B.* The significant spots were picked manually and submitted to trypsin in-gel digestion. The peptides recovered from the gel were subjected to MALDI TOF-MS/MS analysis, and the MS data analyzed with MASCOT database: We successfully identified 100 protein spot, corresponding to 68 proteins (*supplementary Tab. 2*).

Several proteins were found in different isoforms and then detected in multiple spots. Interestingly, among the top ten differentially expressed proteins in Ag^{+1}NPs-EPS treated cells,

we found down regulation of several isoforms of vimentin, an important marker of ETM, and up regulation of NTF2, involved in down regulation of VEGF (Li B et al., 2009). The identified proteins were functionally clusterized by David database (https://david.ncifcrf.gov/home.jsp). We found a high number of proteins with specific biochemical functions. In particular, the identified proteins include mitochondrial and endoplasmic reticulum lumen proteins, and are involved in regulation of apoptosis, response to oxidative stress and glycolysis. The glycolytic enzymes were collectively down regulated, indicating a reversion the Warburg effect (*Fig. 65*).

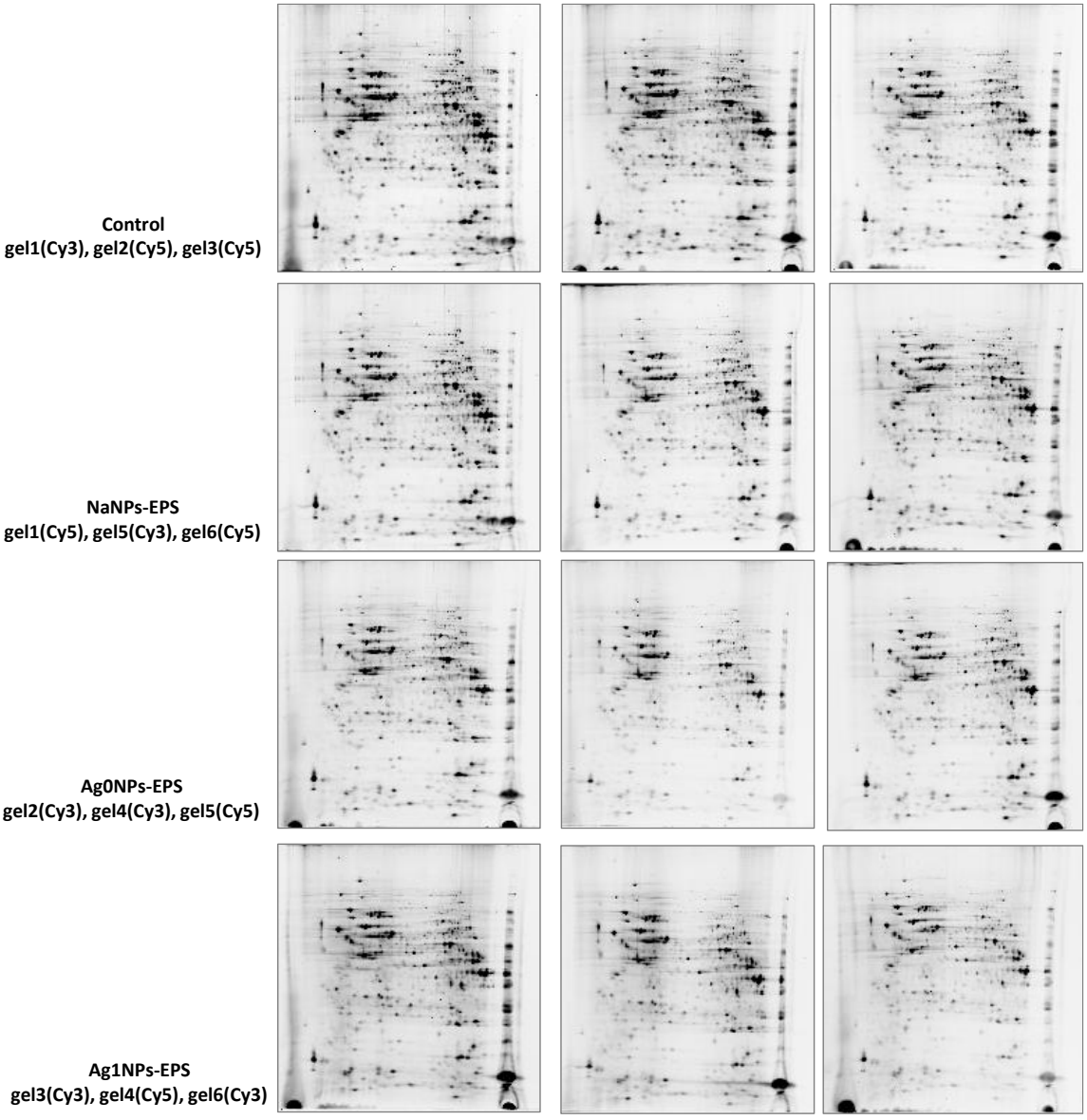

Figure 62. Panel showing the miniatures of the 2D-DIGE maps from control cells and subjected to treatments with Ag^{0}NPs-EPS, Ag^{+1}NPs-EPS e NaNPs-EPS.

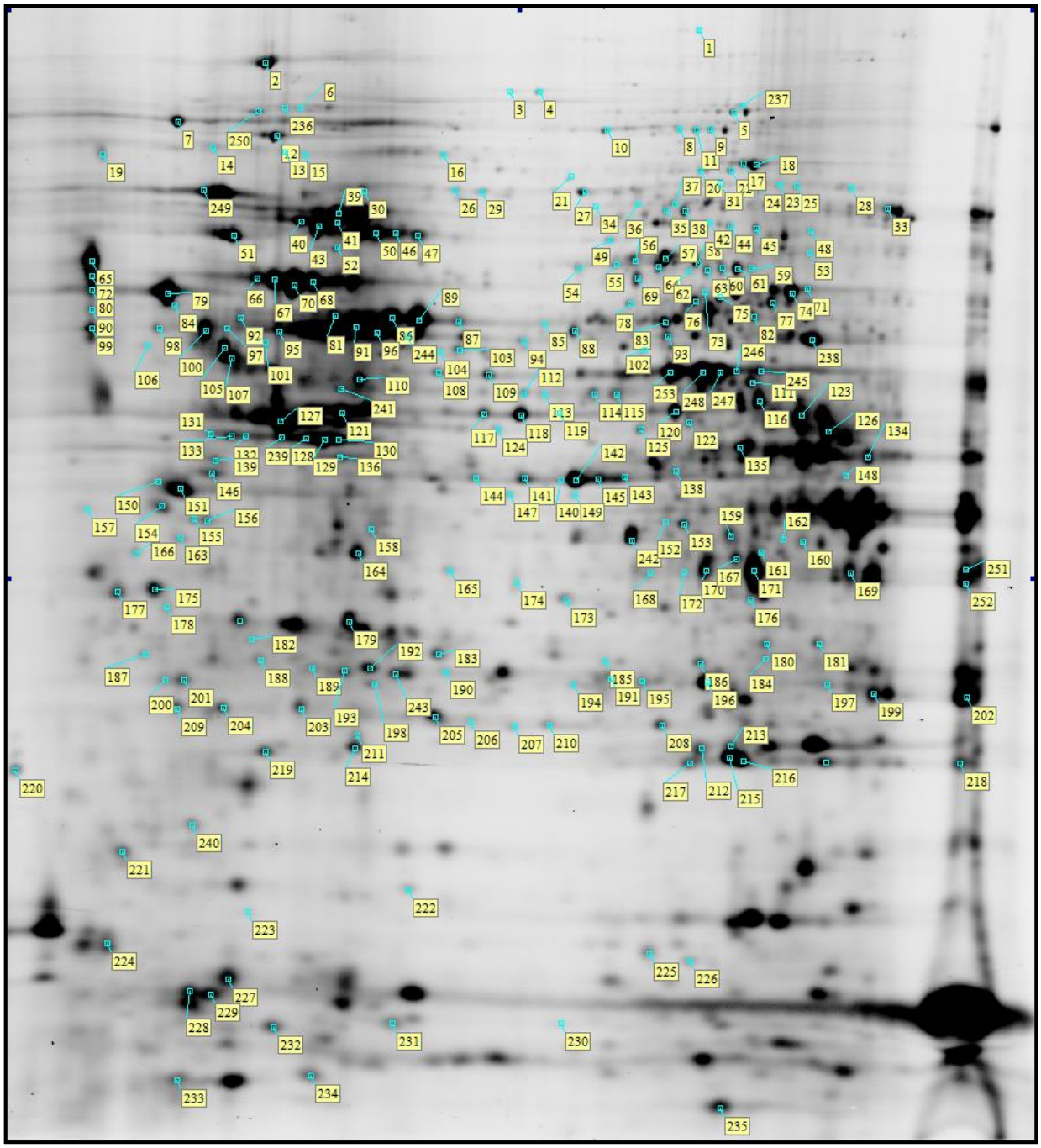

Figure 63. Proteomic map of SKBR-3 cells with the 253 differential protein spots.

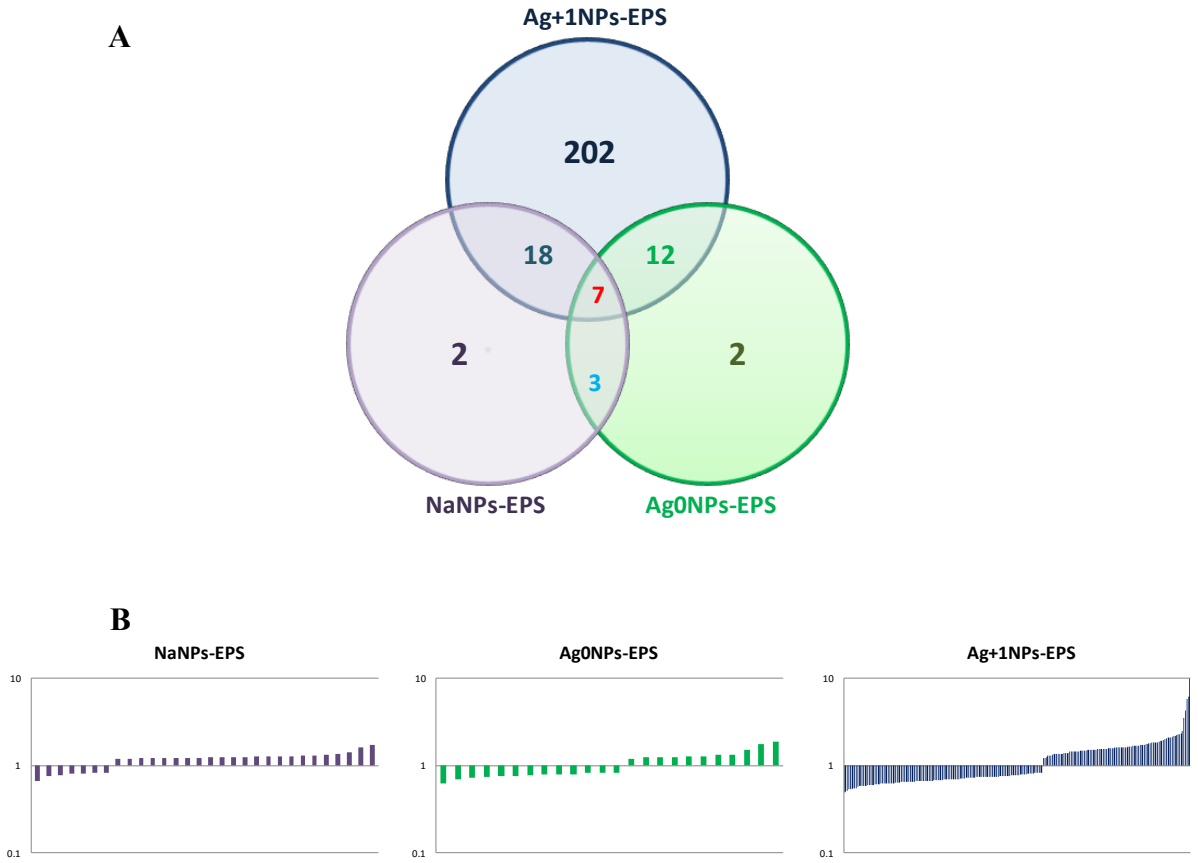

Figure 64. A) Eulero Venn diagram showing the differentially expressed proteins selected based on the threshold settings (fold change ≥1.2, $p<0.05$) in the analyzed groups. B) Up- and down-regulated proteins plotted as fold change compared to the control cells.

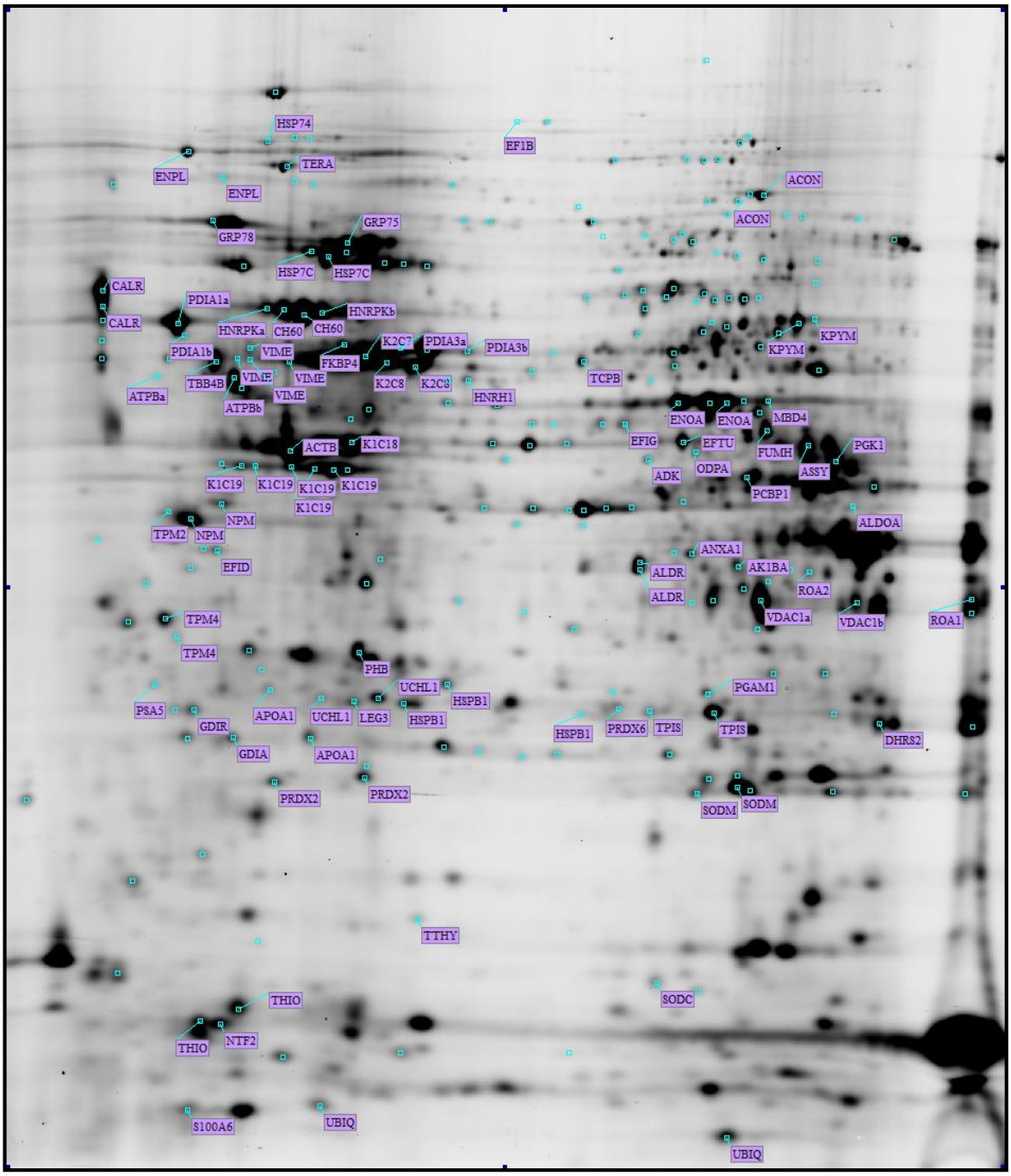

Figure 65. Proteomic map of SKBR-3 cells, with 100/253 protein species identified and labelled with the access number of the Swiss-Prot database.

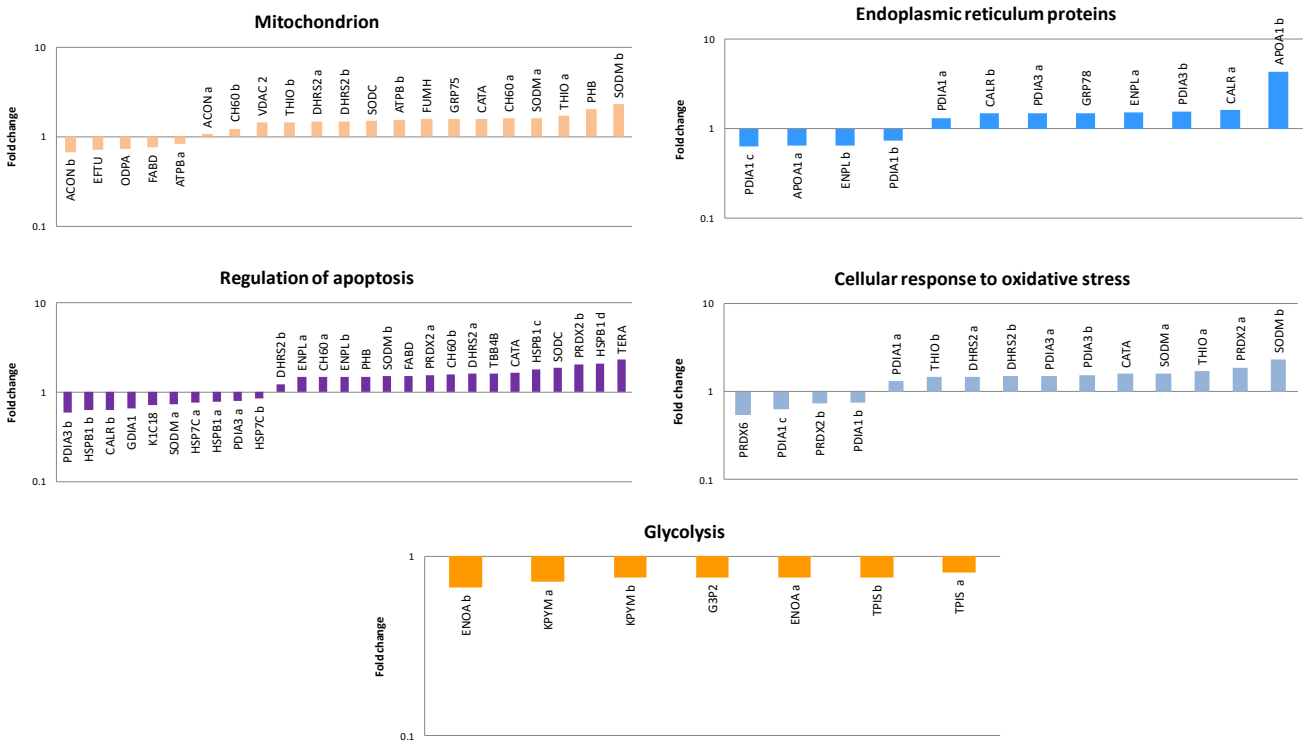

Figure 66. Histograms of the differentially identified proteins in SKBR-3 AgNPs-EPS treated cells, sorted into functional classes and plotted as fold change in log scale.

Nuclear, cytosolic and mitochondrial isolation

In order to detect Ag localization into the cell, cell fractionation was performed by means of sequential centrifugation with a buffered solution of sucrose. The obtained pellets (nuclei, mitochondria, lysosomes and membranes) were analysed with anodic stripping voltammetry, a technique that allows to determinate the release of silver species from the various types of AgNPs-EPS. These measurements allowed obtaining information on the kinetic of silver ions release from AgNPs-EPS and their concentration profiles at the substrate/water interface. As expected, higher Ag^{+1} concentration was released from Ag^{+1}NPs-EPS compared to Ag^{0}NPs-EPS, produced under aerobic and anaerobiotic conditions. Ag^{+1} was released both in nuclei and mitochondria fractions. Obtained data were normalized for protein concentration and the amount released Ag^{+1} was higher in the mitochondria compared to the nuclei (*Tab. 4*).

		Ag µg.L-1	Proteins	Ag/µg pt
Nuclei	Control	<LOD	776,475	-
	Ag^{0}NPs-EPS	83,2	502,425	0,1656
	Ag^{+1}NPs-EPS	254,4	1213,65	0,2096
Mitochondria	Control	<LOD	167,475	-
	Ag0NP-EPS	<LOD	67,425	-
	Ag1NP-EPS	23	70,6875	0,3253
Lysosomes	Control	<LOD	-	-
	Ag0NP-EPS	<LOD	-	-
	Ag1NP-EPS	<LOD	-	-
Membrane	Control	<LOD	-	-
	Ag0NP-EPS	<LOD	-	-
	Ag1NP-EPS	<LOD	-	-

Table 4. Voltammetric analysis on pellets derived from cell fractionation.

A second analysis performed on nuclear and mitochondrial pellets, confirmed that higher release of Ag^{+1} in the mitochondria with respect to the nuclei (*Fig. 67*). To verify if Ag can bind to proteins or DNA, a voltammetric analysis was also performed on DNA extracted both from nuclei and mitochondria, but no results has been obtained. Further investigation will be performed in order to clarify the nature of Ag interactions.

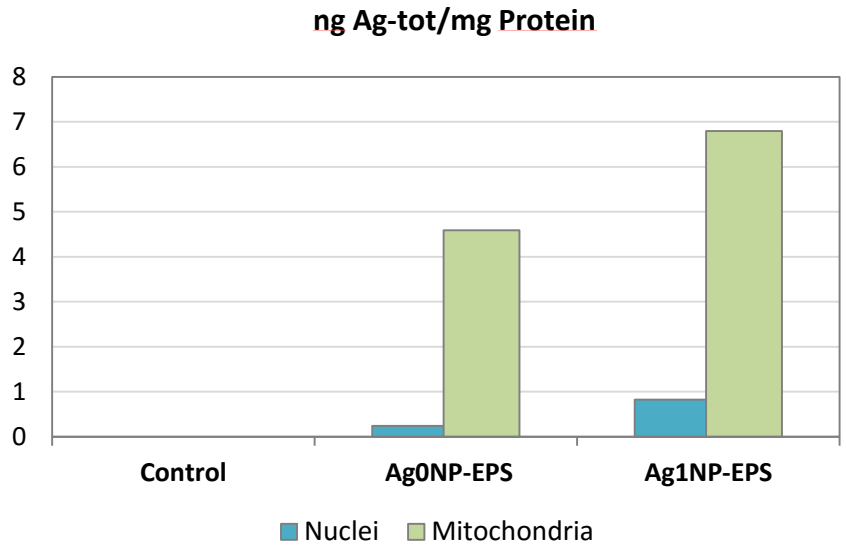

Figure 67. Amount of silver in the mitochondrial and nuclear pellets.

Conclusion

The AgNPs-EPS, produced by Klebsiella oxytoca were tested for its efficiency as a potent cytotoxic agent against breast cancer cell lines. AgNPs-EPS treatment impaired cell morphology consistent with the acquisition of apoptotic features, decrease the migratory and invasive capabilities and determines many proteomic changes. The differentially proteins identified so far, highlights important pathways involved in the mechanism of action of Ag^{+1}NPs-EPS. The protein classes identified in this study can explain the cellular effects of AgNPs-EPS. The endoplasmic reticulum (ER) is a well-orchestrated protein-folding machine composed of protein chaperones, proteins that catalyze protein folding, and sensors that detect the presence of misfolded or unfolded proteins. Accumulating evidence suggests that protein folding and generation of reactive oxygen species (ROS) as a byproduct of protein oxidation in the ER are closely linked events. Persistent oxidative stress and protein misfolding initiate apoptotic cascades. Autophagy is emerging as an important mediator of pathological responses and engages in cross-talk with ROS (reactive oxygen species) and RNS (reactive nitrogen species) in both cell signaling and protein damage. Oxidative stress is inseparably linked to mitochondrial dysfunction, as mitochondria are both generators of and targets for reactive species. Mitochondrial turnover is dependent on autophagy. The crosstalk between autophagy, redox signaling and mitochondrial dysfunction is not well understood and further efforts are necessary to analyze the effects of AgNPs-EPS on oxidative stress-ER stress, ER-mitochondria connectivity and apoptosis/autophagy.

CONCLUSIONS

Discovery of new biomarkers represent the greatest promise for the detection and management of cancer. Although progress in cancer biology has been rapid during the past few years, the complete understanding of molecular basis for cancer initiation, progression and efficacious treatments is still lacking. In this context, the application of proteomic strategies is now holding a focal position. The main reason is that proteins are the functional players that drive cancer phenotypes. Among cancers, breast and colon represent the most frequent forms. The evolution of these types of cancer are not easily predictable since there are several types that behave differently among patients. The biological heterogeneity is consistent with observed varied responses to therapies across patients, also.

A primary objective of this study was to identify differentially expressed proteins in colorectal cancer, to search specific gene-expression patterns associated with colorectal carcinogenesis and progression, especially with metastatic spread to liver. Collectively, a total of one hundred protein spots were found to be differentially expressed, among which some has been suggested to act at multiple tumor progression steps, and already proposed as possible biomarkers. In particular, we pointed on different implication of transgelin and cathepsin D on colon cancer progression. Interestingly, was emerged the considerable function of different isoforms, which deserve further investigations. In conclusion, differential proteomic analysis allowed us to identify proteomic clusters, possibly related to the onset of cancer and metastasis. We believe that present study will contribute to the implementation of the panel of biomarkers useful to the management of colorectal cancer.

In the second part of the thesis, starting from the results obtained by a comparative proteomic screening in a large sample set of patients, supporting the hypothesis that a significant deregulation of multiple S100 protein members was associated with breast cancer progression, we performed *in silico* analysis, using Kaplain Meir-plotter database, to strengthen previous results on the association between gene expression levels of the S100 protein family members and prognosis of patients. Moreover, we investigated the possible correlation between AKT signaling and S100 proteins expression in breast cancer, extending our analysis to IGF-1R and MMPs for their involvement in breast cancer progression. No significant correlation was found between the investigated S100 proteins and AKT-1/p-AKT, but several correlation were found between S100 proteins and Pro-MMP-9 and MMP-2, suggesting a possible molecular mechanism through which S100 contribute to breast cancer progression. We propose that this

may offer a significant contribution to the knowledge and clinical applications of the S100 protein family to breast cancer.

A last objective of this study was to investigate the potential antitumor activity of nano-silver particles on breast cell line in vitro, demonstrating the ability of AgNPs-EPS to inhibit cellular growth, induce significant morphological changes consistent with the acquisition of apoptotic features, decrease the migratory and invasive capabilities. The differential proteomic analysis showed many proteins differentially expressed after the Ag^{+1}NPsEPS-treatment, in line with the hypothesis of the so-called "Trojan-horse" mechanism, in which nanoparticles are internalized within cells and then release high levels of toxic ions. In our study, we found a significant level of Ag^{+1} releasing in mitochondria, which in turn can explain the intracellular reactive oxygen species (ROS) and oxidative stress generation. Moreover, ROS can reacts with AgNPs to form more Ag^{+1}. Mitochondria represent the major site of ROS production within the cell, which may be the primary effect of AgNPs-EPS treatment and causes many secondary problems, such as protein damage, endoplasmic reticulum stress and activation of several chaperones. Finally, mitochondrial damage is the basis of the mechanism of early apoptosis of activation of autophagy. Conclusively, we believe that the results obtained represent a significant contribution for cancer system biology and confirm the powerful of proteomics for biomarker discovery and clinical applications.

REFERENCES

Abulafi AM, Williams NS. Local recurrence of colorectal cancer: the problem, mechanisms, management and adjuvant therapy. Br J Surg 1994;81:7-19.

Adams JM, Cory S. The Bcl-2 apoptotic switch in cancer development and therapy. Oncogene 26, (2007)1324–1337.

Adeli M, Mirab N, Alavidjeh MS, et al. Carbon nanotubes-graft-polyglycerol: Biocompatible hybrid materials for nanomedicine. Polymer, 2009. 50, 3528–3536.

Alivisatos AP, Gu W, Larabell C. Quantum dots as cellular probes. Annu. Rev. Biomed. Eng. 2005. 7, 55–76.

American Society of Clinical Oncology. 1997 update of recommendations for the use of tumor markers in breast and colorectal cancer. J Clin Oncol 1998; 16:793-5.

Ang EZ, Nguyen HT, Sim HL, et al. Annexin-1 regulates growth arrest induced by high levels of estrogen in MCF-7 breast cancer cells. Molecular Cancer Research, 2009, 7(2):266-274.

Arai Y, Miyayama T, Hirano S. Difference in the toxicity mechanism between ion and nanoparticle forms of silver in the mouse lung and in macrophages. Toxicology. 2015 Feb 3; 328:84-92.

Babel I, Barderas R, Díaz-Uriarte R, et al. Identification of tumor-associated autoantigens for the diagnosis of colorectal cancer in serum using high density protein microarrays. Mol Cell Proteomics. 2009 Oct;8(10):2382-95.

Baldi F, Marchetto D, Battistel D, et al. Iron-binding characterization and polysaccharide production by Klebsiella oxytoca strain isolated from mine Acid drainage**.** Journal of Applied Microbiology 107 (2009) 1241–1250.

Baldi F, Marchetto D, Paganelli S, et al. Bio-generated metal binding polysaccharides as catalysts for synthetic applications and organic pollutant transformations. New Biotechnol 29 (2011) 74–78.

Baldi F, Marchetto D, Pini F et al. Biochemical and microbial diversity of shallow marine sediment along the Terra Nova Bay (Ross Sea, Antarctica). Continental shelf research, vol. 30, pp. 1614-1625 (ISSN 0278-4343) (2010).

Baldi F, Minacci A, Pepi M et al. Gel sequestration of heavy metals by Klebsiella Oxytoca isolated from iron mat. Fems Microbiology Ecology, vol. 36, pp. 169-174, 2001 (issn 0168-6496).

Battistel D, Baldi F, Gallo M, et al. Characterisation of biosynthesised silver nanoparticles by scanning electrochemical microscopy (SECM) and voltammetry. Talanta. 2015, 132:294-300.

Bayascas JR, Alessi DR. Regulation of Akt/PKB Ser473 phosphorylation. Mol Cell 18:143–145. 2005.

Belham C, Wu S, Avruch J. Intracellular signaling : PDK1 a kinase at the hub of things. Curr Biol 9:R93–96. 1999.

Berchem G, Glondu M, Gleizes M, et al. Cathepsin-D affects multiple tumor progression steps in vivo: proliferation, angiogenesis and apoptosis. Oncogene. 2002; 21(38):5951–5955.

Bhattacharya R, Mukherjee P. Biological properties of "naked" metal nanoparticles. Adv. Drug Deliv. Rev. 2008. 60, 1289–1306.

Biondi RM, Kieloch A, Currie RA, et al. The PIF-binding pocket in PDK1 is essential for activation of S6K and SGK, but not PKB. EMBO J 2001. 20:4380–4390.

Bouck N, Stellmach V, Hsu SC. How tumors become angiogenic. Adv. Cancer Res (1996). 69, 135–174.

Brown JM, Attardi LD. The role of apoptosis in cancer development and treatment response**.** Nat. Rev. Cancer 5, 231–237 (2005).

Cancemi P, Di Cara G, Albanese NN, et al. Large-scale proteomic identification of S100 proteins in breast cancer tissues. BMC Cancer 2010, 10:476.

Cancemi P, Di Cara G, Albanese NN, et al. Differential occurrence of S100A7 in breast cancer tissues: a proteomic-based investigation. Proteomics Clin Appl. 2012 Aug;6(7-8):364-73. doi: 10.1002/prca.201100072.

Cancer Genome Atlas Network. Comprehensive molecular characterization of human colon and rectal cancer. Nature 487, 330–337, 2012.

Carpenter B, McKay M, Dundas SR, et al. Heterogeneous nuclear ribonucleoprotein K is over expressed, aberrantly localised and is associated with poor prognosis in colorectal cancer. Br J Cancer. 2006 Oct 9;95(7):921-7.

Cataleya C. In Vitro Toxicity Assessment of Silver Nanoparticles in Rat Alveolar Macrophages. 2006, Master of Science (MS), Pharmacology and Toxicology.

Chang YJ, Chen WY, Huang CY, et al. Glucose-regulated protein 78 (GRP78) regulates colon cancer metastasis through EMT biomarkers and the NRF-2/HO-1 pathway. Tumour Biol. 2015 Mar;36(3):1859-69. doi: 10.1007/s13277-014-2788-x.

Chen H, Xu C, Jin Q et al. S100 protein family in human cancer. Am J Cancer Res 2014;4(2):89-115.

Chen X, Ba Y, Ma L et al. Characterization of microRNAs in serum: a novel class of biomarkers for diagnosis of cancer and other diseases. Cell Research, vol. 18, no. 10, pp. 997–1006, 2008.

Chen X, Schluesener HJ. Nanosilver: a nanoproduct in medical application. Toxicol Lett. 2008 Jan 4; 176(1):1-12.

Chin YR, Toker A. The actin-bundling protein paladin is an Akt1-specific substrate that regulates breast cancer cell migration. Mol Cell 2010; 38:333-44.

Chin YR, Toker A. Akt isoform-specific signaling in breast cancer: uncovering an anti-migratory role of palladin. Cell Adhesion & Migration 5:3, 211-214; May/June 2011; © 2011 Landes Bioscience.

Cho CY, Lee KT, Chen WC et al. MST3 promotes proliferation and tumorigenicity through the VAV2/Rac1 signal axis in breast cancer. Oncotarget, Advance Publications, February 20, 2016.

Cho YB, Chun HK, Yun HR, et al. Clinical and pathologic evaluation of patients with recurrence of colorectal cancer five or more years after curative resection. Dis Colon Rectum 2007;50:1204-10.

Choi DS, Choi DY, Hong BS, et al. Quantitative proteomics of extracellular vesicles derived from human primary and metastatic colorectal cancer cells. J Extracell Vesicles. 2012 Sep 11;1.

Choueiri MB, Shen JP, Gross AM, et al. ERCC1 and TS Expression as Prognostic and Predictive Biomarkers in Metastatic Colon Cancer. PLOS ONE | DOI:10.1371/journal.pone.0126898 June 17, 2015.

Chung C, Christianson M. Predictive and prognostic biomarkers with therapeutic targets in breast, colorectal, and non-small cell lung cancers: a systemic review of current development, evidence, and recommendation. J Oncol Pharm Pract. 2014; 20: 11-28.

Cicenas J, Urban P, Vuaroqueaux V, et al. Increased level of phosphorylated Aktmeasured by chemiluminescence-linked immunosorbent assay is a predictor of poor prognosis in primary breast cancer overexpressing ErbB-2. Breast Cancer Research. 2005;7:R394-R401 (DOI 10.1186/bcr1015).

Cidado J, Ho Park B. Targeting the PI3K/Akt/mTOR pathway for breast cancer therapy. J Mammary Gland Biol Neoplasia 2012; 17(0):205-216. doi: 10.1007/s10911-012-9264-2.

Clark AS, West K, Streicher S, et al. Constitutive and inducible Akt activity promotes resistance to chemotherapy, trastuzumab, or tamoxifen in breast cancer cells. Mol Cancer Ther 1: 707-717, 2002.

Clarke SJ, Karapetis CS, Gibbs P, et al. Overview of biomarkers in metastatic colorectal cancer: Tumour, blood and patient-related factors. Critical Reviews in Oncology/Hematology 85 (2013) 121–135.

Cornejo KM, Kandil D, Khan A, et al. Theranostic and Molecular Classification of Breast Cancer. Arch Pathol Lab Med—Vol 138, January 2014.

Coskun U, Yamac D, Gulbahar O, et al. Locally advanced breast carcinoma treated with neoadjuvant chemotherapy: are the changes in serum levels of YKL-40, MMP-2 and MMP-9 correlated with tumor response? Neoplasma. 2007;54:348–352.

Coussens LM, Zitvogel L, Palucka AK. Neutralizing tumor promoting chronic inflammation: a magic bullet? Science 2013, 339:286-291.

Cunningham D, Atkin W, Heinz-Josef L, et al. Colorectal cancer. Lancet (2010) 375: 1030–1047.

Dahm CC, Keogh RH, Spencer EA, et al. Dietary fiber and colorectal cancer risk: a nested case–control study using food diaries. J Natl Cancer Inst. 2010; 102:614–626.

del Rocío Balaguera Gelves M, El Burai-Félix A, De La Cruz-Montoya E, et al. Silver metal colloidal film on a flexible polymer substrate. SPIE Proceedings Vol. 62012C (2006).

Diz AP, Truebano M, Skibinski DO. The consequences of sample pooling in proteomics: an empirical study. Electrophoresis. 2009 Sep;30(17):2967-75.

dos Santos CA, Seckler MM, Ingle AP, et al. Silver nanoparticles: therapeutical uses, toxicity, and safety issues. J Pharm Sci. 2014 Jul;103(7):1931-44.

Duquet A, Melotti A, Mishra S, et al. A novel genome-wide in vivo screen for metastatic suppressors in human colon cancer identifies the positive WNT-TCF pathway modulators TMED3 and SOX12. EMBO Mol Med (2014) 6: 882–901.

Espinosa Arranz E, Fresno Vara JÁ, Gámez-Pozo A, et al. Gene Signatures in Breast Cancer: Current and Future Uses. Transl Oncol. 2012 Dec; 5(6): 398–403.

Fidler IJ. The pathogenesis of cancer metastasis: the 'seed and soil' hypothesis revisited. Nat. Rev. Cancer (2003) 3, 453–458.

Fleming M, Ravula S, Tatishchev SF, et al. Colorectal carcinoma: pathologic aspects. J Gastrointest Oncol, 2012; 3:153-73.

Folkman J. Angiogenesis. Annu. Rev. Med. (2006). 57, 1–18.

Franken N, Rodermond H, Stap J, et al. Clonogenic assay of cells in vitro. doi:10.1038/nprot.2006.339.

Freshney RI. Culture of animal cells, a manual of basic technique. 2nd edn. **(**Alan R. Liss Inc., New York, 1987).

Fu R, Yang P, Wu HL, Li ZW, Li ZY. GRP78 secreted by colon cancer cells facilitates cell proliferation via PI3K/Akt signaling. Asian Pac J Cancer Prev. 2014;15(17):7245-9.

Gallo G, Baldi F, Renzone G et al. Adaptative biochemical pathways and regulatory networks in Klebsiella oxytoca BAS-10 producing a biotechnologically relevant exopolysaccharide during Fe(III)-citrate fermentation. Microbial cell factories, 11:152, 2012.

Gerdes J, Lemke H, Baisch H, et al. Cell cycle analysis of a cell proliferation-associated human nuclear antigen defined by the monoclonal antibody Ki-67. J Immunol. 1984; 133(4):1710–1715.

Goldman ER, Clapp AR, Anderson GP, et al. Multiplexed toxin analysis using four colors of quantum dot fluororeagents. Anal. Chem. 2004. 76, 684–688.

Görg A, Postel W, Günther S. The current state of two-dimensional electrophoresis with immobilized pH gradients. Electrophoresis Volume 9, Issue 9, pages 531–546, 1988.

Guzin'ska-ustymowic K, Zalewsk B, Kasacka I, et al. Activity of Cathepsin B and D in Colorectal Cancer: Relationships with Tumour Budding. Anticancer Research 24: 2847-2852 (2004).

Haber DA, Settleman J. Cancer: drivers and passengers. Nature. 2007 Mar 8;446(7132):145-6.

Hagland HR, Berg M, Jolma IW, et al. Molecular pathways and cellular metabolism in colorectal cancer. Dig Surg 2013; 30:12–25.

Hanahan D, Folkman J. Patterns and emerging mechanisms of the angiogenic switch during tumorigenesis. Cell (1996) 86, 353–364.

Hanahan D, Weinberg RA. The hallmarks of cancer. Cell, 2000. 100(1): p. 57-70.

Hanahan D, Weinberg RA. Hallmarks of cancer: the next generation. Cell, 2011. 144(5): p. 646-74.

Hardy B, Raiter A, Yakimov M, Vilkin A, Niv Y. Colon cancer cells expressing cell surface GRP78 as a marker for reduced tumorigenicity. Cell Oncol (Dordr). 2012 Oct;35(5):345-54.

Hill M, Mazal D, Biron VA, et al. A novel clinically relevant animal model for studying galectin-3 and its ligands during colon carcinogenesis. Journal of Histochemistry & Cytochemistry. Volume 58(6): 553–565, 2010.

Hong BS, Cho JH, Kim H, et al. Colorectal cancer cell-derived microvesicles are enriched in cell cycle-related mRNAs that promote proliferation of endothelial cells. BMC Genomics. 2009 Nov 25; 10:556.

Huang S, Li C, Cheng Z, et al. Magnetic Fe3O4@mesoporous silica composites for drug delivery and bioadsorption. J. Colloid Interface Sci. 2012. 376, 312–321.

Iacobuzio-Donahue C, Shuja S, Cai J, et al. Cathepsin D protein levels in colorectal tumors: divergent expression patterns suggest complex regulation and function. Int J Oncol. 2004 Mar; 24(3):473-85.

Iravani S. Bacteria in Nanoparticle Synthesis: Current Status and Future Prospects. International Scholarly Research Notices Volume 2014, Article ID 359316, 18 pages.

Iravani S, Korbekandi H, Mirmohammadi SV et al. Plants in nanoparticle synthesis. Reviews in Advanced Sciences and Engineering, vol. 3, no. 3, pp. 261–274, 2014.

Iravani S, Zolfaghari B. Green synthesis of silver nanoparticles using Pinus eldarica bark extract. Biomed Research International, vol. 2013, Article ID 639725, 5 pages, 2013.

Jacobson-Raber G, Lazarev I, Novack V, et al. The prognostic importance of cathepsin D and E-cadherin in early breast cancer: A single-institution experience. Oncol Lett. 2011 Nov;2(6):1183-1190. Epub 2011 Aug 24.

Jana NR, Gearheart L, Murphy CJ. Wet chemical synthesis of high aspect ratio cylindrical gold nanorods. J. Phys. Chem. B 2001. 105, 4065–4067.

Jass JR. Classification of colorectal cancer based on correlation of clinical, morphological and molecular features. Histopathology. 2007 Jan; 50 (1):113-30.

Jemal A, Bray f, Center MM, et al. Global cancer statistics. CA Cancer J Clin, 2011. 61(2): p. 69-90.

Jeong B, Kim SW, Bae YH. Thermosensitive sol-gel reversible hydrogels. Adv. Drug Deliv. Rev. 2002. 54, 37–51.

Joyce JA, Pollard JW. Microenvironmental regulation of metastasis. Nat Rev Cancer. 2009 Apr;9(4):239-52.

Jung H, Suh Y. Regulation of IGF -1 signaling by microRNAs. Front. Genet., 13 January 2015.

Kalia M. Biomarkers of Colorectal Cancer. J Cancer Biol Res 3(1): 1058 (2015).

Kang HS, Ahn SH, Mishra SK, et al. Association of polymorphisms and haplotypes in the insulin-like growth factor 1 receptor (IGF-1R) gene with the risk of breast cancer in Korean women. PLoS One. 2014 Jan 2;9(1):e84532.

Kanmani P, Lim ST. Synthesis and structural characterization of silver nanoparticles using bacterial exopolysaccharide and its antimicrobial activity against food and multidrug resistant pathogens. (2013). Process Biochem 48:1099–1106).

Karp NA, Lilley KS. Investigating sample pooling strategies for DIGE experiments to address biological variability.
Proteomics. 2009 Jan;9(2):388-97.

Kim BK, Lee J W, Park PJ, et al. The multiplex bead array approach to identifying serum biomarkers associated with breast cancer**.** Breast Cancer Research 2009, 11:R22.

Kirana C, Shi H, Laing E, et al. Cathepsin D expression in colorectal cancer: from proteomic discovery through validation using western blotting, immunohistochemistry, and tissue microarrays. International Journal of Proteomics, Volume 2012, Article ID 245819, 10 pages. doi:10.1155/2012/245819.

Koontongkaew S. The tumor microenvironment contribution to development, growth, invasion and metastasis of head and neck squamous cell carcinomas. J Cancer. 2013;4(1):66-83.

Korbekandi H, Ashari Z, Iravani S, et al. Optimization of biological synthesis of silver nanoparticles using Fusarium oxysporum. Iranian Journal of Pharmaceutical Research,vol. 12, no. 3, pp. 289–298, 2013.

Kuester D, Lippert H, Roessner A, et al. The cathepsin family and their role in colorectal cancer. Pathol Res Pract. 2008;204(7):491-500

Kurizaki T, Toi M, Tominaga T. Relationship between matrix metalloproteinase expression and tumor angiogenesis in human breast carcinoma. Oncol. Rep. 5 (1998) 673–677.

La Rocca G, Pucci-Minafra I, Marrazzo A, et al. Zymographic detection and clinical correlations of MMP-2 and MMP-9 in breast cancer sera. British Journal of Cancer (2004) 90, 1414 – 1421.

Leone S, De Castro C, Parrilli M, et al. Structure of the iron binding exopolysaccharide produced anaerobically by the Gram-negative bacterium Klebsiella oxytoca BAS-10. European J Org Chem 2007, 31:5183-5189.

Levine AJ. p53, the cellular gatekeeper for growth and division. Cell (1997) 88, 323–331.

Levine B, Kroemer G. Autophagy in the pathogenesis of disease. Cell. 2008 Jan 11; 132(1):27-42.

Li B, Zhang HQ, Shi Y, et al. Overexpression of nuclear transport factor 2 may protect against diabetic retinopathy. Mol Vis. 2009;15:861-9. Epub 2009 Apr 27.

Liefers G-J, Cleton-Jansen A-M, van de Velde CJH, et al. Micrometastases and survival in stage II colorectal cancer. N Engl J Med 1998; 339:223-8.

Lin Y, Buckhaults PJ, Lee JR, et al. Association of the actin-binding protein transgelin with lymph node metastasis in human colorectal cancer. Neoplasia. 2009 Sep;11(9):864-73.

Loo C, Hirsch L, Lee M, et al. Gold nanoshell bioconjugates for molecular imaging in living cells. Opt. Lett. 2005. 30, 1012–1014.

Lowe SW, Cepero E, Evan G. Intrinsic tumour suppression. Nature (2004). 432, 307–315.

Lu W, Fu Z, Wang H, et al. Peroxiredoxin 2 is upregulated in colorectal cancer and contributes to colorectal cancer cells' survival by protecting cells from oxidative stress. Mol Cell Biochem. 2014 Feb;387(1-2):261-70. Epub 2013 Nov 15.

Lynch HT, de la Chapelle A. Hereditary colorectal cancer. N Engl J Med. 2003; 348: 919-932.

Ma Y, Zhang P, Yang Y, et al. Candidate microRNA biomarkers in human colorectal cancer: systematic review profiling studies and experimental validation. International Journal of Cancer, vol. 130, no. 9, pp. 2077–2087, 2011.

Mahapatra SS, Karak N. Silver nanoparticle in hyperbranched polyamine: synthesis, characterization and antibacterial activity. Mater. Chem. Phys. 2008. 112, 1114–1119.

Marisa L, de Reyniès A, Duval A, et al. Gene expression classification of colon cancer into molecular subtypes: characterization, validation, and prognostic value. PLoS Med. 2013;10(5):e1001453.

Martin TD, Der CJ. Differential involvement of RalA and RalB in colorectal cancer. Small GTPases. 2012 Apr-Jun;3(2):126-30. doi: 10.4161/sgtp.19571.

Martin TD, Samuel JC, Routh ED, et al. Activation and involvement of Ral GTPases in colorectal cancer Cancer Res. 2011 Jan 1;71(1): 206-15. doi: 10.1158/0008-5472.CAN-10-1517.

Meding S, Balluff B, Elsner M, et al. Tissue-based proteomics reveals FXYD3, S100A11 and GSTM3 as novel markers for regional lymph node metastasis in colon cancer. J Pathol. 2012 Dec;228(4):459-70.

Menéndez P, Padilla D, Villarejo P et al. Prognostic implications of serum microRNA-21 in colorectal cancer. Journal of Surgical Oncology, vol. 108, no. 6, pp. 369–373, 2013.

Mizushima N. Autophagy: process and function. Genes Dev. (2007). 21, 2861–2873.

Moore MC, Peppas NA. Micro- and nanotechnologies for intelligent and responsive biomaterial-based medical systems. Adv Drug Deliv. Rev. 2009. 61, 1391–1401.

Murugan K, Aruna P, Panneerselvam C, et al. Fighting arboviral diseases: low toxicity on mammalian cells, dengue growth inhibition (in vitro), and mosquitocidal activity of Centroceras clavulatum-synthesized silver nanoparticles. Parasitol Res DOI 10.1007/s00436-015-4783-6.

Naba A, Clauser KR, Whittaker CA, et al. Extracellular matrix signatures of human primary metastatic colon cancers and their metastases to liver. BMC Cancer. 2014 Jul 18;14:518.

Nair RR, Solway J, Boyd DD. Expression cloning identifies transgelin (SM22) as a novel repressor of 92-kDa type IV collagenase (MMP-9) expression. J Biol Chem. 2006;281(36):26424–36.

Naz S, Bashir M, Ranganathan P, et al. Protumorigenic actions of S100A2 involve regulation of PI3/Akt signaling and functional interaction with Smad3. Carcinogenesis vol.35 no.1 pp.14–23, 2014.

Navaladian Subramanian, Balasubramanian Viswanathan. Microwave assisted rapid synthesis of anisotropic Ag nanoparticles by solid state transformation. Nanotechnology. 01/2008; 19(4):045603.

Nelson WJ, Dickinson DJ, Weis WI. Roles of cadherins and catenins in cell-cell adhesion and epithelial cell polarity.
Prog Mol Biol Transl Sci 2013, 116:3-23.

Ngan CY, Yamamoto H, Seshimo I, et al. Quantitative evaluation of vimentin expression in tumour stroma of colorectal cancer. Br J Cancer. 2007 Mar 26;96(6):986-92.

O'Dwyer D, Ralton LD, O'Shea A, et al. The Proteomics of Colorectal Cancer: Identification of a Protein Signature Associated with Prognosis. PLoS ONE 6(11): e27718. (2011).

O'Reilly KE, Rojo F, She QB, et al. mTOR inhibition induces upstream receptor tyrosine kinase signaling and activates Akt. Cancer Res. (2006) 66, 1500–1508.

Oh DY, Kim TW, Park YS, et al. Phase 2 study of everolimus monotherapy in patients with nonfunctioning neuroendocrine tumors or pheochromocytomas/paragangliomas. Cancer. 2012 Dec 15;118(24):6162-70.

Ohtsu N, Nakatani Y, Yamashita D, et al. Eva1 Maintains the Stem-like Character of Glioblastoma-Initiating Cells by Activating the Noncanonical NF-κB Signaling Pathway. Cancer Res. 2016 Jan 1;76(1):171-81.

Otsuki S, Inokuchi M, Enjoji M, et al. Vimentin expression is associated with decreased survival in gastric cancer. Oncol Rep. 2011 May;25(5):1235-42.

Palumbo JS, Kombrinck KW, Drew AF, et al. Fibrinogen is an important determinant of the metastatic potential of circulating tumor cells. Blood. 2000 Nov 15;96(10):3302-9.

Park S, Kim S. Activated Akt signaling pathway in invasive ductal carcinoma of the breast: Correlation with HER2 overexpression. Oncology Reports 18: 139-143, 2007.

Patel P, Clarke C, Barraclough DL, et al. Metastasis-promoting anterior gradient 2 protein has a dimeric thioredoxin fold structure and a role in cell adhesion. J Mol Biol. 2013 Mar 11;425(5):929-43.

Perou CM, Sorlie T, Eisen MB, et al. Molecular portraits of human breast tumours. Nature. 2000;406(6797):747–752.

Petrova DT, Asif AR, Armstrong VW, et al. Expression of chloride intracellular channel protein 1 (CLIC1) and tumor protein D52 (TPD52) as potential biomarkers for colorectal cancer. Clin Biochem. 2008 Oct;41(14-15):1224-36.

Pollak M. Insulin and insulin-like growth factor signaling in neoplasia. Nat Rev Cancer. 2008 Dec;8(12):915-28. doi: 10.1038/nrc2536.

Pritchard CC, Grady WM. Colorectal cancer molecular biology moves into clinical practice. Gut (2011) 60: 116–129.

Pucci-Minafra I, Cancemi P, Marabeti MR, et al. Proteomic profiling of 13 paired ductal infiltrating breast carcinomas and non-tumoral adjacent counterparts. Proteomics Clin Appl. 2007 Jan;1(1):118-29.

Pucci-Minafra I, Cancemi P, Albanese NN, et al. New protein clustering of breast cancer tissue proteomics using actin content as a cellularity indicator. J Proteome Res. 2008 Apr;7(4):1412-8.

Pucci-Minafra I, Fontana S, Cancemi P, et al. Proteomic patterns of cultured breast cancer cells and epithelial mammary cells. Ann N Y Acad Sci. 2002 Jun;963:122-39.

Pucci-Minafra I, Minafra S, La Rocca G, et al. Zymographic analysis of circulating and tissue forms of colon carcinoma gelatinase A (MMP-2) and B (MMP-9) separated by mono- and two-dimensional electrophoresis. Matrix Biology 20 (2001) 419-427.

Puppa G, Sonzogni A, Colombari R, et al. TNM staging system of colorectal carcinoma: a critical appraisal of challenging issues. Arch Pathol Lab Med. 2010; 134(6):837-52.

Qiu Y, Park K. Environment-sensitive hydrogels for drug delivery. Adv. Drug Deliv. Rev. 2001 53, 321–339.

Ratto C, Sofo L, Ippoliti M, et al. Prognostic factors in colorectal cancer. Literature review for clinical application. Dis Colon Rectum 1998; 41:1033-49.

Roy PG, Thompson AM. Cyclin D1 and breast cancer. Breast 2006, 15:718-727

Ryuk JP, Choi G-S, Park JS, et al. Predictive factors and the prognosis of recurrence of colorectal cancer within 2 years after curative resection. Annals of Surgical Treatment and Research 2014;86(3):143-151.

Sadanandam A, Lyssiotis CA, Homicsko K, et al. A colorectal cancer classification system that associates cellular phenotype and responses to therapy. Nat Med. 2013 May;19(5):619-25.

Safari J, Zarnegar Z. Advanced drug delivery systems: Nanotechnology of health design a review. Journal of Saudi Chemical Society (2014) 18, 85–99.

Saku T, Sakai H, Tsuda N, et al. Cathepsins D and E in normal, metaplastic, dysplastic, and carcinomatous gastric tissue: an immunohistochemical study. Gut. 1990 Nov;31(11):1250-5.

Salata OV. Applications of nanoparticles in biology and medicine. Journal of Nanobiotechnology, vol. 2, no. 1, article 3, 2004.

Sanchez-Tillo E, de Barrios O, Siles L, et al. Beta-catenin/tcf4 complex induces the epithelial to mesenchymal transition (EMT)-activator zeb1 to regulate tumor invasiveness. Proc Natl Acad Sci USA 2011, 108:19204-192099.

Sansom OJ, Reed KR, Hayes AJ, et al. Loss of apc in vivo immediately perturbs wnt signaling, differentiation, and migration. Genes Dev 2004, 18:1385-1390.

Sapkota D, Bruland O, Costea DE, et al. S100A14 regulates the invasive potential of oral squamous cell carcinoma derived cell-lines in vitro by modulating expression of matrix metalloproteinases, MMP1 and MMP9. Eur J Cancer. 2011 Mar;47(4):600-10.

Sarbassov DD, Ali SM, Sabatini DM. Growing roles for the mTOR pathway. Curr Opin Cell Biol17:596–603. 2005.

Sayar N, Karahan G, Konu O, et al. Transgelin gene is frequently downregulated by promoter DNA hypermethylation in breast cancer. Clin Epigenetics. 2015 Sep 28;7:104.

Scheid MP, Marignani PA, Woodgett JR. Multiple phosphoinositide 3-kinase-dependent steps in activation of protein kinase B. Mol Cell Biol 2002. 22:6247–6260.

Scorilas A, Karamelis A, Arnogiannaki N, et al. Overexpression of matrix-metalloproteinase-9 in human breast cancer: a potential favourable indicator in node-negative patients. Br. J. Cancer 84 (2001) 1488–1496.

Seshadri R, Matthews C, Dobrovic A, et al. The significance of oncogene amplification in primary breast cancer. Int J Cancer. 1989 Feb 15; 43(2):270-2.

Shevchenko A, Wilm M, Vorm O, et al. Mass spectrometric sequencing of proteins from silver stained polyacrylamide gels. Anal. Chem. 68, 850-858. (1996)

Shields JM, Rogers-Graham K, Der CJ. Loss of transgelin in breast and colon tumors and in RIE-1 cells by Ras deregulation of gene expression through Raf-independent pathways. J Biol Chem. 2002 Mar 22;277(12):9790-9.

Shin IY, Sung NY, Lee YS, et al. The expression of multiple proteins as prognostic factors in colorectal cancer: cathepsin D, p53, COX-2, epidermal growth factor receptor, C-erbB-2, and Ki-67. Gut Liver. 2014 Jan;8(1):13-23.

Shirota Y, Stoehlmacher J, Brabender J, et al. ERCC1 and thymidylate synthase mRNA levels predict survival for colorectal cancer patients receiving combination oxaliplatin and fluorouracil chemotherapy. Journal of clinical oncology. 2001; 19(23):4298–304.

Silva EJ, Argyris PP, Zou X, et al. S100A8/A9 regulates MMP-2 expression and invasion and migration by carcinoma cells. Int J Biochem Cell Biol. 2014 Oct;55:279-87.

Simiczyjew A, Mazur AJ, Popow-Woźniak A, et al. Effect of overexpression of β- and γ-actin isoforms on actin cytoskeleton organization and migration of human colon cancer cells. Histochem Cell Biol. 2014 Sep;142(3):307-22.

Sinha S, Levine B. The autophagy effector Beclin 1: a novel BH3- only protein. Oncogene (2008) 27 (Suppl 1), S137–S148.

Sintubin L, De Gusseme B, Van der Meeren P et al. The antibacterial activity of biogenic silver and its mode of action. (2011) Appl Microbiol Biotechnol 91:153–162.

Slamon DJ, Clark GM, Wong SG, et al. Human breast cancer: correlation of relapse and survival with amplification of the HER-2/neu protooncogene in human breast and ovarian cancer. Science 1989; 244:707-12.

Slamon DJ, Godolphin W, Jones LA, et al. Studies of the HER-2/neu proto-oncogene in human breast and ovarian cancer. Science. 1989; 244(4905):707-12.

Søreide K, Nedrebø BS, Knapp JC, et al. Evolving molecular classification by genomic and proteomic biomarkers in colorectal cancer: potential implications for the surgical oncologist. Surg Oncol (2009) 18: 31–50.

Sridharan M, Hubbard JM, Grothey A. Colorectal Cancer: How Emerging Molecular Understanding Affects Treatment Decisions. February 15, 2014 | Oncology Journal.

Srinivas PR., Verma M, Zhao Y, et al. Proteomics for cancer biomarker discovery. Clin Chem, 2002. 48(8): p. 1160-9.

Sudarsanam S, Johnson DE. Functional consequences of mTOR inhibition. Curr. Opin. Drug Discov. Devel. (2010). 13, 31–40.

Takayama T, Miyanishi K, Hayashi T et al. Colorectal cancer: genetics of development and metastasis. J Gastroenterol 2006; 41:185–192.

Talmadge JE, Fidler IJ. AACR centennial series: the biology of cancer metastasis: historical perspective. Cancer Res. (2010)70, 5649–5669.

Talvensaari-Mattila A, Pääkkö P, Höyhtyä M, et al. MMP-2 immunocreative protein, a marker of aggressiveness in breast carcinoma. Cancer 83 (1998) 1153–1162.

Tan GJ, Peng ZK, Lu JP, et al. Cathepsins mediate tumor metastasis. World J Biol Chem. 2013 Nov 26;4(4):91-101.

Tan IB, Tan P. Genetics: an 18-gene signature (ColoPrint(R)) for colon cancer prognosis. Nat Rev Clin Oncol. 2011;8:131–3.

Tan S, Melek E, Attygalle A, et al. Synthesis of positively charged silver nanoparticles via photoreduction of AgNO3 in branched polyethyleneimine/HEPES solutions. Langmuir 23(19):9836-9843. 2007.

Thomas CD, Franco AMA, Hill. **JK.** Range retractions and extinction in the face of climate warming. Trends Ecol. Evol. 2006, 21, 415-416.

Toker A, Newton AC. Cellular signaling: Pivoting around PDK-1. Cell 103: 185–188. 2000.

Tolaymata TM, El Badawyb AM, Genaidyc A, et al. An evidence-based environmental perspective of manufactured silver nanoparticle in syntheses and applications: A systematic review and critical appraisal of peer-reviewed scientific papers. Science of The Total Environment, Vol. 408, Issue 5, 1 February 2010, Pages 999–1006.

Tomozawa S, Tsuno NH, Sunami E, et al. Cyclooxygenase-2 overexpression correlates with tumour recurrence, especially haematogenous metastasis, of colorectal cancer. British Journal of Cancer (2000) 83(3), 324–328.

Tran PA, Zhang L, Webster TJ. Carbon nanofibers and carbon nanotubes in regenerative medicine. Adv. Drug Deliv. Rev. 2009. 61, 1097–1114.

Turpeenniemi-Hujanen T. Gelatinases (MMP-2 and -9) and their natural inhibitors as prognostic indicators in solid cancers. Biochimie 87 (2005) 287–297.

Urruticoechea A, Smith IE, Dowsett M. Proliferation marker Ki-67 in early breast cancer. J Clin Oncol.2005;23:7212–7220. doi: 10.1200/JCO.2005.07.501.

Ushigome M, Ubagai T, Fukuda H, et al. Up-regulation of hnRNP A1 gene in sporadic human colorectal cancers. Int J Oncol. 2005, 26: 635-640.

Valinluck Lao V, Grady WM. Epigenetics and colorectal cancer. Nat Rev Gastroenterol Hepatol. 2011 October 18; 8(12): 686–700. doi: 10.1038/nrgastro.2011.173.

Vander Heiden MG, Cantley LC, Thompson CB. Understanding the Warburg effect: the metabolic requirements of cell proliferation. Science, 324 (2009), pp. 1029–1033.

Vigneshwaran N, Kathe AA, Varadarajan PV et al. Biomimetics of silver nanoparticles by white rot fungus, Phaenerochaete chrysosporium. Colloids and Surfaces B: Biointerfaces 53.; 55 59 (2006).

Verma S, Salmans ML, Geyfman M, et al. The estrogen-responsive Agr2 gene regulates mammary epithelial proliferation and facilitates lobuloalveolar development. Developmental Biology 369: 249–260 (2012).

Visvader JE. Cells of origin in cancer. Nature 469,314–322(20 January 2011) doi:10.1038/nature09781.

Walsh LA, Damjanovski S. IGF-1 increases invasive potential of MCF 7 breast cancer cells and induces activation of latent TGF-β1 resulting in epithelial to mesenchymal transition. Cell Commun Signal. 2011 May 2;9(1):10.

Wang H, Duan L, Zou Z et al. Activation of the PI3K/Akt/mTOR/p70S6K Pathway is Involved in S100A4-induced Viability and Migration in Colorectal Cancer Cells. International Journal of Medical Sciences 2014; 11(8): 841-849.

Wang G, Wang X, Wang S, et al. Colorectal cancer progression correlates with upregulation of S100A11 expression in tumor tissues. Int J Colorectal Dis. 2008 Jul;23(7):675-82.

Wang L, Shen X, Wang Z, et al. A molecular signature for the prediction of recurrence in colorectal cancer. Molecular Cancer (2015) 14:22.

Wang P, Zhang C, Yu P, et al. Regulation of colon cancer cell migration and invasion by CLIC1-mediated RVD. Mol Cell Biochem. 2012 Jun;365(1-2):313-21.

Wang P, Zeng Y, Liu T, et al. Chloride intracellular channel 1 regulates colon cancer cell migration and invasion through ROS/ERK pathway. World J Gastroenterol. 2014 Feb 28;20(8):2071-8.

Wasinger VC, Cordwell SJ, Cerpa-Poljak A, et al. Progress with gene-product mapping of the Mollicutes: Mycoplasma genitalium. Electrophoresis. 1995 Jul; 16(7):1090-4.

Williams MD, Nguyen T, Carriere PP et al. Protein Kinase CK2 Expression Predicts Relapse Survival in ER_ Dependent Breast Cancer, and Modulates ER_ Expression in Vitro. Int. J. Environ. Res. Public Health 2016, 13, 36;

Wilkins MR, Sanchez JC, Gooley AA, et al. Progress with proteome projects: why all proteins expressed by a genome should be identified and how to do it. Biotechnol Genet Eng Rev. 1996; 13:19-50.

Wright JA, Richer JK, Goodall GJ. Micrornas and EMT in mammary cells and breast cancer. J Mammary Gland Biol Neoplasia 2010, 15:213-223.

Xie W, Herschman HR. v-src induces prostaglandin synthase 2 gene expression by activation of the c-Jun N-terminal kinase and the c-Jun transcription factor. J Biol Chem. 1995 Nov 17;270(46):27622-8.

Xueru Li, Hui Sun, He Zha, et al. Activation of the PI3K/Akt/mTOR/p70S6K Pathway is Involved in S100A4-induced Viability and Migration in Colorectal Cancer Cells.International Journal of Medical Sciences 2014; 11(8): 841-849.

Yarden Y, Ullrich A. Growth factor receptor tyrosine kinases. Ann Rev Biochem.1988; 57:443-78.

You Q, Guo H, Xu D. Distinct prognostic values and potential drug targets of ALDH1 isoenzymes in non-small-cell lung cancer. Drug Des Devel Ther. 2015 Sep 3;9:5087-97.

Zhang Y, Ye Y, Shen D, et al. Identification of transgelin-2 as a biomarker of colorectal cancer by laser capture microdissection and quantitative proteome analysis. Cancer Sci. 2010 Feb;101(2):523-9.

Zhang W, Liu Y, Wang CW. S100A4 promotes squamous cell laryngeal cancer Hep-2 cell invasion via NF-kB/MMP-9 signal. Eur Rev Med Pharmacol Sci. 2014;18(9):1361-7.

Zhao L, Wang H, Deng YJ, et al. Transgelin as a suppressor is associated with poor prognosis in colorectal carcinoma patients. Mod Pathol. 2009 Jun;22(6):786-96.

Zheng G, Dahl JA, Niu Y, et al. ALKBH5 is a mammalian RNA demethylase that impacts RNA metabolism and mouse fertility. Mol Cell. 2013 Jan 10;49(1):18-29.

Zhou X, Tan M, Stone Hawthorne V, et al. Activation of the Akt/mammalian target of rapamycin/4E-BP1 pathway by ErbB2 overexpression predicts tumor progression in breast cancers. Clin Cancer Res 10: 6779-6788, 2004.

Zhou X, Teng L, Wang M. Distinct prognostic values of four-Notch-receptor mRNA expression in ovarian cancer. Tumour Biol. 2015 Dec 12.

SUPPLEMENTARY TABLES

Supplementary Table 1. Identified differentially expressed proteins on the colon proteome. In the ID column are indicated spot number and picking proteomic map: A) pooled colon cancer and paired normal tissues, B) colon tumor and paired normal tissues; C) colon tumor and colon metastatic tissues; g.m = gel matching.

ID	Abbreviated Protein name	Accession number	Score	Sequence coverage	Molecular weight (Da)	Theoretical pI
49/A	1433B	P31946	111	44%	27951,20	4,76
9/B	A1AT	P01009	125	38%	44324	5,37
44/A	A1AT a	P01009	73	38%	44324	5,37
138/A	A1AT b	P01009	120	50%	44324	5,37
137/A	A1AT c	P01009	128	55%	44324	5,37
136/A	A1AT d	P01009	106	47%	44324	5,37
46+/C	ACADS	P16219	243	43%	41721	6,15
67/A	ACON	Q99798	79	20%	82426	6,85
15+/C	ACON	Q99798	69	6%	82426	6,85
130/A	ACTB a	P60709	125	59%	41737	5,29
119/A	ACTB b	P60709	72	35%	41737	5,29
120/A	ACTB c	P60709	74	23%	41737	5,29
63/A	ACTB d	P60709	145	55%	41737	5,29
61/A	ACTB e	P60709	118	44%	41737	5,29
128/A	ACTB f	P60709	78	38%	41737	5,29
62/A	ACTB g	P60709	139	52%	41737	5,29
26/A	ACTB/G fr a	P63261	64	21%	41737	5,29
17/A	ACTB/G fr b	P63261	57	30%	41737	5,29
60/A	ACTG a	P63261	98	25%	41737	5,29
113/A	ACTG b	P63261	76	29%	41737	5,29
2/A	ACTH	P63267	107	43%	41643	5,31
65/A	ACTN4	O43707	64	31%	104854,04	5,27
34-/B	AGR2	O95994	71	54%	17817	9,06
23+/C	AL4A1 a	P30038	121	41%	59034	6,96
22+/C	AL4A1 b	P30038	82	25%	59034	6,96
23+/C	AL4A1 c	P30038	177	46%	59034	6,96
36/A	ALBU a	P02768	114	33%	66472	5,67
51/A	ALBU b	P02768	121	36%	66472	5,67
46/A	ALBU c	P02768	80	25%	66472	5,67
72/A	ALBU d	P02768	142	33%	66472	5,67
103/A	ALBU e	P02768	106	28%	66472	5,67
34/A	ALBU f	P02768	101	27%	66472	5,67
143-/B	ALDOA a	P04075	73	49%	39289	8,39
142-/B	ALDOA b	P04075	73	39%	39289	8,39
141-/B	ALDOA c	P04075	69	47%	39289	8,39
145-/B	ALKBH5	Q6P6C2	76	12%	44256	9,19
75/A	AMPL	P28838	80	38%	56166	8,03
105/A	APOA1	P02647	97	40%	28079	5,27
3/B	APOA1	P02647	94	44%	28079	5,27
17-/B	ARL5B	Q96KC2	63	28%	20243	6,07

ID	Abbreviated Protein name	Accession number	Score	Sequence coverage	Molecular weight (Da)	Theoretical pI
95/A	BICR2	A1A5D9	58	22%	56834	4,99
99/A	BLVRB	P30043	68	65%	21988	7,31
115/A	CAH1	P00915	68	40%	28739	6,63
21+/C	CATA a	P04040	73	37%	59624	6,95
22+/C	CATA b	P04040	54	22%	59624	6,95
68+/C	CATD a	P07339	83	18%	37852	5,60
115-/C	CATD b	P07339	62	24%	37852	5,60
41/A	CCNI	Q14094	61	37%	42557	8,23
70/A	CH60	P10809	62	25%	57963	5,24
160-/B	CH60 a	P10809	99	35%	57963	5,24
159-/B	CH60 b	P10809	61	26%	57963	5,24
168-/B	CLTA	P09496	58	16%	23662	4,45
119/A	CLIC1	O00299	92	60%	26791,54	5,09
53-/B	CLIC1	O00299	g.m.	g.m.	26791,54	5,09
13/A	COF1	P23528	61	36%	18371	8,26
130-/B	COF1	P23528	73	42%	18371	8,26
25-/B	COLEC10	Q9Y6Z7	61	17%	27617	6,28
2+/C	CPSM a	P31327	193	26%	160550	5,92
3+/C	CPSM b	P31327	91	11%	160550	5,92
52+/C	CRB1 a	P16152	73	36%	30244	8,55
51+/C	CRB1 b	P16152	93	63%	30244	8,55
113-/B	DDAH1	O94760	64	20%	30991	5,53
48/A	DESM a	P17661	75	37%	53536	5,21
52/A	DESM b	P17661	113	47%	53536	5,21
49+/C	ECH1	Q13011	115	43%	32206	5,99
59-/B	EF1B	P24534	61	24%	24633	4,50
134/A	ENOA a	P06733	168	50%	47038	6,99
33+/B	ENOA a	P06733	82	22%	47038	6,99
143/A	ENOA b	P06733	202	50%	47038	6,99
148-/B	ENOA b	P06733	111	44%	47038	6,99
149-/B	ENOA c	P06733	86	34%	47038	6,99
150-/B	ENOA d	P06733	79	29%	47038	6,99
76-/B	ENOA fr a	P06733	129	29%	47038	6,99
112-/B	ENOA fr b	P06733	99	33%	47038	6,99
1+/C	ENPL	P14625	66	17%	90178	4,73
7+/C	ERG7	P48449	64	11%	83178	6,15
165-/B	ERP29 a	P30040	119	49%	25853	6,08
117-/B	ERP29 b	P30040	92	31%	25853	6,08
54+/C	ETFB	P16219	83	47%	27712	8,29
84-/B	EVA1C	P58658	58	21%	44122	5,85
135/A	EXOC7	P08670	59	32%	53520	5,05
8+/C	EXOC7	Q96BU6	59	9%	83382	6,33
83/A	FABPL	P07148	g.m.	g.m.	14208	6,6
45/A	FIBB	P02675	66	35%	50762,93	7,95
85-/C	FUMH a	PO7954	98	23%	50081	6,99

ID	Abbreviated Protein name	Accession number	Score	Sequence coverage	Molecular weight (Da)	Theoretical pI
86-/C	FUMH b	PO7954	78	30%	50081	6,99
126/A	G3P2 a	P04406	128	47%	35922	8,58
125/A	G3P2 b	P04406	148	41%	35922	8,58
124/A	G3P2 c	P40926	99	40%	35922	8,58
93-/C	G3P2 a	P04406	67	38%	35922	8,58
92-/B	G3P2 b	P04406	60	31%	35922	8,58
91-/C	G3P2 c	P04406	80	42%	35922	8,58
31+/C	GATM	P50440	86	39%	44283	6,42
104/A	GDIR1	P52565	86	32%	23076	5,01
68/A	GRP78	P11021	76	35%	70479	5,01
80-/B	GRP78	P11021	120	33%	70479	5,01
39-/B	GRPEL1	Q9HAV7	61	47%	21336	6,03
56+/C	GSTA1	P08263	94	33%	25499	8,92
101/A	GSTP1	P09211	90	58%	23225	5,44
16/A	HBA	P69905	64	42%	15126	8,73
83/A	HBB a	P68871	g.m.	g.m.	14208	6,6
12/A	HBB b	P68871	73	57%	15867	6,81
55/A	HBB b	P68871	62	57%	15867	6,81
24/A	HBB d	P68871	107	72%	15867	6,81
19/A	HBB e	P68871	68	45%	15867	6,81
114/A	HBB f	P68871	66	61%	15867	6,81
32/A	HBB g	P68871	63	56%	15867	6,81
31/A	HBB h	P68871	78	63%	15867	6,81
20/A	HCD2	Q99714	63	48%	26792	7,87
45-/B	HEBP2	Q9Y5Z4	61	24%	22875	4,55
133/A	HMCS2	P54868	72	15%	52383	6,64
32+/C	HMCS2	P54868	81	26%	52383	6,64
44+/C	HPT	P00738	86	25%	43341	6,13
122/A	HS71A	P0DMV8	56	21%	69921,04	5,48
2/B	HSPB1	P04792	60	40%	22782	5,98
4+/C	HYOU1	Q9Y4L1	65	13%	107660	5,07
132/A	IDHC	O75874	158	57%	46528	6,53
107/A	IGKC	P01834	75	56%	10821	5,58
82-/B	IMPDH2	P12268	88	21%	55673	6,46
39+/C	IVD	P26440	60	23%	43069	6,90
90/A	K1C9 a	P35527	74	23%	62064	5,14
106/A	K1C9 b	P35527	106	40%	62064	5,14
55+/C	KAD3	Q9UIJ7	85	42%	25434	9,16
63/A	KCRB	P12277	87	42%	42513	5,35
124-/B	CMPK1	P30085	74	39%	22222	5,44
85/A	LEG1H	P09382	93	49%	35858	5,79
120-/B	GLO1	Q04760	67	36%	20647	5,12
124/A	MDHM	P04406	101	45%	35922	8,58
93/A	NDKA	P15531	71	50%	17149	5,81
19-/B	NDKA	P15531	67	51%	17149	5,81

ID	Abbreviated Protein name	Accession number	Score	Sequence coverage	Molecular weight (Da)	Theoretical pI
129-/B	NDKB	P22392	59	55%	17298	8,52
5/A	NDKB a	P22392	61	44%	17298	8,52
6/A	NDKB b	P22392	57	53%	17298	8,52
37/A	NDUF7	Q7L592	62	27%	44244	7,31
20+/C	NLTP	P22307	75	32%	58993	6,44
114-/B	NPM	P06748	68	30%	32575	4,64
118-/B	PARK7	Q99497	92	66%	19891	6,26
50+/C	PBLD	P30039	88	43%	31785	6,06
73/A	PDIA1	P30101	146	41%	55294,02	4,69
155-/B	PDIA3 a	P30101	168	58%	54265	5,61
154-/B	PDIA3 b	P30101	118	46%	54265	5,61
111-/C	PEBP1	P30086	108	74%	20926	7,43
26-/B	PFDN5	Q99471	65	41%	17328	5,94
38/A	PGK1 a	P00558	103	47%	44483	8,3
89-/B	PGK1 a	P00558	125	27%	44483	8,30
131/A	PGK1 b	P00558	150	60%	44483	8,3
88-/C	PGK1 b	P00558	70	24%	44483	8,30
89/A	PPIA a	P62937	80	50%	18012	7,68
131-/B	PPIA a	P62937	71	46%	17881	7,82
7/A	PPIA b	P62937	104	46%	17881	7,82
8/B	PPIA b	P62937	114	41%	17881	7,82
88/A	PPIA c	P62937	104	56%	18012	7,68
26a/A	PPIA d	P62937	84	53%	17881	7,82
133-/C	PRDX1	Q06830	101	56%	21979	8,27
4/B	PRDX2	P32119	123	48%	21761	5,67
94/A	PRDX2 a	P32119	85	39%	15819	9,14
96/A	PRDX2 b	P32119	85	35%	15819	9,14
11/A	PROF1	P07737	56	47%	14923	8,47
29/A	PSB3	P49720	69	37%	22818	6,12
103-/B	PSB6	P28072	68	21%	21904	4,91
116-/B	PSME1	Q06323	76	31%	28723	5,78
139-/B	RALB	P11234	73	40%	23079	6,24
79/A	RL40	P0CG47	81	28%	8565	6,56
8-/B	RL40	P62987	65	42%	8565	6,56
18/A	ROA2	P22626	79	32%	37430	8,97
81/A	S10AB	P31949	64	36%	11609	6,82
128-/B	S10AB	P31949	101	52%	11609	6,82
91/A	TAGL a	Q01995	100	59%	22480	8,88
92/A	TAGL b	Q01995	85	35%	22480	8,88
87/A	TAGL c	Q01995	110	42%	22480	8,88
86/A	TAGL d	Q01995	134	58%	22480	8,88
119-/B	TCTP	P13693	62	41%	19595	4,84
66/A	TERA	P55072	191	40%	89191	5,14
39+/C	THIL a	P24752	67	37%	41386	8,16
40+/C	THIL b	P24752	85	26%	41386	8,16

ID	Abbreviated Protein name	Accession number	Score	Sequence coverage	Molecular weight (Da)	Theoretical pI
41+/C	THIL c	P24752	72	23%	41386	8,16
84/A	THIO	P10599	g.m.	g.m.	11606	4,82
110/A	TPIS	P60174	135	39%	30791	5,65
50/A	TPM1	P09493	83	39%	32709	4,69
4/A	TPM2	P07951	98	46%	32851	4,66
57-/B	TPM3	P06753	69	26%	32819	4,68
58-/B	TPM4	P67936	68	32%	28391	4,67
52/A	TPM4 a	P67936	70	46%	28391	4,67
121/A	TPM4 b	P67936	122	41%	28391	4,67
17+/C	TRFE a	P02787	88	19%	75195	6,70
18+/C	TRFE b	P02787	79	17%	75195	6,70
79/A	UBB	P62987	83	50%	6181	10,32
25+/C	UGPA a	Q16851	123	47%	56940	8,15
26+/C	UGPA b	Q16851	149	40%	56940	8,15
61+/C	UK114	P52758	67	40%	14362	8,73
104-/B	VDAC1	P21796	74	28%	30641	8,63
95-/B	VDAC2	P45880	62	29%	31566	7,50
135/A	VIME	Q96BU6	58	22%	83382	6,33
48/A	VIME a	P08670	93	36%	53520	5,05
3/A	VIME b	P08670	94	38%	53520	5,05
100/A	VIME c	P08670	62	27%	53520	5,05
65/A	VINC	P18206	145	35%	123668	5,51
139/A	VTDB	P02774	61	54%	51243	5,22

Supplementary Table 2. Identified differentially expressed proteins on the SKBR-3 proteome after treatments with NaNPs-EPS, Ag^{0}NPs-EPS and Ag^{+1}NPs-EPS; g.m. = gel matching.

ID	Abbreviated Protein name	Accession number	Score	Sequence coverage	Molecular weight (Da)	Theoretical pI
17	ACON a	Q99798	g.m.	g.m.	82426,00	6,85
18	ACON b	Q99798	g.m.	g.m.	82426,00	6,85
127	ACTB	P60709	130	42%	41737,00	5,29
125	ADK	P55263	95	30%	40414,24	6,25
159	AK1BA	O60218	g.m.	g.m.	35888,39	7,81
148	ALDOA	P04075	g.m.	g.m.	39289,00	8,39
242	ALDR	P15121	g.m.	g.m.	35722,21	6,55
153	ANXA1	P04083	g.m.	g.m.	38583,05	6,64
188	APOA1 a	P02647	g.m.	g.m.	28079,00	5,27
203	APOA1 b	P02647	g.m.	g.m.	28079,00	5,27
123	ASSY	P00966	87	26%	46530,37	8,06
106	ATPB a	P06576	70	27%	51769,25	5
105	ATPB b	P06576	156	44%	51769,25	5
111	BUB3	O43684	g.m.	g.m.	37154,78	6,36
65	CALR a	P27797	g.m.	g.m.	46466,37	4,29
72	CALR b	P27797	79	31%	48200,00	4,29
75	CATA	P04040	100	25%	59624,00	6,95
67	CH60 a	P10809	g.m.	g.m.	57963,00	5,24
70	CH60 b	P10809	g.m.	g.m.	57963,00	5,24
199	DHRS2 a	Q13268	145	43%	27307,00	8,9
202	DHRS2 b	Q13268	124	43%	27307,00	8,9
3	EF1B	P24534	g.m.	g.m.	24633,00	4,5
156	EF1D	P29692	72	35%	30990,64	4,9
115	EF1G	P68104	71	35%	49987,62	6,27
120	EFTU	P49411	92	22%	45045,00	6,31
253	ENOA a	P06733	167	44%	47037,77	6,99
247	ENOA b	P06733	150	45%	47037,77	6,99
7	ENPL a	P14625	199	40%	90178,00	4,73
14	ENPL b	P14625	g.m.	g.m.	90178,00	4,73
48	FABD	Q8IVS2	59	27%	40631,74	8,15
81	FKBP4	Q02790	117	39%	51804,56	5,35
116	FUMH	P07954	104	31%	50081,00	6,99
64	G3P2	P04406	115	49%	35922	8,58
204	GDIA1	P31150	g.m.	g.m.	50582,72	5
201	GDIR1	P52565	g.m.	g.m.	23075,92	5,01
39	GRP75	P38646	97	26%	68759,00	5,44
249	GRP78	P11021	97	28%	70479,00	5,01
103	HNRH1	P31943	60	27%	49484,00	5,89
66	HNRPK a	P61978	80	32%	50976.25	5.39
68	HNRPK b	P61978	116	32%	50976.25	5.39
250	HSP74	P34932	g.m.	g.m.	94330,92	5,1
40	HSP7C a	P11142	86	24%	70766,90	5,37
43	HSP7C b	P11142	89	25%	70766,90	5,37
243	HSPB1 a	P04792	94	52%	28672,74	6,75

ID	Abbreviated Protein name	Accession number	Score	Sequence coverage	Molecular weight (Da)	Theoretical pI
183	HSPB1 b	P04792	85	51%	28672,74	6,75
194	HSPB1 c	P04792	g.m.	g.m.	28672,74	6,75
186	HSPB1 d	P04792	71	51%	28672,74	6,75
121	K1C18	P05783	143	30%	47926,62	5,34
239	K1C19	P08727	311	69%	44106,00	5,05
133	K1C19 a	P08727	296	69%	44106,00	5,05
132	K1C19 b	P08727	261	63%	44106,00	5,05
128	K1C19 c	P08727	223	63%	44106,00	5,05
129	K1C19 d	P08727	262	65%	44106,00	5,05
130	K1C19 e	P08727	316	68%	44106,00	5,05
91	K2C7	P08729	103	36%	51254,47	5,39
96	K2C8 a	P05787	173	48%	53704,25	5,52
244	K2C8 b	P05787	253	52%	53704,25	5,52
74	KPYM a	P14618	g.m.	g.m.	57805,70	7,95
71	KPYM b	P14618	g.m.	g.m.	57805,70	7,95
193	LEG3A	P17931	g.m.	g.m.	26021,14	8,6
245	MBD4	O95243	68	17%	66050,90	9,01
229	NTF2	P61970	g.m.	g.m.	14478,48	5,1
122	ODPA	P08559	71	32%	40081,77	6.51
135	PCBP1	Q15365	68	24%	37497,81	6,66
79	PDIA1 a	P07237	217	52%	55294,02	4,69
84	PDIA1 b	P07237	131	35%	55294,02	4,69
151	PDIA1 c	P07237	79	21%	55294,02	4,69
86	PDIA3 a	P30101	94	27%	54265,00	5,61
87	PDIA3 b	P30101	68	29%	54265,00	5,61
126	PGK1	P00558	124	41%	44483,00	8,3
179	PHB	P35232	76	31%	29672,91	5,57
219	PRDX2 a	P32119	g.m.	g.m.	21761,00	5,67
214	PRDX2 b	P32119	82	39%	21761,00	5,67
191	PRDX6	P30041	103	45%	24903,79	6,02
187	PSA5	P28066	g.m.	g.m.	26411,03	4,74
251	ROA1	P09651	100	38%	38746,65	9,17
233	S100A6	P06703	g.m.	g.m.	10179,74	5,32
225	SODC	P00441	g.m.	g.m.	15804,55	5,7
217	SODM a	P04179	g.m.	g.m.	22204,14	6,86
215	SODM b	P04179	g.m.	g.m.	22204,14	6,86
100	TBB4B	P68371	145	38%	49831,01	4,79
88	TCPB	P78371	93	35%	57357,02	6,02
12	TERA	P55072	241	37%	89190,61	5,14
228	THIO a	P10599	g.m.	g.m.	11606,30	4,82
227	THIO b	P10599	g.m.	g.m.	11606,30	4,82
195	TPIS a	P60174	67	43%	30791,00	5,45
196	TPIS b	P60174	141	61%	30791,00	5,45
150	TPM2	P07951	g.m.	g.m.	32850,73	4,66

ID	Abbreviated Protein name	Accession number	Score	Sequence coverage	Molecular weight (Da)	Theoretical pI
175	TPM4 a	P67936	94	50%	28390,62	4,67
178	TPM4 b	P67936	140	66%	28390,62	4,67
222	TTHY	P02766	g.m.	g.m.	13761,41	5,31
234	UBB a	P0CG47	g.m.	g.m.	8564,84	6,56
235	UBB b	P0CG47	g.m.	g.m.	8564,84	6,56
189	UCHL1 a	P09936	g.m.	g.m.	24554,01	5,22
192	UCHL1 b	P09936	g.m.	g.m.	24554,01	5,22
75	UGDH	O60701	82	40%	55024,09	6,73
171	VDAC 2	P21796	79	32%	31500,00	7,5
97	VIME a	P08670	147	45%	53520,49	5,05
92	VIME b	P08670	235	61%	53520,49	5,05
95	VIME c	P08670	59	23%	53520,49	5,05

ACKNOWLEDGEMENT

I would like to express my gratitude to those who have permission to carry out this research project.

*My deepest thanks go firstly to my supervisor **Dott.ssa Patrizia Cancemi**, for giving me this important opportunity, sharing not only lab experiments but also moments of daily life, encouraging me always. Thanks for having been an incredible mentor for me, for guidance and support, for innovative ideas and contribution in the interpretation of the results.*

*I would like to express my special gratitude to Centre of Experimental Oncobiology (C.Ob.S) staff at the Maddalena Hospital and, in particular, to **Prof. Ida Pucci-Minafra**, for giving me the opportunity to make the first part of the doctorate in the laboratory of C.Ob.S.*

*This work would not materialize without the technical support of **CHAB** (Mediterranean Center for Human Health Advanced Biotechnologies) and without the financial and technical support of **Prof. Salvatore Feo**, leaving total freedom and confidence at his laboratory of Genomics and Proteomics in the Department of Science and Technology Biological, Chemical and Pharmaceutical (STEBICEF).*

*I would also like to recognize the important roles of **Prof. Franco Baldi** (University of Venice) and **Dott.ssa Claudia Faleri** (University of Siena) in accomplished results.*

Thanks also to my lab colleagues and undergraduates met during this time of PhD, it was a great pleasure working with them and I appreciated their ideas, help and good humour.

*Finally, I cannot thank enough my parents, **Nino** and **Beny**, and my husband **Francesco**, for supporting me for all, and especially for encouraging me throughout this experience.*

*To my beloved little **Giacomo**, who so patiently, every day he has waited his mom.*